UNIVERSITY OF BIRMINGHAM

MICROFLUIDIC ENCAPSULATION OF BACTERIA IN EMULSION DROPLET

Nur Suaidah Mohd Isa

A thesis submitted to

The University of Birmingham

for the degree of

DOCTOR OF PHILOSOPHY

School of Chemical Engineering

The University of Birmingham

September 2019

Abstract

The encapsulation of bacteria in emulsion droplet has gained significant interest due to its various applications such as in the study of complex bacterial interactions and as a mean of protection for bacteria against harsh conditions. The application of droplet microfluidics allows for the encapsulation of bacteria in a highly controlled manner. Nevertheless, relevant studies of the effect of bacteria on emulsion stability remain scarce. Therefore, this thesis is focused on determining the effect of microfluidic-encapsulated bacteria on droplet stability and bacterial viability during ambient and cold temperature storage.

The study began by encapsulating bacteria in single water-in-oil (W/O) droplet. The inclusion of the Gram-negative *E. coli* with green fluorescent protein (*E. coli*-GFP) in W/O showed better droplet stability as compared to the Gram-positive *L. paracasei* as the droplet size distribution was maintained during storage at 25°C. Dead *E. coli*-GFP cells showed better stabilization effect as compared to live cells indicating the ability of dead cells to act as Pickering's particles in stabilizing the interface of the droplet. Encapsulation in W/O caused a reduction in bacterial viability while promoting the formation of bacterial clustering.

The study is then followed by the encapsulation of bacteria in double water-in-oil-in-water ($W_1/O/W_2$) droplet. The ability of $W_1/O/W_2$ droplet in supporting bacterial growth was observed due to the presence of an outer W_2 phase. In addition, the controlled release of bacterial cells induced by osmotic alterations was also determined with a high bacterial release observed at high sodium chloride concentration and low Tween 80 concentration.

Finally, the stability of W/O and $W_1/O/W_2$ droplet during cold temperature storage were also investigated whereby storage in freezing temperature caused an extensive droplet destabilization. This lead to complete bacterial release into the W_2 phase upon thawing. The

results obtained from these studies provide a better understanding of the feasibility of using emulsion droplet for bacterial encapsulation and controlled release that are beneficial for laboratory and industrial applications.

Acknowledgements

Firstly, I would like to express my gratitude to Allah. Alhamdulillah for the opportunity to embark on the journey of knowledge at the University of Birmingham.

I would like to thank my supervisors, Dr Kostas Gkatzionis and Dr Daniele Vigolo for their precious guidance and invaluable support throughout this journey. I will always be grateful for the encouragement that you have provided to assist me in becoming a confident researcher.

In addition to that, special thanks to Mrs Elaine Mitchell and Mr David French for technical support and precious knowledge. Also, to Lynn Draper who has been helpful and reassuring throughout my PhD.

To the members of my research group and lab mates, I am personally thankful for your kindness and support. Thank you for making the time in the laboratory cheerful and fun.

Special thanks to my beloved parents, siblings, relatives, especially my husband who has been standing next to me through thick and thin.

I am also very grateful to my fellow PhD friends Hani, Gina, Iqram, Mashitah, Naeemah, Faiqa, Anisa, Hajar, Hafiza and my sweet 13 Dawlish buddies, Mawaddah, Husnur and Fatin for the unending support. Also to everyone in The Malaysian Community in Birmingham. Although I cannot mention each name, I will always keep you guys in my prayers.

And to my son, Idris Raphael, thank you.

Table of content

List of Tables

List of Figures

Abbreviations

AO	Acridine orange
BATH	Bacterial adhesion to hydrocarbons
CFU	Colony Form Unit
CV	Coefficient of variance
DIW	Deionised water
DSC	Differential scanning calorimetry
GFP	Green fluorescent protein
HLB	Hydrophilic-lipophilic balance
LB	*Luria Bertani*
min	Minute
MO	Mineral oil
MRS	*de Man, Rogosa and Sharpe*
NaCl	Sodium Chloride
O	Oil
OD	Optical density
PAH	Poly(allylamine hydrochloride)
PBS	Phosphate buffer saline
PDMS	Polydimethylsiloxane
PEM	Polyelectrolyte multilayer
PGPR	Polyglycerol polyricinoleate
PI	Propidium iodide
PSS	Poly(sodium-4-styrenesulfonate)
rpm	Rotation per minute
SEM	Standard error of mean
W	Water (subscript 1 represents the inner phase, subscript 2 for outer phase)

Nomenclatures

°C	Degree Celsius
mL	Millilitre
µm	Micrometre
g	Gram
Q_d	Dispersed phase flow rate
Q_c	Continuous phase flow rate
µL	Microliter
nm	Nanometre
mN/m	Millinewton per meter
cm	Centimetre
P	Pressure
mbar	Millibar
w/v	Mass per volume ratio (%)
V	Volume
Mw	Molecular weight
L	Litre
T	Time
mW	Milliwatt
M	Molar

Chapter 1
Introduction

1.1 Context of the study

Bacterial encapsulation in emulsion droplet is not only beneficial for complex bacterial studies such as quorum sensing where droplet served as microreactors, but also for industrial applications in order to protect bacteria against adverse conditions during processing up to the point of consumption (Pimentel-González *et al.*, 2009; Zhang *et al.*, 2013; Barlow *et al.*, 2017; Devanthi *et al.*, 2018). The application of droplet microfluidics for encapsulating bacteria in emulsion droplet is more favourable as compared to other encapsulation methods such as homogenization technique due to its ability to control droplet size and maintain bacterial viability as the sample is not subjected to high mixing force (Zhang *et al.*, 2013; Chang *et al.*, 2015; Barlow *et al.*, 2017). Furthermore, the application of microfluidics for small scale emulsions study is also favourable as it helps in reducing the amount of substance used while the production of monodisperse droplet allows for a detailed study of emulsion stability without taking into account the effect of polydispersity (Teh *et al.*, 2008; Tadros, 2013).

The encapsulation of bacteria in emulsion droplet is highly depended on the stability of the emulsion system. Therefore, further studies are required in order to understand the effects of bacteria on emulsion stability, especially during storage as it is not only the key to successful bacterial assay but also important in ensuring the shelf life of industrial products such as food emulsions. Bacterial responses such as growth, death and production of by-products during storage may affect the stability of the emulsion system. It has been reported that bacterial

surface properties play a key role in droplet stabilization, forming particle-stabilized emulsions known as Pickering emulsions (Dorobantu *et al*., 2004; Firoozmand and Rousseau 2016; Wongkongkatep *et al*., 2012). However, the mechanism of droplet stability by bacterial cells is highly complex and therefore requires extensive study in order to clearly understand the factors related to this process.

Although the instability of emulsions is unfavourable especially for maintaining product quality during long-term storage, the destabilization of water-in-oil-in-water ($W_1/O/W_2$) emulsion is beneficial for the controlled release of bacteria and other materials such as flavours and drugs in food and pharmaceuticals products (Jaimes-Lizcano, Lawson and Papadopoulos, 2011; Dluska *et al.*, 2017; Devanthi *et al.,* 2018). It has been reported that the controlled release of hydrophilic materials/cargo from the $W_1/O/W_2$ droplet can be induced by several factors such as osmotic imbalances (El Kadri *et al.*, 2015; Hou *et al.*, 2017; Zhang *et al.*, 2017), change in pH (Ngai, Behrens and Auweter, 2005; Park *et al.*, 2015), and change in temperature (Ngai, Behrens and Auweter, 2005; Rojas *et al.*, 2008). Nevertheless, valuable studies on the mechanisms behind bacterial release and the destabilization of $W_1/O/W_2$ emulsions in the presence of bacteria remain scarce.

Cold temperature storage of emulsion-based products is commonly practiced especially for storing emulsions containing temperature-sensitive materials such as bacteria and drugs (Damin *et al.*, 2008; Choi, Zhang and Xia, 2010). The long-term storage of bacteria in freezing temperature is beneficial in order to maintain its viability and functionality (Fonseca, Béal and Corrieu, 2000). However, the detrimental effects of freezing on bacteria are still causing major concerns. Other than the use of cryoprotectants, the beneficial effect of bacterial encapsulation in maintaining bacterial viability during cold temperature storage has also been reported previously (Goderska and Czarnecki, 2008; Priya, Vijayalakshmi and Raichur, 2011;

Dianawati, Mishra and Shah, 2013). When using emulsions for bacterial encapsulation, another important aspect that needs to be addressed is the stability of the emulsion droplet as they tends to destabilize when stored in freezing temperatures. The freezing process of an emulsion caused droplet destabilization such as droplet coalescence and rupture that eventually lead to complete phase separation (Rojas *et al.*, 2008; Ghosh and Rousseau, 2009) while the presence of bacteria in emulsion droplet during cold temperature storage may affect droplet stability and bacterial viability. Therefore, it is crucial to understand the stability of emulsion droplet in the presence of bacteria not only during ambient temperature storage but also in cold temperature storage in order to assess the flexibility of this system for bacterial encapsulation.

This thesis aimed to investigate the interaction between bacteria and emulsion stability in order to ensure the effectiveness of emulsions to be used for encapsulation. The stability of emulsion droplet in the presence of bacteria is discussed in detail for single W/O emulsion and double $W_1/O/W_2$ emulsion in chapter three and 4 of this thesis. The study is then followed by the determination of droplet stability in cold temperature storage (chapter five). In addition, the application of double $W_1/O/W_2$ droplet for the controlled release of bacteria, induced by the changes in osmotic balance and the freeze-thawing process will also be described in chapter four and five, respectively. The application of microfluidics in this study helps in developing a model emulsion system in a controlled manner with monodisperse and tuneable droplet size. The results obtained from the designed experiments may give more insights on the stability of such systems and its flexibility to be used for various applications, not only for laboratory-based bacterial studies but also for the industrial development of functional emulsions for food, pharmaceutical and cosmetic applications.

1.2 Public presentations

i. Poster presentation in the Q-safe international conference: Qualitative tools for sustainable food and energy in the Food chain, Ermoupoli (Syros island), Greece on the 10-12 April 2017.

   Poster title: The effects of bacterial growth on microfluidic-generated water-in-oil droplet stability during storage

ii. Poster presentation in the Microfluidics 2018 - New Technologies and Applications in Biology, Biochemistry and Single-Cell Analysis.

   EMBL, Heidelberg, Germany on the 15-17 July 2018.

   Poster title: The effect of bacteria on the stability of microfluidic-generated single and double emulsions

Chapter 2
Literature Review

2.1 Types of emulsions and emulsion stability

An emulsion system is a dispersion of one liquid into another as droplet whereby both liquids are immiscible in nature. It has various applications such as in food, pharmaceutical and cosmetic industries whereby emulsion plays a major role in formulating products beneficial for consumers (Chappat, 1994).

An emulsion can be characterised into single and duplex emulsions with single emulsions being the most common and comprised of water-in-oil (W/O), oil-in-water (O/W), oil-in-oil (O/O) and aqueous type of water-in-water (W/W) emulsions. Duplex emulsions consist of single emulsions further emulsified into another continuous phase forming multiple emulsions of double (eg. Water-in-oil-in-water [$W_1/O/W_2$] emulsions and vice versa), triple (eg. Water-in-oil-in-water-in-oil [$W_1/O_1/W_2/O_2$] emulsions and vice versa) and quadruple emulsions (McClements, 2004). Single emulsions are the simplest form of emulsion system and are commonly being used industrially while the more complex form of duplex emulsions has recently been applied extensively in modern biological and chemical research including industrial applications.

There are several aspects that need to be considered in order to ensure the stability of emulsions such as choice of surfactants, methods used for emulsification, size of droplet formed and storage conditions (Binks *et al.*, 1998). The most crucial aspect is the choice of surfactants that can be classified into ionic and non-ionic surfactants. Anionic surfactant can be used for stabilizing emulsions by absorbing on the droplet and creating a charge that provides an

electrostatic repulsion between the droplet. However, the use of ionic surfactants is usually limited by its sensitivity towards the presence of electrolytes (Tadros, 2013). When used with bacteria, the charged head groups of ionic surfactants may interact with the charged molecules of the bacterial cells resulting in denaturation, making it less biocompatible as compared to non-ionic surfactants (Marcoux *et al.*, 2011). The use of cationic surfactant, for example, cetyltrimethylammonium bromide (CTAB) has been reported to induce a lethal effect on bacteria such as *Bacillus subtilis* and *Pseudomonas aeruginosa* (Zeng *et al.*, 2007) and eukaryotic cells, for example, *Saccharomyces cerevisiae* (Fadnavis *et al.*, 1990). Moreover, anionic surfactants such as sodium dodecyl sulfate (SDS) have also been reported to exhibit antibacterial effects (Mariani *et al.*, 2006). Therefore, the use of non-ionic surfactants such as polyglycerol polyricinoleate (PGPR) and polysorbate 80 (Tween 80) is deemed suitable for making emulsions containing bacteria as it is less likely to interact with bacterial cells (Marcoux *et al.*, 2011). It has also been shown previously that the use of both PGPR and Tween 80 surfactants in the production of emulsions containing bacteria does not affect the viability of *Escherichia coli* and *Lactobacillus paracasei* (El Kadri *et al.*, 2015, 2018).

Emulsion stability is associated with its capability to resist changes with time that can be divided into physical and chemical changes (McClements, 2004). Emulsion breakdown may be due to physical changes such as creaming and sedimentation, flocculation, Ostwald ripening, coalescence and phase inversion as summarized in Figure 2.1 (Mao and Miao, 2015) while chemical changes are due to processes such as oxidation and hydrolysis (Coupland and McClements, 1996; Morales Chabrand *et al.*, 2008). The rate of emulsion destabilization and the mechanism involved in this process depended on several factors such as the microstructure and composition of the specific emulsions and the environmental conditions by which the emulsion was exposed to for example storage conditions, changes in temperatures and

mechanical agitation (McClements, 2004). The quality of emulsion based products can be achieved by controlling the stability and physicochemical properties of the emulsions. Therefore, it is important to understand the importance of the mechanisms involved in emulsion destabilization, the relationship between these mechanisms and factors that lead to the destabilization process (McClements, 2004).

Creaming and sedimentation usually resulted from external forces such as gravitational and centrifugal (Binks *et al.*, 1998). Generally, the dispersed emulsion droplet exhibited a different density than the continuous phase which leads to net gravitational force to act on this droplet (Walstra, 2002; McClements, 2004; Muschiolik and Dickinson, 2017). Depending on its density, these forces cause the droplet to move towards the top (for droplet with lower density than the continuous phase) known as creaming or downwards (for droplet that has a higher density than the continuous phase) which is known as sedimentation. Creaming or sedimentation is usually unfavourable for emulsion based products especially food emulsions as it may affect consumer acceptance. A visually separated emulsion with an opaque layer containing high droplet concentration and a less opaque layer with fewer droplet is undesirable as consumer expectation is towards homogenous emulsion products. In addition, this mechanism may bring the droplet to be in close proximity to each other, therefore enhancing the possibility of droplet flocculation and coalescence that eventually resulted in the formation of a pure oil or water layer (McClements, 2004). The separation rate of an emulsion can be predicted by Stokes law given by:

$$V_0 = \frac{2R^2 \Delta p g}{9\eta} \qquad (2.1)$$

Whereby V_0 refers to as the rate of separation, R the radius of the droplet, Δp is the difference in density between the oil and water phases, g indicates the gravitational or centrifugal force involved while ŋ is the viscosity of the system (Hunter and White, 1987). From the equation, it is shown that reducing the size of the droplet during emulsion production or increasing the system's viscosity may help to slow down the process (Tadros, 2013; Mao and Miao, 2015). This can be achieved by inducing high mechanical force and the addition of thickeners during emulsion production (Mao and Miao, 2015). However, it should be noted that the Stokes law is not applicable to droplet that is smaller than 0.1 μm due to the fact that droplet with smaller size experiences stronger Brownian motion which enables it to resist the separation. Further decrease in droplet size to less than 10 nm leads to complete inhibition of emulsion separation making it thermodynamically stable (Russel, 1981).

In addition, flocculation may also cause emulsion destabilization as the droplet aggregates due to Van der Waals attraction. The associated droplet does not merge with each other and was individually separated by their own interfacial films and therefore, the process is reversible by mixing or by diluting the emulsions with more continuous phase (Mao and Miao, 2015). Droplet aggregation occurred due to insufficient repulsion force to push the droplet apart from each other to the point where the Van der Waals attraction became weak. Therefore, flocculation in emulsions can be overcome by increasing the repulsion forces between the droplet either through electrostatic or steric hindrance repulsion (Mao and Miao, 2015).

Coalescence refers to a process in which two or more droplet diffuse and form into larger droplet due to thinning of the interface (Tadros, 2013). Both flocculation and coalescence may result in an increase in average droplet size but different from that of flocculation where the individual identity of the droplet remains, the coalescence process resulted in the loss of

individual interfacial films as the droplet fused together forming larger droplet where the content of both droplets is combined (Mao and Miao, 2015). Coalescence may lead to a complete separation between the two immiscible phases due to strong Var der Waals forces between the droplet that are keeping them close together and fuse (Tadros, 2013). Active droplet coalescence also resulted in the acceleration of the creaming process as larger droplet tends to move quickly to the top of the emulsion. As coalescence is mainly due to the rupture of interfacial films, any means that may help in strengthening the interfacial films, for example, the adsorption of polymers such as proteins onto the interface can minimize the occurrence of droplet coalescence (Mao and Miao, 2015).

Other than that, Ostwald ripening may also occur as a result of mutual solubility between immiscible liquids. Ostwald ripening is driven by the difference in Laplace pressure between the small and the large droplet whereby in a polydisperse emulsion system, the smaller droplet have larger solubility compared to larger droplet thus, causing the smaller droplet to disappear as they solubilise into the larger droplet (Leal-Calderon, Bibette and Schmitt, 2007). It is a thermodynamically spontaneous process as larger particles tend to be more energetically stable as compared to smaller ones (Mao and Miao, 2015). It may occur due to the formation of a large droplet at the expense of smaller droplet as the disperse phase diffuses through the continuous phase or by the increase in solubility of the entrapped materials within the spherical droplet as it decreases in radius (McClements, 2009). Longer storage time will cause the droplet size distribution to shift to a larger value and eventually lead to phase separation (Tadros, 2013). The rate of droplet coarsening is determined by the rate of molecule diffusion through the continuous phase and its movements across the surfactant films (Leal-Calderon, Bibette and Schmitt, 2007).

In addition, the emulsion may also go through phase inversion whereby the process involves an exchange between the continuous and disperse phase. With an increase in storage time or changes in storage conditions, an oil-in-water (O/W) emulsion may change into water-in-oil (W/O) and vice versa (Tadros, 2013). For example, the increase in temperature of O/W emulsion prepared with polyoxyethylene nonionic surfactants such as Tween 20 and 80, will cause the surfactants to become more hydrophobic and thus change the emulsion into W/O as the dispersed oil phase became the continuous phase (Sherman and Parkinson, 1978). Besides that, this process may also lead to the formation of multiple emulsions as it passes through the state of transition (Tadros, 2013).

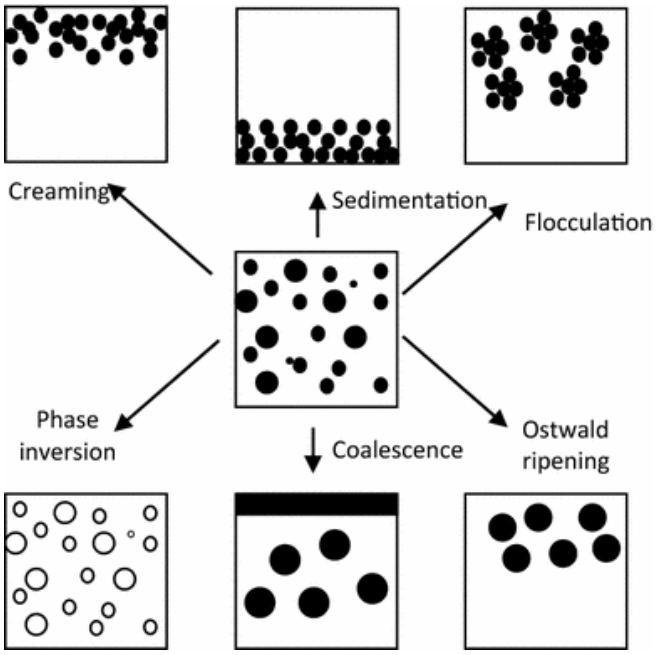

Figure 2.1 Emulsion breakdown processes. Adapted from Mao and Miao (2015)

The multiple water-in-oil-in-water emulsions ($W_1/O/W_2$) exhibit a different destabilization mechanism as compared to single emulsions due to their complex structure (Ficheux *et al.*, 2002). Some of the mechanisms involved in the destabilization of multiple emulsions during processing or storage are the coalescence of the inner W_1 droplet or the oil globule. The coalescence between the inner W_1 phase is termed as internal coalescence whereas the coalescence between the inner W_1 phase and the outer W_2 phase is termed as external coalescence (Villa *et al.*, 2003). In addition, the fusion between oil globule may also occur resulting in samples with larger oil globule size that eventually leads to phase separation (Schuch, Köhler and Schuchmann, 2013).

In order to maintain the stability of the multiple emulsions, it is crucial to balance the osmotic pressure between the aqueous phases. The osmotic balance does not have to be absolute zero in order to maintain its stability but it has to be low enough to prevent droplet coalescence and rupture due to swelling of the W_1 phase (Muschiolik and Dickinson, 2017). One of the most commonly used methods in order to control droplet destabilization due to osmotic imbalances is by separating the W_1 phase and the W_2 phase with a soft-solid like membrane such as starch or globular proteins (Oppermann *et al.*, 2015). Nevertheless, the stability of droplet with the absence of solid-like membrane can also be achieved by careful development of a formulation that can tailor the osmotic imbalances. The addition of salt, sugar or a combination of both in formulating multiple emulsions helps in regulating the osmotic imbalances (Muschiolik and Dickinson, 2017). Moreover, droplet stability also depended on the Laplace and osmotic pressure balance. In $W_1/O/W_2$ emulsion, the presence of NaCl for example in the W1 phase resulted in droplet swelling that helps to minimize the shrinkage of droplet due to Laplace pressure. The balance between the Laplace and osmotic pressure is given by the Walstra equation (Walstra, 1993):

$$2\gamma = 3mRT \qquad (2.2)$$

Where γ is the interfacial tension, m is the molar concentration of NaCl, R is the universal gas constant and T is temperature.

Furthermore, the stability of the multiple emulsion can also be achieved by protein-polysaccharide interactions on the interface (Dickinson, 1993). This result in surface elasticity and also provide a steric barrier that prevents droplet coalescence and aggregation. It is also beneficial in inhibiting water migration between the inner W_1 phase and the outer W_2 phase while minimizing the release of the encapsulated materials (Muschiolik and Dickinson, 2017). Other than that, emulsion stabilization can also be improved by increasing the emulsion viscosity or gelation, for example, the addition of sodium alginate in the production of multiple emulsion (Gaonkar, 1994). The inclusion of gelatine or whey protein as a gelling agent in the W_1 phase has also been reported to enhance the stability of the multiple $W_1/O/W_2$ emulsions during storage while maintaining the sensory quality of the emulsions (Oppermann *et al.*, 2016).

Other than maintaining the stability of the multiple emulsions, the percentage of encapsulated materials in the W_1 phase also indicates the overall quality of the produced multiple emulsions. The encapsulation efficiency is often determined when the multiple emulsions are being used as a means of encapsulation by measuring the free compound available in the outer W2 phase immediately after emulsion production and subtracting the measured amount from the original concentration of the compound prior to encapsulation.

2.2 Methods to produce an emulsion

Two immiscible liquids such as water and oil tend to be in their thermodynamically stable state that separates them into two layers, one on top of the other depending on its density when placed in a container as this minimizes its contact area. With a sufficient amount of energy such as from mechanical agitation, one of these phases may break and disperse in the other phase depending on its concentration (McClements, 2004). The mixing of these immiscible liquids into, for example, O/W emulsions resulted in high interfacial free energy for the oil due to the high surface area of the small oil globule which is unstable and will tend to revert back into its bulk original state with lower interfacial energy (Grumezescu, 2019). In addition, the high cohesive forces between the molecules in oil or water as compared to the adhesive force between them leads to phase separation as the liquids try to keep a low interfacial area (Grumezescu, 2019). The amount of free energy change involved in the formation of an emulsion is represented as follows:

$$\Delta G = \gamma \Delta A \qquad (2.3)$$

Where G is the interfacial energy, γ the interfacial tension and A represents the interfacial area (McClements, 2004). Therefore, in order to ensure the long-term stability of emulsions, it is crucial to add in a sufficient amount of emulsifier that will bridge the immiscible liquids together thus, reducing the interfacial tension and prevent the droplet from fusing together (Walstra and Smulders, 1998). During the emulsion preparation process, the surfactants will adsorb onto the interface and improve the miscibility of the water and oil leading to the formation of emulsions (Grumezescu, 2019).

Homogenization is one of the processes involved in the production of emulsions whereby it can be divided into primary and secondary homogenization. The primary

homogenization is responsible for mixing two completely separated liquids into coarse emulsions while the secondary homogenization helps in reducing the size of the droplet into the smallest possible size to maintain their stability (Figure 2.2). Several processes occur during homogenization such as mixing, droplet breaks up and coalescence. Although secondary homogenization is conducted in order to produce emulsions with small droplet size, this is not usually the case. Emulsions with distinctively small droplet can also be produced directly by using homogenizers such as microfluidizers, membrane homogenizers and ultrasound (McClements, 2004).

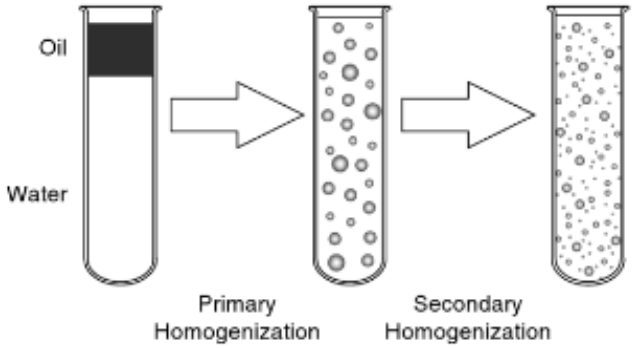

Figure 2.2 Primary and secondary homogenization process in emulsion preparation. Adapted from McClements (2004)

Direct homogenization of the oil and aqueous phases can be done by using high-speed mixers (Figure 2.3). These consist of a vessel that can accommodate from as small as few cm^3 of mixtures for lab-scale applications and up to few m^3 for industrial applications. The emulsions are produced by agitation which is induced by the rotation of the mixing head at high speed. This creates a combination of forces such as rotational and radial velocity that breaks the interface between oil and water producing smaller droplet that is dispersed in one of the phases. The droplet size of the produced emulsions depends on the rotation speed and

homogenization time as an increase in rotation speed and homogenization time resulted in a decrease in droplet size (McClements, 2004).

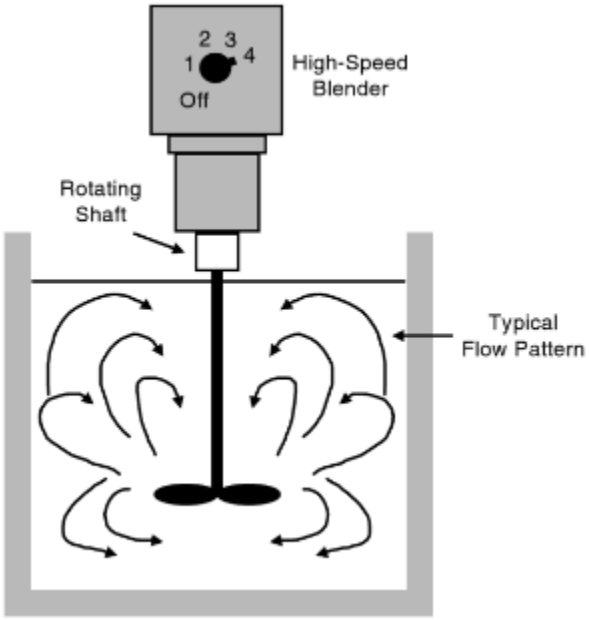

Figure 2.3 High-speed mixer used in the industry. Adapted from McClements (2004)

The high-pressure homogeniser is also one of the pieces of equipment commonly used in the industry to produce emulsions (Aguilera and Lillford, 2007). This method is mostly used to produce emulsions with a smaller droplet from coarse emulsions that were produced by a high-speed mixer (McClements, 2004). These coarse emulsions were fed into the high-pressure homogenisers and were then pumped through a small valve or gap. As the emulsion pass through the valve, disruptive forces were exerted onto the emulsions that further breaks the droplet into smaller sizes creating finer emulsions (Phipps, 1985). The mechanisms involved for droplet disruption in the high-pressure homogenizers are shear forces within the fluids as a result of velocity gradients, the collision between the droplet and hard surfaces within the valve and cavitation (Berk, 2013). Cavitation takes place as the liquids passed through the narrow gap causing a decrease in pressure as it accelerates to a very high velocity. The pressure was reduced

locally to be lower than the water vapour pressure thus resulting in evaporation. This process leads to the formation of vapour bubbles that expands and collapsed resulting in shock waves that break the droplet into smaller sizes (Berk, 2013). Industrial lab-scale homogeniser functions in turbulent flow regime while small lab-scale homogeniser works under laminar flow regime (Aguilera and Lillford, 2007). On top of the standard nozzle used in a typical high-pressure homogenizer, other types of nozzles were used for various applications such as microfluidizer, jet and orifice valve. Some of the industrial homogenizers were also equipped with an adjustable valve in order to adjust the gap size. This way, smaller droplet size can be produced as a greater degree of droplet disruption can be achieved by decreasing the gap size (McClements, 2004).

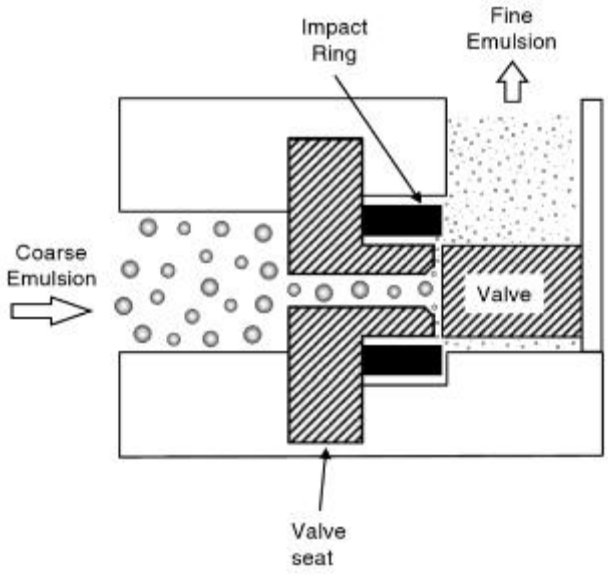

Figure 2.4 High-pressure homogenizer for producing small droplet. Adapted from Mc Clements (2004)

Furthermore, turbulent flow and cavitation effect can also be achieved by using the ultrasound method. Sounds involve propagating pressure oscillation whereby large oscillation created by high-intensity sound creates a pressure that is lower than the vapour pressure of water. This leads to the formation of small imploding bubbles that eventually creates turbulence and cavitation effect similar to high-pressure homogenisation that aid in droplet breakup. A frequency of higher than 20 kHz (ultrasound) is normally being used in this process to create emulsions with very fine droplet size. This method, however, is not suitable for large-scale production of emulsions as small chambers are usually required for high efficiency. Large chambers will lead to less droplet breakup efficiency as the ultrasound generated by the actuator declines with increased chamber size.

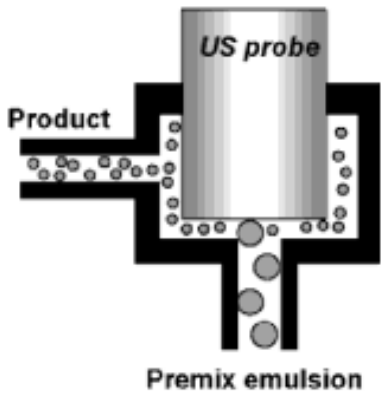

Figure 2.5 Schematic picture of an ultrasound homogenizer. Adapted from Aguilera and Lillford (2007)

Besides that, the production of highly monodisperse emulsion droplet could be achieved by using micro-channel emulsification. By using this technique, an emulsion is produced by permeating the dispersed phase into the continuous phase through microchannels with predefined geometries. The size of the droplet produced depends on the velocity of the phases and the dimension of the microchannels (Kawakatsu *et al*., 2000; McClements, 2004). This method was described in studies by Kawakatsu *et al.* (2000). Monodispersed W/O and O/W

droplet were produced by using a cross-flow microchannel plate. With this method, the dispersed phase was pushed through the microchannel and approximately 10 μm size droplet was produced by squeezing the dispersed phase through the continuous phase. O/W droplet were produced by using hydrophilic channels with a glass plate while W/O droplet was made by using hydrophobic channels and a silane coupler treated glass plate. Membrane homogenizers also work in a similar way as the microchannel homogenizer except that the dispersed phase was introduced through a solid membrane with well-defined pore sizes. Several factors affecting the size of the droplet produced are the size of the pores, the continuous phase flow rate, the interfacial tension between the phases and the membrane pressure (Suzuki, Shuto and Hagura, 1996). The production of a highly monodispersed droplet can be achieved by manufacturing membrane with uniform pores size. However, this is not always the case as the manufactured membrane may have different pore sizes that lead to the production of a fairly polydisperse emulsion. The strength of the membrane along with its polarity is important in order for it to withstand strong pressure and also for producing different types of emulsions (Suzuki, Shuto and Hagura, 1996; McClements, 2004).

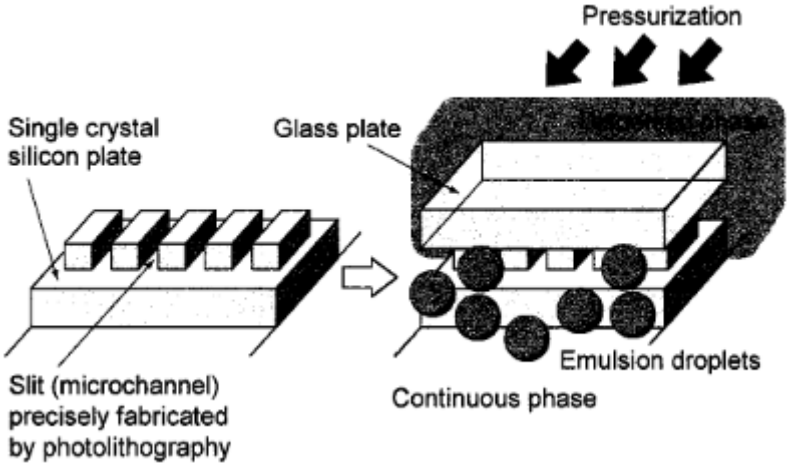

Figure 2.6 Schematic diagram of microchannel emulsification. Adapted from Kawakatsu *et al*. (2000)

In order to produce W/O emulsion, a hydrophobic membrane was used while to produce O/W emulsion, a hydrophilic membrane is used. Both microchannel and membrane homogenizers can be used to produce a variety of emulsions from single W/O or O/W emulsions to multiple emulsions such as $W_1/O/W_2$ depending on the wettability of the materials in which they are made of (Suzuki, Shuto and Hagura, 1996; Kawakatsu, Kikuchi and Nakajima, 1997; Vladisavljevic, 2014). By using these homogenizers, monodispersed emulsion droplet may be produced and the size of the droplet produced can be adjusted by choosing the right microchannel or pore sizes.

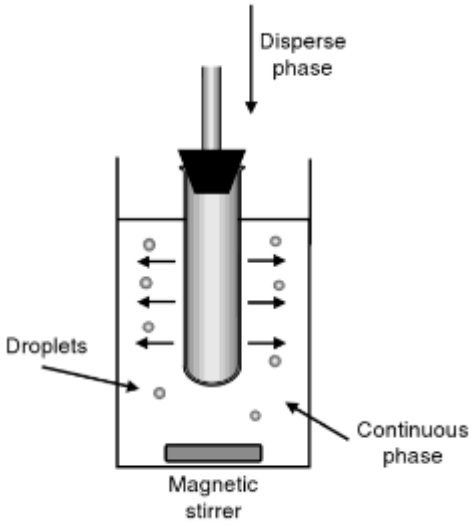

Figure 2.7 Schematic diagram of a batch membrane homogenizer. Adapted from Mc Clements (2004)

2.3 Droplet microfluidics

2.3.1 Droplet microfluidics for producing emulsion

Droplet microfluidics involves the production of the discrete droplet by using immiscible phases such as oil and water and its manipulation within the microchannel (Shang, Cheng and Zhao, 2017). The production of discrete droplet inside the microchannel enables independent control over these droplets, producing microreactors that can be individually transported, merged and analysed (Link *et al.*, 2006; Fair, 2007). This helps in acquiring large data sets for a particular experiment as multiple microreactors can be produced within a short period of time. Moreover, the usage of a droplet with high surface area to volume ratio resulted in shorter distances and time for diffusion, heat and mass transfer thus improving reaction time (Shang, Cheng and Zhao, 2017). To date, droplet microfluidics has been used in numerous studies whereby irregular particles, microbubbles, multiple emulsions and microcapsules were formed for its applications in biomolecules synthesis, diagnostic testing and as a drug carrier (Teh et al. 2008).

Depending on the design of the microfluidic chip, it can be used to produce monodispersed single droplet or multiple droplet whereby the size and format of the droplet can be controlled by changing the dimensions of the microchannels and also by tuning the flow rates of the different phases (Ward *et al.*, 2005). Some of the materials used for microfluidic device fabrication were Polydimethylsiloxane (PDMS) which is hydrophobic in nature, Poly (methyl methacrylate) (PMMA) that has a partially hydrophilic nature, glass (hydrophilic in nature), silicone and thiolene (Teh *et al.*, 2008). PDMS is widely chosen in the production of microfluidic chips as it is cheaper and can be mould easily. However, surface modification of the PDMS microfluidic device may be required in order to make it hydrophilic for the production of O/W and $W_1/O/W_2$ emulsion droplet to ensure effective wetting of the aqueous continuous phase while preventing the oil droplet from adhering onto the channel (Bauer *et al.*, 2010).

Figure 2.8 shows several designs of the microfluidic chips used for droplet generation such as the T-junction, flow-focusing and co-flow (Vladisavljević, Al Nuumani and Nabavi, 2017; Loizou, Wong and Hewakandamby, 2018). The flow-focusing device is commonly used for monodispersed droplet generation as it allows for better control and stable production of the droplet. This is attributed to the fact that the flow-focusing geometry produces a symmetrical flow that eases droplet formation at the junction as compared to the asymmetric T-junction (Tan *et al.*, 2008; Elveflow, 2019). Droplet breaks up at the wall as observed in the T-junction was replaced with the water or oil interface in the flow-focusing whereby, the wall effect is minimized while the shear force effect of the continuous phase is maximized (Elveflow,2019). For producing single emulsions droplet, a single junction device may be used while a device with double or multiple junctions may be used for producing multiple emulsions.

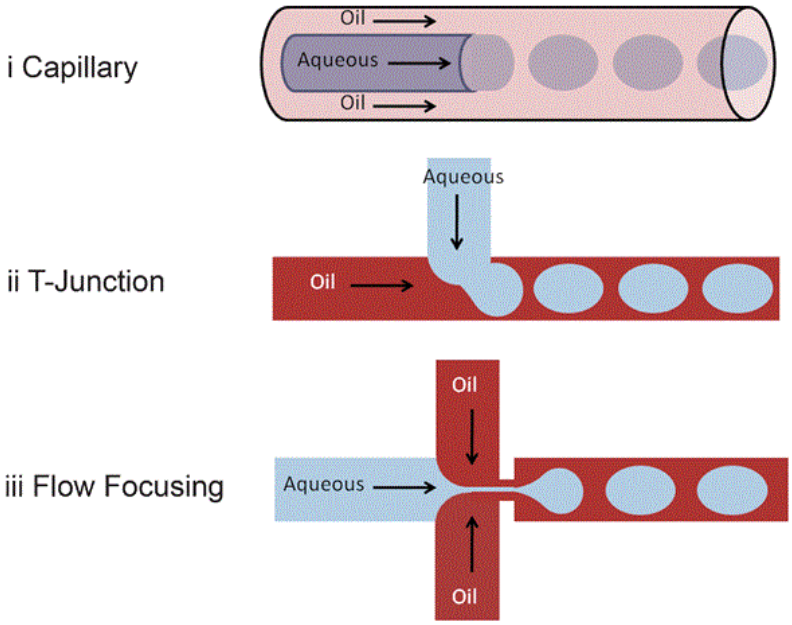

Figure 2.8 Different formats of microfluidic chips. Adapted from Casadevall I Solvas and deMello (2011)

2.3.2 The biological applications of droplet microfluidics

The increasing interest in microfluidics had led to various applications of this technology in ranges of research fields, not only in the field of engineering but also in biology (Gravesen, Branebjerg and Jensen, 1993). The compatibility of microdroplet with various chemical and biological reagents makes them suitable for encapsulation. This allows for successful application of droplet microfluidics in the field of biology for example, in polymerase chain reaction (PCR) amplification whereby the reaction efficiency is significantly improved. The compartmentalization of the reactants significantly improves amplification efficiency by inhibiting reagent dispersion and adsorption on the channel surfaces. It has been shown that the application of droplet microfluidics in PCR allows for single-copy DNA amplification in a short period of time (Schaerli et al. 2009). In addition, biochemical assays such as DNA, protein and enzyme expression have also benefited from the encapsulation of reagents and bacteria through

droplet microfluidic for example, the *in-vitro* synthesis of proteins by bacteria as it allows for the on-chip manipulation of these droplets thus, creating a suitable condition that is important for inducing the production of proteins (Wu *et al.*, 2009).

The application of droplet microfluidics also provides the possibility for capturing individual cells in microdroplet and allows for the production of a droplet containing a predetermined number of cells. These microfluidic-generated microenvironments can be manipulated to assist in cellular studies such as quorum sensing, biofilm formation, detection and identification of pathogens and antibiotics assay (Boedicker, Vincent and Ismagilov, 2009; Neethirajan *et al.*, 2011; Chang *et al*., 2015; Barlow *et al*., 2017). Selective diffusion across the oil phases allows for complete control of the microenvironment (Zhang *et al.*, 2013). In the study done by Boedicker *et al*. (2009), the encapsulation single *P. aeroginosa* cells in small volume was conducted in order to challenge the hypothesis that a high population of cells is needed for quorum sensing initiation. That study successfully demonstrated that quorum sensing initiation is affected by biomass per unit volume whereby confinement itself without host interaction may promote quorum sensing in a single cell. It showed that when a single cell is entrapped in a small volume, it will have enough biomass to activate quorum sensing.

Microfluidic-generated double and triple emulsion droplet also served as microenvironments to investigate biofilm formation of *Bacillus subtilis* in which direct observations of cell differentiation and biofilm microstructure were visualized microscopically within each droplet. The rapid production of thousands of these microenvironments demonstrated its potential to be applied in high-throughput screening of bacterial biofilms (Chang *et al.*, 2015). Recent work has also been done on the development of functional droplet containing *Bacillus subtilis* for selenium remediation. The microencapsulation of *Bacillus subtilis* aids in the entrapment of sodium selenite and converting it into selenium nanoparticles

that were kept inside the droplet. In addition to developing a method of bacterial manipulation for water treatment application, that study also demonstrated the rapid formation of bacterial biofilms in the droplet by ensuring a continuous supply of nutrients across the interface (Barlow *et al.*, 2017).

2.4 Bacteria encapsulation in an emulsion droplet

Probiotic bacteria play an important role in human health and are often used in the development of functional foods and pharmaceutical products (Chavarri, Maranon and Carmen, 2012). In order to effectively provide health benefits to humans, the strains should be kept viable throughout processing, shelf life and during consumption to ensure maximum delivery to the targeted area (Rokka and Rantamäki, 2010; Chavarri, Maranon and Carmen, 2012). Previous reports indicated the poor viability of free probiotics cells in food products and also a decrease in their viability during consumption due to the adverse gastrointestinal conditions, making them less effective in promoting health benefits at targeted areas such as in the gut environment (Rokka and Rantamäki, 2010; Rodríguez-Huezo *et al.*, 2014; Mao and Miao, 2015).

Microencapsulation has been shown to enhance bacterial viability especially of the beneficial probiotics in the intestinal tract and in food products (Pimentel-Gonzalez *et al.*, 2009; Chavarri, Maranon and Carmen, 2012; Lalou, Kadri and Gkatzionis, 2017). Successful bacterial encapsulation has been reported in several studies using various methods and materials for encapsulation such as spray drying, freeze and vacuum drying, emulsion-based technique and the use of food-based materials such as hydrocolloids (Jankowzki *et al*., 1997; Kebary *et al*., 1998; Khalil and Mansour, 1998; Lee and Heo, 2000; Rodriguez-Huezo *et al*., 2007; Annan *et al*., 2008; Rokka and Rantamäki, 2010; Chavarri, Maranon and Carmen, 2012; Larsen *et al.*, 2018). The microencapsulation process involves the entrapment of cells and/or reagents in a membrane or membrane-like materials. The materials used for encapsulation consist of thin,

strong, spherical, semipermeable or non-permeable microcapsules with liquid or solid core and varies in diameter (few microns to 1mm). Increasing demands of encapsulation for food applications give way to the development of food-grade polymers as encapsulation materials with hydrocolloids being the most common for example, alginate, carrageenan, pectin and gelatine (Anal and Singh 2007).

However, there are several important challenges that need to be considered for cell encapsulation. One of the main challenges is the large bacterial size that limit their inclusion into small-sized capsules or the production of relatively large-sized capsules that is unfavourable to the texture and sensorial quality of the food products (Pimentel-Gonzalez *et al.*, 2009). Moreover, the encapsulation process itself may also affect the viability of the probiotics, for example, the use of high temperature during spray drying may lower the viability of bacteria in the produced food products, making them less stable during storage (Chavarri, Maranon and Carmen, 2012). Thus, it is important to select an encapsulation method that is suitable for sensitive probiotic organisms. Encapsulation of bacteria into emulsion droplet especially in double $W_1/O/W_2$ may serve as an alternative method (Shima *et al.,* 2006). Studies done on the encapsulation *Lactobacillus acidophilus* in $W_1/O/W_2$ droplet show that the viability of the encapsulated *Lactobacillus acidophilus* was higher compared to the unencapsulated bacteria. Bacterial viability was affected by the overall size of the produced droplet and the volume of the inner aqueous phase whereby droplet produced with larger oil droplet and inner phase volume show higher viability (Shima *et al.*, 2006). Moreover, the encapsulation of *Lactobacillus rhamnosus* in $W_1/O/W_2$ emulsions also improve the survival of cells against low pH and bile salts condition with similar results observed from *in vitro* studies (Pimentel-Gonzalez *et al.*, 2009). Further studies conducted in real food environments such as yoghurt and cheese also show the ability of emulsions especially double emulsions in improving the

survival of bacterial cells during processing and storage (Rodríguez-Huezo *et al.*, 2014; Lalou, Kadri and Gkatzionis, 2017). Although these studies reveal the potential use of emulsions for bacterial encapsulation, further studies are still required in order to assess the stability of such system under different storage conditions.

2.5 Pickering emulsions and the importance of bacteria in emulsion stability

Recently, there has been an increasing interest in the study of bacteria that act as particles for emulsion stability forming a system known as Pickering emulsion. Pickering emulsion is an emulsion system that forms as a result of solid particle absorption onto interfaces. It has been of interest for decades especially in the development of consumer products where the addition of surfactants is not favourable and may cause adverse effects especially in health-related and cosmetic products (Kalashnikova *et al.*, 2011). The use of solid particles for stabilization in Pickering emulsions not only improves the stability of the emulsion but also helps in reducing the use of surfactants which are known to cause adverse effects on the environment (Wongkongkatep *et al.*, 2012).

In Pickering emulsion, droplet stability was improved due to the accumulation of colloidal particles onto interfaces that creates a layer with a steric barrier that prevents coalescence (Binks *et al*., 2006; Dickinson, 2010). The limit to the steric barrier depended on how strong the particles attached to the interface. The contact angle of the particles at the interface determines the adherence properties and its suitability to be used in the emulsion system. For example, hydrophilic colloidal particles have less than 90° of contact angle and are suitable to be used for O/W emulsions while hydrophobic particles with more than 90° contact angle contribute to the formation of W/O emulsions. Various types of inorganic particles have been studied for their use in the formation of Pickering emulsion such as nanocrystals, silica

and graphene oxide sheet (Binks *et al*., 2005; Colard *et al*., 2010; Kim *et al*., 2010; Kalashnikova *et al.*, 2011; Tzoumaki *et al*., 2011).

The non-biodegradable and compatible characteristics of inorganic solid particles limit its application as Pickering particles for consumer-based products such as foods. Therefore, studies have focused on food-grade particles for Pickering emulsions such as hydrophobic cellulose, soy protein, quinoa starch, β-lactoglobulin and whey protein (Wege *et al*., 2008; Liu and Tang 2013; Rayner *et al*., 2012; Nguyen *et al*., 2013; Destribats *et al*., 2014). However, limitations in the use of food-grade particles, for example, the high tendency to aggregate, has opened up recent researches on the ability of bacterial cells as particles in Pickering emulsions. Microbial cells have shown to be able to adhere to hydrocarbons (Rosenberg, Gutnick and Rosenberg, 1980). A recent study on microbial cells as Pickering particles involves bacteria and yeast with a fine micron-size that was proven suitable for stabilization of O/W emulsions and may be used as an alternative to synthetic surfactants (Firoozmand and Rousseau, 2016). Furthermore, it has also been reported that bacteria with the aid of a self-assembled chitosan network were able to provide stability for O/W emulsions (Wongkongkatep *et al.*, 2012). In addition, stabilization of O/W emulsions by several bacteria with hydrophobic properties has also been reported in which the adherence of such bacteria onto oil droplet prevents coalescence without significant change in interfacial tension (Dorobantu *et al.*, 2004).

The mechanism of bacteria as Pickering emulsion is mostly attributed to their surface properties which vary between strains and conditions in which the bacteria were suspended. Most studies reported that the wettability of bacteria (hydrophobicity or hydrophilicity) play an important role in emulsion stabilization although this characteristic may change with bacterial conditions (Dorobantu *et al.*, 2004; Wongkongkatep *et al.*, 2012). Despite many studies that

have been done on the ability of bacteria for emulsion stabilization (Dorobantu *et al.*, 2004; Wongkongkatep *et al.*, 2012; Firoozmand and Rousseau, 2016), it has also been reported that the presence of bacteria in an emulsion system with ionic surfactants may cause instability (droplet flocculation and aggregation) due to interactions of bacteria with charged droplet (Li *et al*., 2001). In addition, changes in emulsion properties during storage may also affect the ability of bacteria as a stabilizer. Therefore, further studies are still required in order to gain a better understanding on the complexity of bacterial interactions with emulsion especially in the water-in-oil droplet (W/O) whereby studies related to the effects of encapsulated bacteria on W/O emulsion stability is still scarce.

2.6 The application of emulsion for the controlled release of bacteria

Emulsions are suitable for the controlled release and targeted delivery of nutrients or bacteria. For example, bioactive peptides and lactic acid bacteria were delivered in the small intestine following protection against the gastrointestinal conditions (Mao and Miao, 2015; Larsen *et al.*, 2018; Giroux *et al.*, 2019). Studies conducted on the emulsion-based delivery of various functional ingredients such as vitamins and flavour compounds reveals that the controlled release of these materials at a specific stage during digestion could be achieved by formulating emulsions that exhibit reversible or irreversible destabilization when induced by changes in pH, temperature and osmotic balance (Mao and Miao, 2015).

The production of emulsion with pH-responsive switchable behaviour has attracted a lot of interest as it allows for the controlled release of nutrients and bioactive (Patel *et al.*, 2013). Examples of the pH-responsive materials that were used are pH-responsive latexes, pH-sensitive microgel particles and natural materials such as xanthan gum with shellac and chitosan nanoparticles (Amalvy *et al.*, 2003; Wei *et al.*, 2012; Patel *et al.*, 2013). The use of pH-responsive latex in O/W emulsions creates a reversible destabilization of emulsions in which

by lowering the pH, the structure of the emulsion was destabilized due to the desorption of particles from the interface while increasing the pH back to approximately 8.4 with homogenization caused the emulsion to be re-emulsified (Amalvy *et al.*, 2003).

Other than that, the controlled release of materials from emulsions can also be induced by the change in temperature. A study on the development of emulsions stabilized with pH and temperature-sensitive poly(*N*-isoproylacrylamide) (PNIPAM) microgels reveals its potential use for the controlled release of materials from O/W emulsions (Ngai, Behrens and Auweter, 2005). By raising the temperature from 25 °C to 60 °C, the prepared emulsions become unstable due to an increase in the hydrophobicity of the gels causing it to be completely immersed in the oil phase. This eventually leads to complete phase separation and release of the encapsulated compounds. Another example of temperature-induced release is by freezing the oil phase of $W_1/O/W_2$ double emulsions while the aqueous phases of inner and outer phase remain liquid (Rojas *et al.*, 2008; Jaimes-Lizcano, Lawson and Papadopoulos, 2011). Reducing the temperature to approximately 4°C ensures a complete crystallization of the oil phase (*n*-hexadecane) and maintained the stability of the emulsions. In order to trigger the release of compounds from the emulsion, the sample is then thawed at 25°C that caused the oil phase to become liquid. This leads to external coalescence that releases the compound from the inner W_1 phase to the outer W_2 phase. A similar result was also reported by Jaimes-Lizcano, Lawson and Papadopoulos (2011) in which double emulsions containing protein in the inner W_1 phase and ethanol in the W_2 phase were initially stored at 5°C to crystallize the oil phase leaving the aqueous phase in liquid form. Subsequent thawing at 35°C completely released the protein from the W_1 phase to the W_2 phase. The formulation was also tested *in vitro* on porcine skin that reveals its potential to be applied for macromolecular delivery as 86µm penetration into the

skin was achieved by using the developed formulation. The presence of ethanol in the W_2 phase aid in enhancing the penetration rate.

The controlled release of bacteria can be achieved by altering the osmotic balance of the double $W_1/O/W_2$ emulsions. This can be done for example, by changing the sodium chloride concentration that leads to the controlled release of *E. coli*-GFP from the inner W_1 phase into the outer W_2 phase as reported by Kadri *et al.* (2016). This process is dependent on the solute concentration in both of the aqueous phases and also the concentration of the hydrophilic and lipophilic surfactants. According to that study, the bursting of the oil globule leads to the complete and immediate release of bacteria into the outer aqueous phase which could potentially be applied in food emulsions to control the release of bacteria at a desirable time during the fermentation process. However, the study of the release mechanism in a more homogenous system with highly monodispersed droplet size may provide a better understanding of this process.

2.7 Emulsions in cold storage

2.7.1 The freezing mechanism of emulsions

Freezing involves phase transition of a solution from liquid to solid state which is divided into several stages namely supercooling, crystallization and recrystallization. The crystallization stage is further divided into the nucleation stage followed by crystals formation and growth (Sun, 2005). The freezing of emulsions involves the freezing of the aqueous and the oil phase and depending on the freezing point of these phases, the crystallization sequence between the two phases may affect the stability of the emulsion during storage (Cramp *et al.*, 2004; Ghosh and Rousseau, 2009; Degner *et al.*, 2014). Although the freezing of both phases is important in determining emulsion stability, the phase transition of the aqueous phase plays a major role in

the freezing process and therefore, the phase behaviour of water will be explained in detail followed by the critical role of oil phase crystallization on emulsions stability.

The freezing process of the aqueous phase begins with the supercooling or the supersaturation stage whereby these conditions resulted in the formation of ice crystals as the emulsion is cooled below its freezing point or with an increase in solute concentration that exceeds its saturation point (Degner *et al.*, 2014). The change in temperature during this stage is fairly constant due to the phase transition of a liquid to ice crystals that releases heat (the latent heat of crystallization). The freezing of the aqueous phase in O/W emulsions usually occurs heterogeneously as compared to homogeneous crystallization due to the presence of dust or impurities in the continuous aqueous phase that catalyses the formation of ice crystals (Schuch, Köhler and Schuchmann, 2013; Degner *et al.*, 2014). In contrast, the crystallization of the dispersed aqueous phase in W/O emulsions usually occurred homogeneously (self-induced) as the small size of water droplet caused it to be less likely to contain any ice nuclei or impurities (Koop, 2004). In a case where ice nuclei are present in one of the droplet, the crystallization will only occur in this droplet while the other droplet remains liquid and crystallizes homogeneously (Figure 2.9). This lowers the crystallization temperature and leads to broader crystallization curve as the freezing process occurred in a much broader temperature range as compared to bulk aqueous phase that exhibits sharp crystallization temperature (Schuch, Köhler and Schuchmann, 2013). Both of these freezing mechanisms were observed during the freezing process of the double $W_1/O/W_2$ whereby the outer W_2 aqueous phase shows heterogeneous crystallization while the inner W_1 phase exhibits homogeneous crystallization (Schuch, Köhler and Schuchmann, 2013). This is beneficial in distinguishing the thermal properties between both of the phases as it resulted in two distinguish cooling curves in the DSC (differential scanning calorimetry) (Schuch, Köhler and Schuchmann, 2013).

Nevertheless, the presence of solute for example bacteria encapsulated in the inner W_1 phase may result in heterogeneous crystallization of the droplet and therefore leads to the formation of only one cooling curve in the DSC. However, further studies are required in order to confirm this hypothesis.

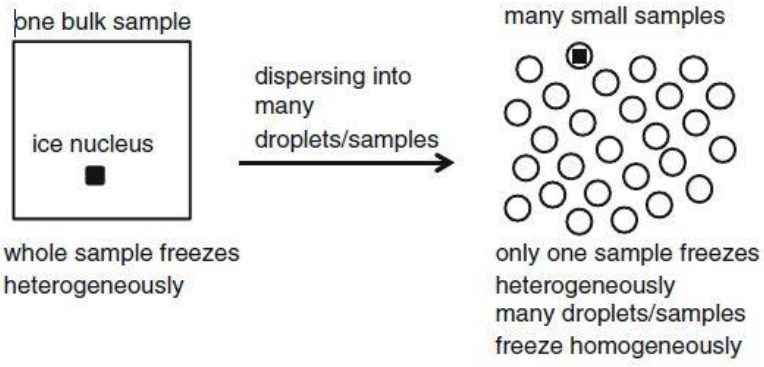

Figure 2.9 The difference in the crystallization process between the bulk aqueous phase and dispersed aqueous phase in emulsions. Adapted from Schuch, Köhler and Schuchmann (2013)

In addition, the presence of encapsulated materials such as bacteria in the dispersed aqueous phase for W/O emulsions or in the continuous aqueous phase of the O/W emulsions may cause a further reduction in the freezing temperature of the emulsions due to freezing point depression. This is due to the presence of non-volatile solute that caused a reduction in the vapour pressure of the solvent. According to the example three-phase diagram (Figure 2.10), the triple point of a solution depends on its vapour pressure and as the vapour pressure decreased with an increase in solute concentration, the triple point of a solution is shifted towards a lower temperature. This reduces the freezing point of a solution as a reduction in temperature is required for the solid-liquid system to reach equilibrium (Reger, Goode and Ball, 2009).

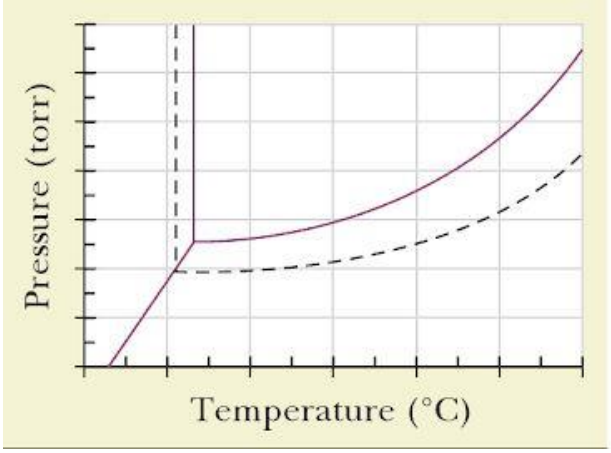

Figure 2.10 An example of freezing point depression of a solution shown in a triple-phase diagram. The behaviour of a solution is shown by the dotted line as opposed to pure solvent that is represented by the solid line. The presence of solute reduces the vapour pressure and the triple point of the solution resulting in a lower freezing point than that of a pure solvent. Adapted from Reger, Goode and Ball (2009)

The formation of ice nuclei within the solution leads to the growth of ice crystals that spreads throughout the solution and will continue to grow until an equilibrium state is achieved within the system (Sun, 2005; Degner *et al.*, 2014). As the water phase crystallizes, the solute will be forced into the still-liquid region of the aqueous phase and away from the solid-liquid border. This leads to frozen-concentration whereby the accumulation of solute in the still-liquid region increases the solute concentration of this region. As the presence of solutes causes a decrease in the freezing point of the solution, a gradual decrease in melting point occurred in this region as water crystallizes resulting in a region with crystallizing water and another region containing highly concentrated non-frozen solutes. This process may cause changes in the original physicochemical characteristics of the solution such as changes in pH value, ionic strength, osmotic pressure as well as viscosity which will later affect the stability and quality of the product after the thawing process (Degner *et al.*, 2014).

Another important factor that may affect emulsion stability is the freezing rate of the samples as this determines the number and size of the ice crystals. At a high cooling rate, the

formation of ice nuclei is much faster compared to crystal growth leading to the formation of smaller ice crystals as opposed to lower cooling rate as the slow formation of ice nuclei resulted in the formation of a few but large ice crystals. This process also depended on the presence of additives as it promotes the formation of ice nuclei. The freezing process will then continue until the crystallization of the freeze-able water is completed (Sun, 2005). However, temperature fluctuations that occur during storage may cause recrystallization process that affects stability (Walstra, 2002; Degner *et al.*, 2014). This process resulted in the formation of larger ice crystals that will be detrimental to the quality of the encapsulated material especially bacteria as the large ice crystals puncture the cell membrane leading to cell damage (Gao, Smith and Li, 2007). Therefore, it is recommended to keep the product such as food emulsions at/below -18°C to prevent the occurrence of recrystallization (Erickson and Hung, 1997).

2.7.2 Emulsion destabilization in cold storage and its applications

The storage of emulsions under cold temperature caused changes in the phase behaviour of the oil and aqueous phase which affects the overall stability of the emulsions as the oil and aqueous phase gradually crystallizes depending on their freezing point (Vanapalli, Palanuwech and Coupland, 2002; Cramp *et al.*, 2004; Ghosh and Rousseau, 2009; Tippetts and Martini, 2009). According to Degner *et al.* (2013), several destabilization conditions were observed after the freeze-thawing of O/W emulsions such as oiling off or phase separation due to the presence of a free oil layer and the creaming process as the oil droplet was concentrated at the top layer of the emulsion. In addition, the presence of oil droplet with a larger size as compared to before the freeze-thawing process was also observed due to coalescence along with partial coalescence due to partial crystallization process that links neighbouring droplet. Droplet flocculation also occurs as the droplet were closely associated forming clusters while the aggregation of droplet leads to gelation or thickening as the freezing process caused an increase in viscosity.

It has been reported that the stability of water-in-oil emulsions (W/O) during freezing is based on the freezing sequence of the oil and the aqueous phase (Ghosh and Rousseau, 2009). The crystallization of the continuous oil phase prior to the dispersed aqueous phase caused an extensive emulsion destabilization as compared to continuous phase that crystallizes at a much lower temperature than the dispersed phase. This is due to the freeze-concentration process as the liquid droplet was forced into the still-liquid region of the continuous oil phase as it crystallizes. This leads to droplet clustering that accelerates emulsion destabilization. Similar effects have also been reported by Cramp *et al.* (2004) in samples of O/W emulsions whereby the crystallization of the continuous aqueous phase freeze-concentrated the oil-droplet into the still-liquid region of the continuous phase causing the water layer that separates neighbouring droplet to be withdrawn from the region as it crystallizes leading to droplet ruptures and eventually emulsion destabilization.

The freeze-concentration process is then followed by partial coalescence that occurs as the freezing process continues with the crystallization of the dispersed droplet. Partial coalescence takes place due to gradual crystallization of the droplet whereby crystallized droplet with protruding crystals puncture the membrane of the neighbouring still-liquid droplet causing the liquid to flow out forming a linkage between the two droplet as it freezes. This resulted in droplet flocculation that eventually leads to complete coalescence and phase separation upon thawing (Vanapalli, Palanuwech and Coupland, 2002; Lin *et al.*, 2007; Ghosh and Rousseau, 2009). A similar effect was also observed in a loosely packed emulsion sample in which the collision between the still-liquid oil droplet and crystallized oil droplet with protruding crystals may cause membrane rupture that resulted in the droplet with still-liquid oil to flow out and linked the two droplets as they freeze. This mechanism also leads to droplet

flocculation that eventually leads to complete coalescence during the thawing process (Lin *et al.*, 2007).

Several factors that affect the stability of emulsions against partial coalescence are size, droplet concentration and the nature of the fat components in the oil phase during crystallization. In addition, the type and concentration of the surfactants that determine the nature of the interfacial layer and the application of mechanical forces also affect the rate of partial coalescence (Walstra, 2002). Emulsions containing large-sized and high concentration of dispersed droplet are more prone to destabilization while the application of mechanical force accelerates the rate of partial coalescence as it increases the rate of droplet collision. Increasing the thickness of the interfacial layer or by using solid-state surfactants such as glycerol monostearate (GMS) that crystallizes at 25°C may help in improving emulsion stability. Ghosh and Rousseau (2009) reported that the use of liquid-state surfactant such as PGPR accelerates droplet destabilization as it can be easily drawn out from the emulsion especially during freeze-concentration and weakens the droplet barrier against coalescence. The use of crystallized surfactants such as glycerol monostearate (GMS) that crystallizes at 25°C help in minimizing emulsion destabilization as it creates a barrier against droplet coalescence during the thawing process (Ghosh and Rousseau, 2009). Zhu *et al.* (2017) also reported that the Pickering stearic stabilization along with the formation of a gel-like network due to the presence of soy and whey protein particles helps in preventing coalescence and creaming during the freeze-thaw process. Moreover, freezing the emulsion at a high cooling rate also helps in preventing partial coalescence as the rapid cooling minimizes the time of contact between crystallized and liquid droplet (Walstra, 2002; Degner *et al.*, 2014).

The freezing of multiple emulsion such as $W_1/O/W_2$ from ambient temperature to freezing temperature begins heterogeneously with the crystallization of the outer aqueous phase

whereby the presence of impurities for example surfactants trigger the formation of ice crystals. The formation of an ice germ on these impurities leads to the crystallization of the whole aqueous phase while the crystallization of the inner W_1 droplet occurred homogeneously as the possibility of these small droplets to contain impurities are small (Schuch, Köhler and Schuchmann, 2013). However, by using the $W_1/O/W_2$ as a means for encapsulation, the presence of materials such as bacteria in the W1 inner phase may induce heterogeneous nucleation. During the freezing process, the inner W1 aqueous phase remains intact as reported previously by Rojas and Papadopoulos (2007). The destabilization mechanism for multiple emulsions namely water-in-oil-in-water ($W_1/O/W_2$) emulsions in low-temperature storage mainly occurred during the thawing process due to the external coalescence of the inner W_1 phase with the outer W_1 phase. Several factors that affect the susceptibility of multiple emulsions towards external coalescence are the size of the inner W_1 phase and the thickness of the surfactant layer that helps in creating a boundary between the W_1 inner phase and the outer W_2 phase (Rojas and Papadopoulos, 2007; Rojas *et al.*, 2008). The intact W_1 phase during the freezing phase and the immediate droplet destabilization during the thawing process makes it suitable for the encapsulation and controlled release of material from the $W_1/O/W_2$ droplet.

The destabilization of food emulsions is undesirable as it can negatively affect product quality. Nevertheless, emulsion destabilization is highly beneficial for other applications such as during the Emulsion Liquid Membrane processing (ELM) and also for the processing of unwanted emulsions such as oil sludge (He and Chen, 2002; Lin *et al.*, 2007, 2008). These processes require an effective technique of emulsion destabilization in order to obtain a high percentage of demulsification. Some of the conventional techniques used for emulsion demulsification are chemical treatment, thermal, electrical and mechanical techniques. There were several setbacks encountered when using these conventional methods such as the need for

using high voltage electricity for electrical treatment (Lin *et al.*, 2007). The freeze-thaw process has been reported as an alternative method to oil refinery whereby 90% of emulsion demulsification was achieved by using freeze-thaw treatment to demulsify used lubricating oil which consists of complex emulsions that were hard to break under conventional demulsification processes (He and Chen, 2002). Other than for oil processing applications, the freeze-thaw induced destabilization of $W_1/O/W_2$ emulsions has also been applied for the controlled and immediate release of materials from double emulsion droplet (Rojas and Papadopoulos, 2007; Rojas *et al.*, 2008; Jaimes-Lizcano, Lawson and Papadopoulos, 2011). Rojas *et al.* (2008) reported on the application of freeze-thaw induced controlled release of protein from emulsions. FITC-BSA was used as a model protein and was encapsulated in $W_1/O/W_2$ and the droplet was kept in cold temperature that freezes the oil phase while the aqueous phase remains liquid. While the inner W_1 phase remains intact during storage under freezing temperatures, the thawing process of the emulsions leads to the complete and immediate release of the encapsulated proteins as the oil melted (Rojas *et al.*, 2008). Further studies on the application of this system for the development of dermal macromolecular delivery formulations revealed its potential to be used in cutaneous vaccine delivery system whereby the *in vitro* study conducted on porcine skins shows up to 86 μm penetration when using the emulsions for encapsulation (Jaimes-Lizcano, Lawson and Papadopoulos, 2011). Those studies show an interesting application of the freeze-thaw process for the controlled release of materials in which will be further explored in chapter five of this thesis by using live bacterial cells as the encapsulated material.

2.8 Bacteria in cold storage

2.8.1 Bacteria viability and survival in cold temperature

Bacterial survival in cold temperature storage especially during freezing varies between species and depends on the conditions during storage. Different strains exhibited different resistance against freezing, for example, *Streptococci* showed better resistance compared to *Lactobacilli* (Tsvetkov and Shishkova, 1982; Fonseca, Béal and Corrieu, 2000) and mainly due to cell size and structure as larger cells with more complex structure survived less than smaller cells (Bozoğlu, Özilgen and Bakir, 1987). In general, Gram-positive bacteria are more susceptible to freezing conditions as compared to Gram-negative bacteria (Georgala and Hunt, 1963). In a previous study by Lowry and Gill (1985), the enrichment of the Gram-positive spoilage strains such as lactobacilli and *Brochothrix thermosphacta* were observed during the slow-freezing process of meat at the expense of the Gram-negative bacteria that were usually predominant in the air-stored meat. Besides that, the medium used during storage may also affect bacterial survival against freezing. For lactic acid bacteria, it has been reported that the addition of Tween 80 allows for better survival. The addition of Tween 80 increases the ratio of unsaturated fatty acids in the cell's membrane that changes the permeability of the membrane. Other than that, the addition of calcium in the growth medium also maintains the stability of *Lactobacillus delbrueckii* subsp. *bulgaricus* during freezing (Wright and Klaenhammer, 1981, 1983).

The freezing of microorganisms also leads to water removal from cells (intracellular freezing) or its surrounding (extracellular freezing) as the formation of ice crystals reduces the percentage of free water. The cell's resistance to freezing damage depends on the membrane ability to withstand freezing stress as it has been identified as the primary site of ice crystals formation (Souzu, 1989). The membrane layer of a Gram-negative bacteria consists of the cytoplasmic membrane, peptidoglycan layer and the outer membrane. The outer membrane is

known to be water permeable which allows for the transport of nutrients across the membrane while the cytoplasmic membrane is known to be less permeable to water (Osborn *et al.*, 1972; Nakae, 1976). The freeze-induced structural change in the cell membrane is mainly attributed to the change in phospholipid conformation of the outer membrane. During the freezing process of *Escherichia coli* B cells, significant alterations in the membrane caused a significant change in the membrane permeability that eventually leads to cell damage. This process is dependent on the freezing rate whereby slow freezing leads to extensive cell damage that lowers the bacterial viability as compared to rapid freezing in which the cells suffers a much smaller amount of cells impairment and is able to maintain high cells viability (Souzu, 1989).

Moreover, the freezing process of *Escherichia coli* cells also caused the cell membrane component to be liberated such as phospholipids and proteins. Lower cell viability was observed with the higher release of membrane component which can be observed at a slow freezing rate. During a slow freezing process, the component released from the cell is mainly from the outer cell membrane whereas rapid freezing leads to the release of both cytoplasmic and outer cell membrane constituents. The released fragments exhibit different chemical composition as compared to its original state (Souzu, 1980). In slow freezing, the phase separation of the lipid bilayer leads to increased fragmentation of the outer membrane whereas, with rapid freezing, the phase separation effect was minimized as the cells were only exposed to the transition temperature in a short period of time (Souzu, 1980). The short exposure time to transition temperature with rapid freezing resulted in lipid freezing without allowing much time for the rearrangement of the intramembrane protein leading to less damaging effect in the cell membrane. Moreover, rapid freezing also decreases the rate of cell shrinkage resulting in less separation of the membrane (Souzu, 1980).

Other than the structural change of the cell membrane, the effect of water crystallization is also one of the most common factors responsible in cell damage (Mazur, 2017; Powell-Palm *et al.*, 2018). As opposed to changes in the membrane structure that was minimized at the high freezing rate, the detrimental effect of water-crystallization on bacterial viability is minimized at the low-freezing rate as compared to high-freezing rate. This is due to the cryoconcentration effect that helps in preventing the lethal intracellular water crystallization as the intracellular water was drawn out of the cells during the freezing process. During slow-freezing, the water crystallization process will most likely begin with extracellular crystallization of the surrounding liquid. The gradual crystallization of the extracellular water forces the cells to be concentrated in the unfrozen region of the medium whereby a continuous decrease in temperature caused the region to be increasingly concentrated. This leads to cell dehydration as the cells were exposed to high concentrated solution creating a concentration gradient that draws water out from the cell during the freezing process thus preventing the formation of intracellular ice crystals. Meanwhile, the rapid freezing of bacterial suspension resulted in extensive supercooling that caused the crystallization of the intracellular water as it is not able to flow out of the cells fast enough resulting in extensive cell damage (Simonin *et al.*, 2015). These indicate that the degree of cell damage during the freezing process also depended on the availability of intra- and extracellular water in which it can be controlled by changing the freezing rate of the samples.

In conclusion, the storage of bacteria in freezing temperatures can lead to irreversible cell damage. Therefore, the development of cryoprotectant formulations such as the combination of glycerol as a cryoprotectant together with cell encapsulation may help in protecting the cells against freeze-damage. This will be discussed in detail in the next section

along with an experiment designed in order to determine the effect of cell encapsulation in emulsion droplet on the viability of bacteria (chapter five).

2.8.2 The effect of encapsulation on bacterial survival in freezing temperature

Several cryoprotective formulations have been developed that can best protect bacteria against freeze-damage (Chen *et al.*, 2015; Wang *et al.*, 2019). One of the most commonly used cryoprotectants is glycerol in which it helps in promoting supercooling by depressing the freezing point of bacterial cells. Glycerol forms strong hydrogen bonds with water molecules, thus reducing hydrogen bonding between water molecules leading to the disruption of the ice crystal lattice formation (Pegg, 2007). Besides that, it has been reported that the mixture of trehalose, sucrose, glycerol and skimmed milk significantly improves the viability of lactobacilli during the freezing process (Wang *et al.*, 2019). Moreover, the mixture of skim milk, lactose and sodium ascorbate was shown to significantly improve the number of viable cells after the freeze-thaw process (Chen *et al.*, 2015). Other than the development of suitable formulations of cryoprotectants, the pre-freezing treatment of bacterial cells may also aid in improving their viability. In a study by Simonin *et al.* (2015), osmotic treatments on *E. coli* cells during freezing at -20 °C that mimics the cryoconcentration effect helps in minimizing cell damage. Moreover, cells that were exposed to cold stress also shows an increased resistance towards freeze-damage.

In addition, the effect of encapsulation in improving bacterial viability during the freeze-thaw process has been reported extensively in previous studies (Goderska and Czarnecki, 2008; Priya, Vijayalakshmi and Raichur, 2011; Dianawati, Mishra and Shah, 2013). Some examples of the application of microencapsulation for protecting bacteria against freeze-damage include the encapsulation of *Lactobacillus acidophilus* in the self-assembled polyelectrolyte layers of

chitosan and carboxymethyl cellulose that not only provide a protection barrier for bacteria against the adverse effect of simulated GI tract but also against cell-damage during the freeze and freeze-drying processes (Priya, Vijayalakshmi and Raichur, 2011). Similar protective effects were also observed from the microencapsulation of *Bifidobacterium longum* in milk proteins and sugar alcohols whereby it works in enhancing the protective effect of cryoprotectants such as glycerol, resulting in better bacterial viability and function after the freeze and freeze-drying processes (Dianawati, Mishra and Shah, 2013). The freezing of an emulsion-based product such as milk has also been reported to cause small changes in the viability of bacteria, indicating the ability of the emulsion structure in protecting bacteria against extensive cell damage. A study by Sánchez *et al.* (2003) shows that the freezing of goat milk at -20°C or even after extended storage at -80°C does not significantly affect the viability of *E. coli* as opposed to cow milk due to differences in milk composition. A similar result was also reported by Nurliyani, Suranindyah and Pretiwi (2015) whereby the frozen storage of Ettawah Crossed bred goats milk sample for 60 days does not cause changes in the total bacteria while changes in emulsion stability were only observed after 30 days of storage.

2.9 Aim and objectives

The research conducted in this thesis is focused on determining the interaction between encapsulated bacteria and emulsion droplet of W/O and $W_1/O/W_2$ in ambient and cold temperature storage with the application of droplet microfluidics. The objectives of this work are listed as follows:

i. To determine the effect of different bacterial responses (growth and death) on the stability of W/O droplet.
ii. To investigate the effect of bacterial encapsulation in W/O and $W_1/O/W_2$ droplet on bacterial viability in ambient and cold temperature storage.
iii. To study the stability of single W/O and double $W_1/O/W_2$ droplet in the presence of bacteria during cold temperature storage.
iv. To study the effect of osmotic balance alterations and cold temperature storage on the release of bacteria from the $W_1/O/W_2$ droplet.

Chapter 3

The effect of bacteria on the stability of microfluidic-generated water-in-oil droplet

3.1 Introduction

Microencapsulation of emulsion droplet, as discussed in section 2.4, has been extensively used in the encapsulation of bacteria for various applications such as to increase their viability in food products, to protect bacteria against the harsh conditions in gastrointestinal tract and for high-throughput bacterial studies (Lalou *et al*. 2017; Klojdová *et al*. 2019; Shima *et al*. 2006; Pimentel-Gonzalez *et al*. 2009; Marcoux *et al.* 2011). Nevertheless, the successful applications of emulsions droplet for bacterial encapsulation is highly depended on their stability during processing, storage and during consumption. Understanding the effects of the encapsulated bacteria on emulsion stability is still limited and therefore requires further studies on bacterial response such as growth, death and production of by-products and their effect on stability.

Previous studies revealed the potential use of bacteria for emulsion stabilization as discussed in section 2.5 where bacterial surface properties played a key role in stabilization (Dorobantu *et al.*, 2004; Wongkongkatep *et al.*, 2012; Firoozmand and Rousseau, 2016). However, the mechanism of droplet stability with the aid of bacterial cells is highly complex thus, further studies may provide beneficial information in order to clearly understand the factors involved in this process.

Therefore, this chapter aimed to investigate the interrelationship between bacterial response and emulsion stability with microfluidics application. The stability of model emulsion systems in the presence of *Escherichia coli (E. coli*-GFP*),* the most common Gram-negative bacteria used in biotechnology applications such as *in vitro* synthesis of biomolecules (Idalia and Bernardo, 2017) and *Lactobacillus paracasei (L. paracasei*) which is one of the most common Gram-positive bacteria used in the food industry for making dairy products such as yoghurt, were investigated during storage. The viability of the bacteria and its effect on droplet stability was investigated by measuring changes in droplet distribution during storage and by characterising factors that affect stability through bacterial hydrophobicity and zeta potential test. The developed model emulsion system and the study of bacterial interactions may help to give more insights on the stability of such systems that can later be applied in the industrial production of emulsion-based products.

3.2 Materials and methods

3.2.1 Materials and bacterial cultures

Microfluidic device fabrication was done by using a Polydimethylsiloxane (PDMS) preparation set (Sylgard 184, Dow-corning, United States) which includes the curing agent and pre-polymer. Oil-soluble surfactant, polyglycerol polyricinoleate (PGPR) was obtained from Danisco (Denmark) while mineral oil and acridine orange stain (AO) were purchased from Sigma Aldrich (United Kingdom). For bacterial culture preparation, the materials used were nutrient agar, De Man, Rogosa and Sharpe (MRS) agar and broth, Luria Bertani broth (LB broth) and phosphate buffer saline (PBS) all by Oxoid Ltd. (United Kingdom). Propidium iodide stain (PI) was purchased from Invitrogen (United Kingdom). *Escherichia coli* strain SCC1 (MG1655-GFP mutation) expressing green fluorescent protein (*E. coli*-GFP) and *Lactobacillus paracasei* subsp. *paracasei* DC412 (*L. paracasei*) stock cultures were obtained from Biochemical Engineering Laboratory, University of Birmingham, United Kingdom.

3.2.2 Microfluidic device fabrication

The microfluidic device was produced using a standard soft lithography technique (Kim *et al.*, 2008). The device was designed according to Bauer *et al*. (2010) using AutoCAD 2016 (Autodesk) software. A device with 100 µm width at the junction, 200 µm width at the exit channel and 50 µm (depth) dimension was used for producing water-in-oil (W/O) droplet with diameters between 40-50 µm (Figure 3.1a). The design was then printed onto high-resolution photo-masks. A patterned mould was produced by exposing a silicon wafer (Si-Mat, Germany) that was spin-coated with SU-8 photoresist (SU-8, Microchem) to UV light through the photomasks (Figure 3.1b). The device was then prepared by mixing the PDMS and curing agent at the recommended mixing ratio of 1:10. The prepared PDMS was then poured onto the mould, degassed and baked in the oven at 70°C for 1 hour. The device was then cut out of the mould

and the inlet and outlet holes were punched followed by corona discharge treatment for approximately 30s that bonds the device onto a glass slide to close the channels. The prepared device was then left on the hot plate for approximately 15 mins at 100°C. A new device was prepared for every experiment in order to minimize contamination.

a

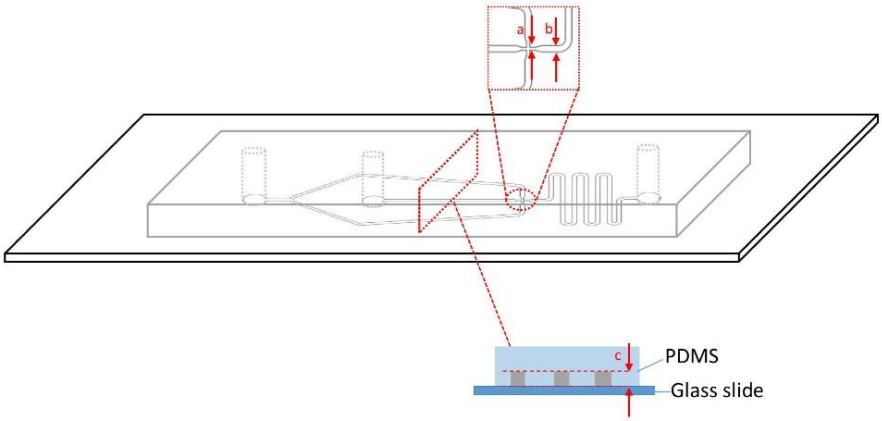

b

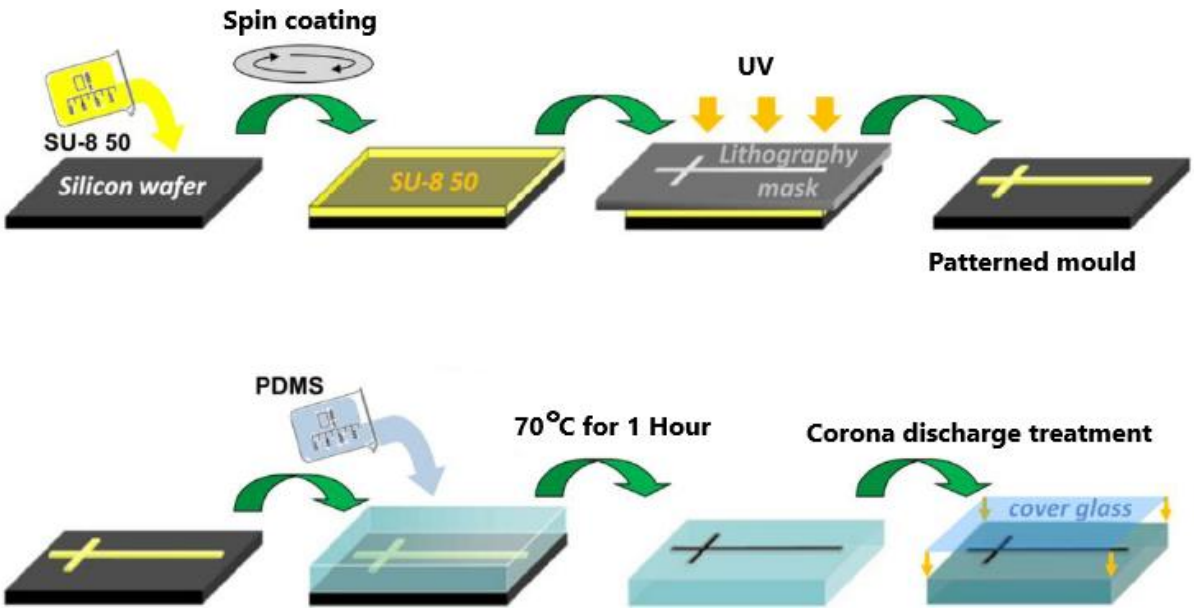

Figure 3.1 Flow-focusing microfluidic device fabrication for W/O droplet generation with (a) the dimension of the device whereby, width at the junction (a): 100 µm, width at the exit channel (b): 200 µm and depth (c): 50 µm. The design of the device was printed on a high resolution mask and a patterned mould was produced by spin-coating SU-8 photoresist on a silicon wafer and exposing it to UV light through the photomask (b). The patterned mould was then used to prepare microfluidic devices by using PDMS.

3.2.3 Optical microscopy for determining the effect of flow rates on droplet size and stability changes during storage

The effect of different dispersed to continuous phase flow rate ratios (Q_d:Q_c) on the production of monodispersed W/O droplet was determined by measuring the size of the droplet immediately after formation. In addition, droplet size was also measured daily for all W/O emulsion samples during the five days of storage at 25°C. Droplets were formed by pumping the continuous oil phase (mineral oil with 1.5% PGPR) through inlet a and the dispersed aqueous phase (sterilised deionised water [DIW]) through inlet b of the flow-focusing microfluidic device (Figure 3.2). The W/O droplets were produced at the flow-focusing junction and collected in an Eppendorf tube at outlet c (Figure 3.2). The solutions were pumped into the microfluidic device by using syringe pumps (AL-1000, World Precision Instruments, United States) at varying flow rate ratios (Q_d:Q_c) of 1:1, 1:2, 1:4, 1:6, 1:8 and 1:10.

Droplet formation in the microfluidic device was observed at 10x magnification by using a Nikon Eclipse Ti-U microscope equipped with Photron FASTCAM SA3 high-speed camera software. In order to measure the size of the droplet, optical microscopy was done by placing the W/O sample on a glass slide and observed at 10× magnification by using the same microscope. Images of the droplet were taken and analysed by using MATLAB software for size measurement using the circular Hough transform. For characterisation of droplet size distribution, changes in the coefficient of variation (CV) was determined by dividing the standard deviation with the mean droplet size (Romoscanu *et al.*, 2010; Maan, Schroën and Boom, 2013; Muijlwijk, Berton-Carabin and Schroën, 2016).

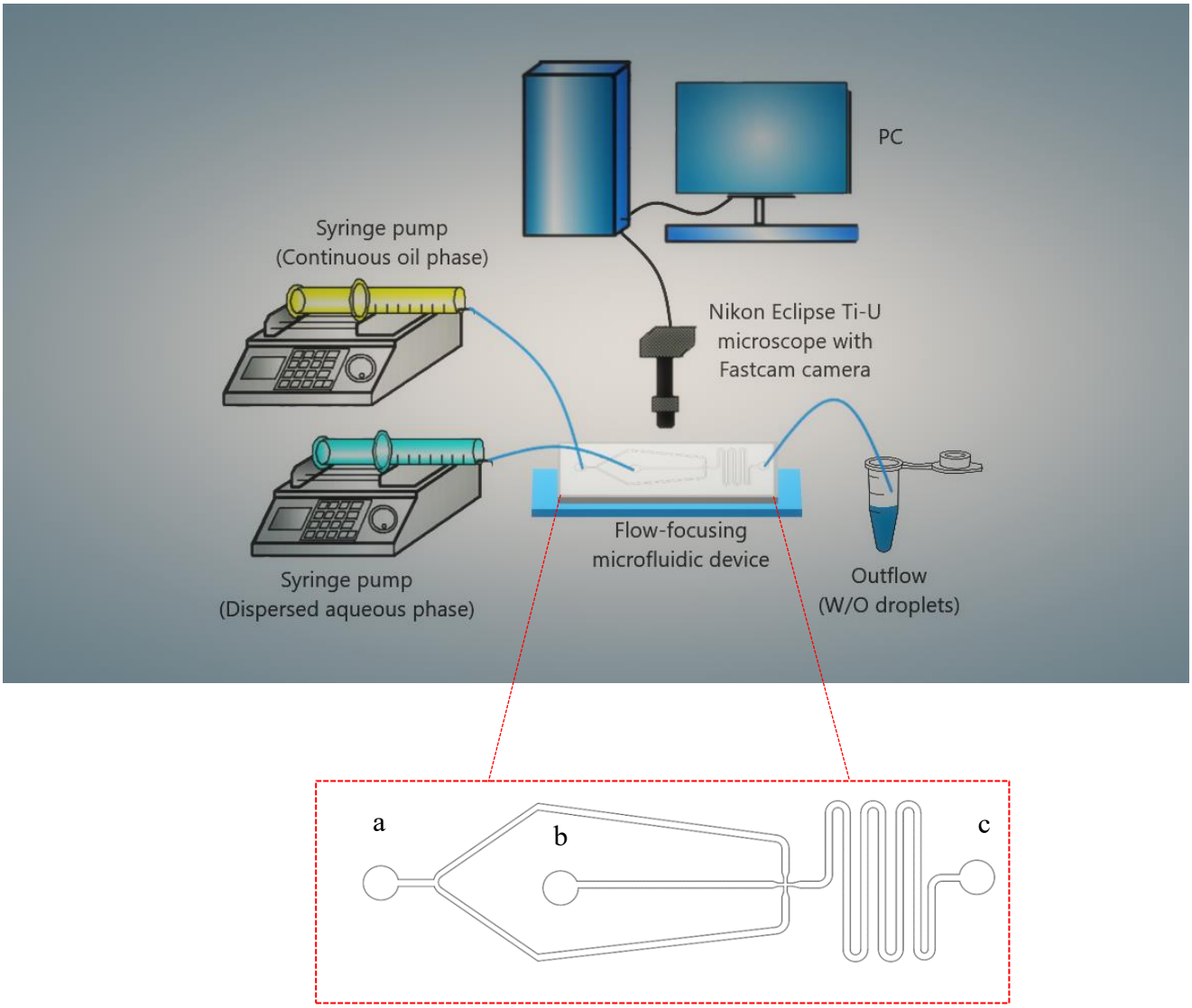

Figure 3.2 The formation of W/O droplet by using a flow-focusing microfluidic device. The continuous oil phase was pumped through inlet a while the dispersed aqueous phase was pumped through inlet b by using syringe pumps at varying flow rate ratios. The W/O droplet were formed at the flow-focusing junction and the sample was then collected in an Eppendorf tube at outlet c. Droplet formation was observed by using Nikon Eclipse Ti-U microscope equipped with Fastcam SA3 camera. Images of the droplet were taken and analysed for size measurement by using MATLAB software.

3.2.4 Bacterial cells preparation

Bacterial cultures for encapsulation in W/O emulsion were prepared by culturing *E. coli*-GFP on nutrient agar at 37 °C for 24 hours. The cultured bacteria were kept at 4°C prior to the experiment. The bacterial cells were then inoculated into 50 mL of Luria Bertani broth (LB Broth) in a shaking incubator at 37°C, 150 rpm for 24 hours and sub-cultured into LB broth (1:50) and incubated for another 2 hours. The bacterial culture was then centrifuged (10000 × g, 10 mins) and washed two times with 50 mL of PBS. After centrifugation, the supernatant was discarded and was replaced with 50 mL of fresh LB broth or DIW to re-suspend bacterial cells for encapsulation. The bacterial cell concentration was prepared to 10^8 CFU/mL. *L. paracasei* bacteria culture was maintained on MRS agar at 4°C. The bacterial cells were inoculated into 50 mL of MRS broth and incubated for 48 hours at 25°C, sub-cultured into 50 mL of fresh MRS broth and incubated for another 12 hours. Approximately 10^8 CFU/mL of *L. paracasei* cells were obtained by centrifuging 50 mL of cell suspension at 10000 × g for 10 minutes. The cells were washed twice with PBS and re-suspended into 50 mL of MRS broth or sterilised deionized water for encapsulation into W/O droplet.

Samples of dead cells were prepared for determining the characteristics of both live and dead cells by suspending bacterial cultures of 10^8 CFU/mL in DIW and heat-treated at 80°C for 30 minutes using an Eppendorf thermomixer. 80°C is the temperature used in pasteurization that resulted in the total reduction of viability for many bacterial strains including *E. coli* and *Lactobacillus* strains (Petruzzi *et al*. 2017). The heat-treatment of cells may result in dead cells and viable-but-not-culturable (VBNC) cells that were extensively injured to the point where they were unable to grow on nutrient agar (for *E. coli*-GFP) and MRS agar (for *L. paracasei*). In this study, the viability of bacteria was determined based on membrane integrity thus, a

bacterial cell with the inability to grow on agar plates together with positive staining of PI was termed as dead or thermally-inactivated.

3.2.5 Bacteria encapsulation in single Water-in-oil emulsion

E. coli-GFP in LB broth and *L. paracasei* in MRS broth were then used as the aqueous phase of the W/O droplet with 10^8 CFU/mL of cell concentration. The continuous oil phase consisted of mineral oil with 1.5% w/v PGPR surfactant. The bacterial encapsulation was conducted by using a flow-focusing microfluidic device as described in section 3.2.3. The suitable flow rates used for droplet production were determined from the experiment described in section 3.2.3 whereby the chosen flow rates were, 3 µl/min for the dispersed aqueous phase containing bacteria and 30 µl/min for the continuous oil phase, forming a droplet of approximately 40-50 µm in diameter. The average cell number per droplet was not determined in this study due to the high density of cell used (10^8 CFU/mL). According to Lu *et al*. (2017), the high density of cells leads to a lack of precision in cell counting per droplet due to high droplet occupancy. This is due to the high possibility of cells overlapping that affected the accuracy of the cell count. W/O droplet with *E. coli*-GFP or *L. paracasei* in DIW as the inner aqueous phase were used as non-nutrient controls. In addition, the empty droplet of LB broth, MRS broth and DIW were also produced as controls to determine the effects of bacteria on droplet stability. All samples were kept statically in Eppendorf tubes at 25 °C for five days.

3.2.6 Determination of bacterial viability

Viability was determined for bacteria encapsulated in W/O droplet with or without nutrient. Unencapsulated bacteria dispersed in sterilised DIW or LB broth (for *E. coli*-GFP) and MRS broth (for *L. paracasei*) were prepared as controls. Encapsulated samples were centrifuged at 15 800 × g for 10 min in order to break the emulsion and release the entrapped cells. Viable cells were counted daily for both encapsulated and unencapsulated samples during the five days

of storage using the Miles and Misra method (Miles and Misra, 1931). Serial dilutions were done on the sample with PBS. For *E. coli*-GFP 10 µL of diluted sample was pipetted onto nutrient agar and incubated at 37°C for 24 hours while for *L. paracasei*, samples were pipetted onto MRS agar and incubated at 25°C for 48 hours. The detection limit for both *E. coli*-GFP and *L. paracasei* was 10^3 CFU/mL.

3.2.7 Fluorescence microscopy for bacterial response observation

Fluorescence microscopy was conducted in order to distinguish the viability of the encapsulated bacteria in W/O emulsion droplet. Dead cell observation was done by staining *E. coli*-GFP and *L. paracasei* with PI. Additionally, *L. paracasei* was stained with AO for viable cell observation. It has been reported that the use of PI stain with GFP provides a better distinction of *E. coli* viability as compared to SYTO9-PI dual staining (Lehtinen, Nuutila and Lilius, 2004). GFP produces a green signal indicating viable *E. coli* cell whereas PI produces a red signal that indicates dead cell as the stain is only able to bind with the DNA of the damaged cell. As the viability of bacteria in this study were classified based on membrane integrity, the use of GFP with PI stain is suitable for the determination of *E. coli* cell viability. Besides that, the use of AO with PI for determining the viability of *L. paracasei* is suitable for this study as they possess different exciting and emission wavelengths that aid in distinguishing between live and dead cells. The AO can easily traverse the cell membrane of a viable cell to bind with the DNA producing green signal whereas PI can only bind with the DNA of damaged cells producing a red signal. However, in order to distinguish between the live *E. coli*-GFP cell from the live AO stained *L. paracasei* cell, the AO stained cell was coloured as yellow in this study. The AO/PI stain has been used effectively for determining cell viability in a study done by Hussein *et al.* (2019).

The samples were prepared for microscopy by placing 1 drop of sample onto a glass slide and covering it with a coverslip. The samples were then observed at 100× magnification with immersion oil and micrographs of the samples were acquired using the Axiocam ICm1 digital camera system of 1.4-megapixel camera and Axiovision software (Zeiss). The emission was observed at 509 nm (GFP), 502 nm (AO) and 645nm (PI) using a mercury arc lamp. The micrographs obtained was overlaid and image analysis was done using ImageJ to determine the size of bacterial clustering with respect to droplet size.

3.2.8 Observation of bacterial clustering with confocal microscopy

In order to clearly observe the clustering of bacteria in the W/O droplet, images of *E. coli*-GFP clustering in the droplet containing LB Broth were taken using Leica TCS SPE confocal scanning microscope at 100× oil magnification. GFP excitation was observed at 509 nm. Images were taken at 3 µm intervals over a 30-60 µm of sample depth. The images were reconstructed to produce z-projections and 3D images of the samples to provide clear observation of the overall structure of bacterial clustering in the W/O droplet.

3.2.9 Bacterial hydrophobicity test

Bacterial hydrophobicity was tested in order to determine the difference in hydrophobicity between live and dead cells of *E. coli*-GFP and *L. paracasei*. The assay was conducted according to Rosenberg *et al*. (1980). Washed bacterial cells (1.2 mL of live or dead) in sterilised DIW were added into four round bottom test tubes and the initial absorbance (before treatment with oil phase) was measured at 600 nm. Different volumes of mineral oil (0.2, 0.15, 0.1, 0.05 mL) were then added into the test tubes. After 10 minutes of incubation at room temperature, the samples were mixed by vortexing the test tubes for 2 minutes. After mixing, the samples were left upright at room temperature to allow the separation of the oil and bacterial suspension. The aqueous phase was then carefully drawn out of the test tubes by using a pipette

and the absorbance of the aqueous phase was measured at 600 nm for the samples after being mixed with mineral oil. The percentage of absorbance was calculated for samples after treatment relative to samples before treatment with different volumes of mineral oil.

3.2.10 Interfacial tension determination between bacteria and mineral oil

The test was done in order to determine the affinity of *E. coli*-GFP and *L. paracasei* towards the mineral oil and to compare the difference between live and dead bacterial cells. The interfacial tension between bacterial suspension and mineral oil was measured by the pendant drop method using Attension Theta optical tensiometer and comparisons were made between live and dead bacterial cells suspended in sterilised deionised water (DIW) against mineral oil (with or without 1.5% PGPR). Different cell concentrations were prepared for both live and dead cells (OD_{600} values of 0.07, 0.4, 0.7, 2.3) with samples without bacteria as control. The samples were prepared by serial dilutions and the OD_{600} were measured by using a spectrophotometer (Jenway 6305, Bibby Scientific Ltd., United Kingdom) to determine the effect of different bacterial concentrations on interfacial tension. Samples containing a mixture of live and dead cells at different ratios (Live: Dead, 30:70, 50:50, 70:30) were also tested. A drop of the sample (11 μL) was introduced into the mineral oil and was left to stabilise for 3 minutes. Interfacial tension readings (mN/m) were then measured and the process was repeated for 3 droplet replicates.

3.2.11 Bacterial surface zeta potential determination

The zeta potential of bacterial suspension was measured for both live and dead cells of *E. coli*-GFP and *L. paracasei* in different suspension solutions in order to determine colloidal stability. Samples were prepared by suspending live or dead cells in different suspensions (LB broth for *E. coli*-GFP, MRS for *L. paracasei* or DIW). In addition, mixed samples containing both live and dead cells suspended in DIW with different ratios (L:D, 70:30, 50:50, 30:70) were also

prepared. Approximately 1 mL of diluted sample (OD_{600}= 0.34) was carefully loaded into folded capillary zeta cell (Figure 3.3) and the zeta potential was measured using dynamic light scattering zeta sizer nano by Malvern Instruments.

Figure 3.3 Folded capillary zeta cell used for zeta potential measurements. Adapted from Malvern Instruments Ltd. (2013).

3.2.12 Statistical analysis

The experiments were conducted with three replicates. For the experiment that determines the effect of variables on droplet diameter, a total of 900 droplets were measured for diameter (N=900). The generated data were analysed with Excel (Microsoft Corp.) in order to calculate the mean, standard deviation (SD), standard error of mean (SEM) and coefficient of variation (CV) values. Data on droplet size was presented with SD as it described the variability in the diameter of the droplet produced with the microfluidic method and also during storage. SD also gives an indication of the monodispersity of the droplet produced and changes during storage through the measurement of CV (standard deviation divided by mean). Other data such as bacterial viability were presented with SEM as it indicates the precision of the sample mean and the level of uncertainty around the sample mean by taking into account the sample size (Altman and Bland, 2005). Student's T-test was conducted in order to compare two means while one-way ANOVA with Tukey's HSD was conducted to compare several means by using IBM

SPSS statistical software version 21. The difference between the means was considered significant at $P < 0.05$.

3.3 Results and discussion

3.3.1 Generation of monodispersed water-in-oil droplet incorporated with bacteria

Droplet generation experiments were done in order to determine the ability of the flow-focusing microfluidic device to generate monodispersed droplet and their compatibility with bacteria. The effects of different flow rate ratios on droplet size were studied to determine the stable dripping regime in which droplet can be formed (Figure 3.4). The dimensions of the flow-focusing microfluidic device used for droplet generation was 100 µm (width at the junction), 200 µm (width at exit channel) 50 µm (height) as shown in Figure 3.5.

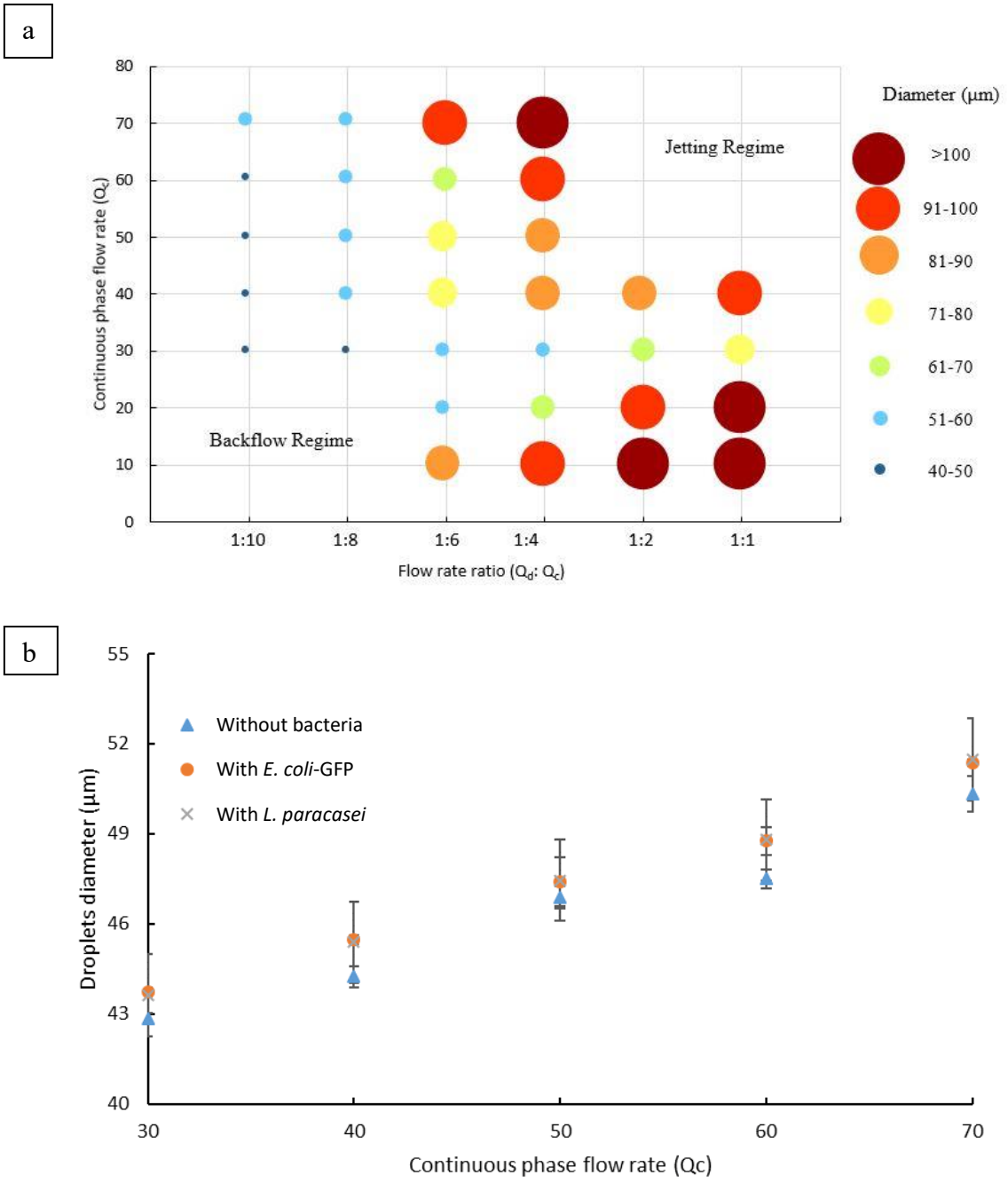

Figure 3.4 The average diameter of droplet generated with a flow-focusing microfluidic device with respect to (a) flow rate ratio, whereby an increase in the ratio of dispersed aqueous phase (Q_d) with respect to the continuous oil phase (Q_c) resulted in an increase in average droplet diameter. No droplet was formed at the backflow and jetting regime. The effect of bacteria on droplet formation (b) shows no significant difference in droplet diameter between the samples (P = 1.00). Bars represent mean ± SD taken from 3 independent experiments with N= 900. The data were analysed with one-way ANOVA at a significant level of $P < 0.05$.

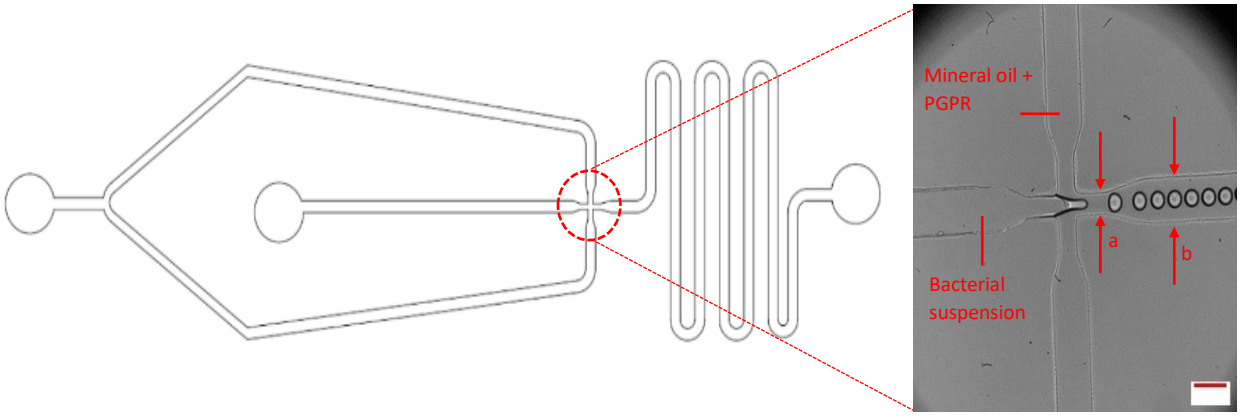

Figure 3.5 Monodispersed W/O droplet formation with a flow-focusing microfluidic device. W/O droplet was formed at the flow-focusing junction (in the circle). The widths of the channel were (a) 100 µm and (b) 200 µm. Scale bar represents 200 µm.

Figure 3.4 (a) shows the average diameter of W/O droplet generated with a flow-focusing device at different flow rate ratios of dispersed phase to the continuous phase (Q_d/Q_c). From the graph, it was determined that the size of the droplet formed depended on the flow rate ratio whereby droplet generated at a lower flow rate ratio had a smaller droplet diameter compared to droplet generated with a higher flow rate ratio. This is because, at a lower flow rate ratio, the difference in flow rate between the continuous phase and the dispersed phase was larger and therefore, the droplet broke easily at the junction producing smaller droplet. However, no droplet were formed at a continuous flow rate of 10 µL/min or 20 µL/min with flow rate ratios of 1:10 and 1:8 as the dispersed phase were not able to enter the junction (backflow) due to the large difference in flow rate between the dispersed and continuous phase (Christopher and Anna, 2007).

Increasing the flow rate ratio to 1:1 at a continuous flow rate of 10 µL/min or 20 µL/min caused the formation of droplet with larger diameter as the droplet was not able to break easily at the junction due to lower shear stress, causing the dispersed phase to be elongated at the junction before breaking. However, further increasing the continuous flow rate to 50 µL/min, 60 µL/min or 70 µL/min at a high flow rate ratio of 1:2 or 1:1 had caused zero formation of droplet as the system reached the unstable jetting regime. Monodispersed W/O droplet was formed at the stable dripping regime by tuning the continuous phase flow rate to 30 µL/min or 40 µL/min where droplet was generated at every flow rate ratios (Figure 3.4 b). Therefore, these flow rates were chosen in order to produce droplet incorporated with bacteria. The flow rate ratio of 1:10 with a continuous flow rate of 30 µl/min was chosen as it is able to produce droplets with 40-50 µm in diameter. In addition, the effects of bacteria on droplet generation was also determined as in Figure 3.4 (b). The droplet was formed at a flow rate ratio of 1:0 with different

continuous phase flow rate. From the graph, it was observed that no significant (P = 1.00) difference in droplet size was observed with the addition of bacteria.

3.3.2 The effect of bacteria on droplet stability

In order to understand the effects of bacteria on the stability of W/O emulsion, changes in droplet size were observed daily by optical microscopy and droplet diameter was measured by analysing photomicrographs using MATLAB software during five days of storage. The data obtained were plotted as in Figure 3.6 to determine changes in droplet size distribution during storage for samples of bacteria (*E. coli*-GFP *or L. paracasei*) encapsulated with nutrient (LB broth for *E. coli*-GFP and MRS for *L. paracasei*) or sterilised DIW to investigate the effect of bacterial growth on stability. In addition, the control samples of empty droplet with only nutrient (LB or MRS broth) or sterilised deionised water was also measured for changes in droplet size. The droplet size distribution was characterized by measuring the CV whereby a CV below 25% indicates monodispersed droplet while emulsions with CV above 25% are regarded as polydispersed (Romoscanu *et al.*, 2010).

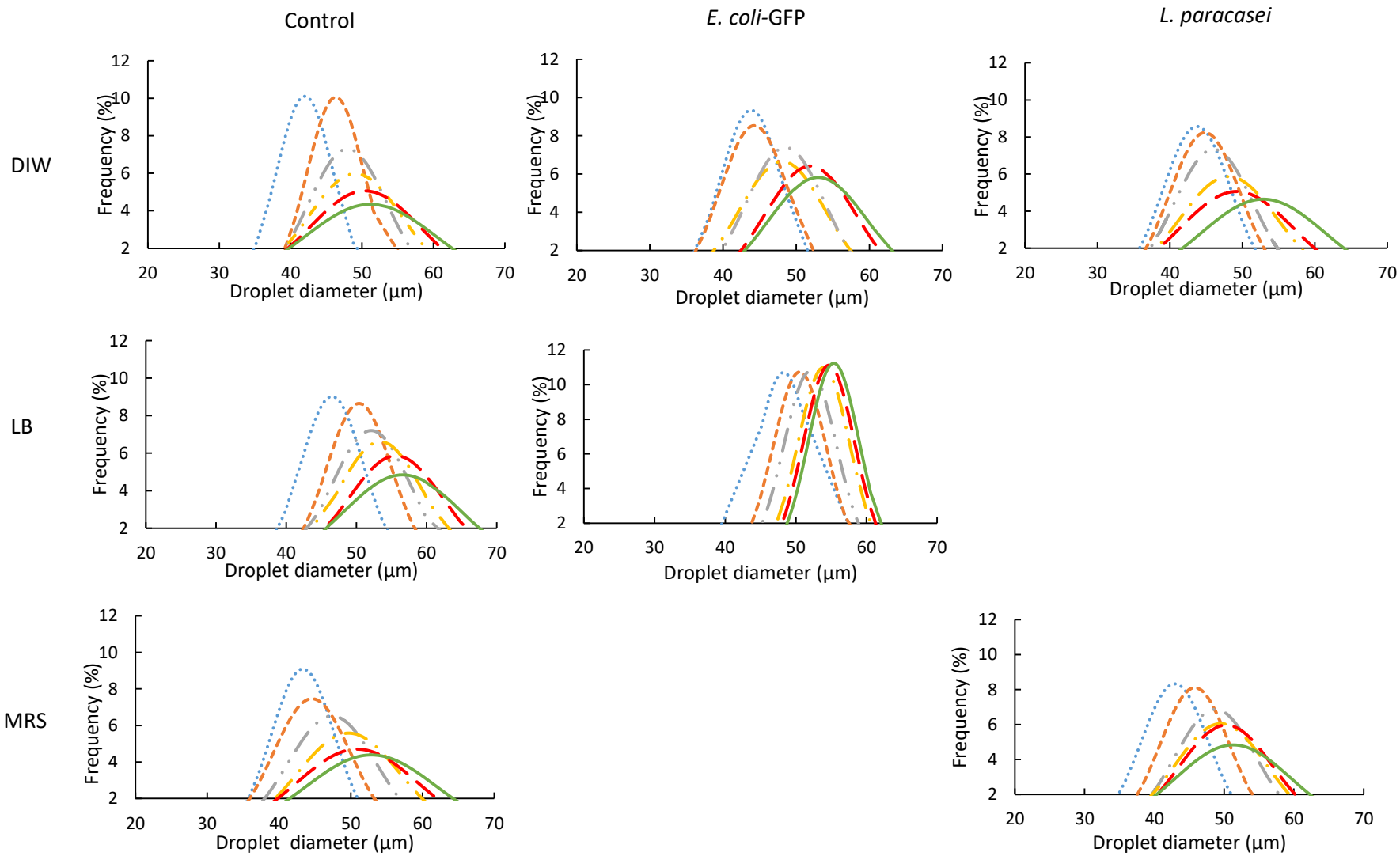

Figure 3.6 Droplet size distribution at Day 0 (⋯⋯), Day 1 (----), Day 2 (- ··), Day 3 (- · -), Day 4 (- - -), Day 5 (—). Frequency (%) refers to the percentage of droplet. Data was analysed with N=900 droplet.

Table 3.1 Summary of changes in droplet stability during five days of storage at 25°C. Data represent the mean ± standard deviation from 3 independent experiments with N=900 droplet. The average diameters were measured daily during five days of storage and the overall change in diameter (%) was measured based on the diameter at day 0 with respect to day 5. The CV values were measured by dividing the standard deviation with the average droplet diameter for each storage days. The average diameters at different storage day were compared within each sample while the overall diameter changes were compared between samples.

Samples	Days	Average diameter (µm)	Overall diameter changes (%)	Coefficient of variance (%)
Empty DIW	0	42.0 ± 3.9^{a}	21.2 ± 10.7^{a}	9.3
	1	46.3 ± 4.0^{b}		8.6
	2	48.0 ± 5.5^{bc}		11.5
	3	49.0 ± 6.7^{cd}		13.6
	4	50.4 ± 7.9^{d}		15.7
	5	51.2 ± 9.2^{d}		18.0
Empty LB broth	0	46.5 ± 4.4^{a}	21.3 ± 6.2^{a}	9.5
	1	50.4 ± 4.6^{b}		9.1
	2	52.1 ± 5.5^{c}		10.6
	3	53.4 ± 6.0^{cd}		11.2
	4	55.6 ± 6.8^{de}		12.2
	5	56.6 ± 8.2^{e}		14.5
***E. coli*-GFP in DIW**	0	43.8 ± 4.3^{a}	20.6 ± 3.9^{a}	9.8
	1	44.3 ± 4.7^{a}		10.6
	2	48.5 ± 5.4^{b}		11.1
	3	48.1 ± 6.0^{b}		12.5
	4	51.9 ± 6.2^{c}		11.9
	5	53.0 ± 6.9^{c}		13.0
***E. coli*-GFP in LB broth**	0	48.3 ± 3.7^{a}	14.8 ± 1.4^{b}	7.7
	1	50.6 ± 3.7^{ab}		7.3
	2	52.0 ± 3.7^{bc}		7.1
	3	53.9 ± 3.6^{cd}		6.7
	4	54.7 ± 3.6^{d}		6.6
	5	55.4 ± 3.6^{d}		6.4
Empty MRS broth	0	43.3 ± 4.4^{a}	21.6 ± 8.7^{a}	10.2
	1	44.6 ± 5.3^{b}		11.5
	2	47.4 ± 6.1^{b}		12.7
	3	49.7 ± 7.2^{c}		14.5
	4	50.9 ± 8.5^{c}		16.7
	5	52.9 ± 9.1^{d}		17.3
***L. paracasei* in DIW**	0	43.7 ± 4.7^{a}	20.6 ± 6.8^{ac}	10.8
	1	44.8 ± 4.8^{ab}		10.7
	2	46.0 ± 5.4^{b}		11.7
	3	48.1 ± 6.8^{c}		14.1
	4	49.2 ± 7.9^{c}		16.1
	5	52.9 ± 8.6^{d}		16.3
***L. paracasei* in MRS broth**	0	42.9 ± 4.8^{a}	19.1 ± 6.1^{c}	11.2
	1	45.8 ± 4.9^{a}		11.0
	2	48.8 ± 5.8^{b}		11.9
	3	49.5 ± 6.6^{b}		13.3
	4	50.3 ± 6.7^{bd}		13.3
	5	51.3 ± 8.3^{d}		16.1

The data were analysed with one-way ANOVA.

^{abcde}mean ± standard deviation with different letters are significantly different at $P < 0.05$

From the results obtained, it was observed that at day 0, the measured diameter of the droplet generated by the microfluidic device for all samples was approximately 40-50 μm and monodispersed droplet was produced for all samples indicating the ability of the designed flow-focusing microfluidic device to produce monodispersed droplet (Figure 3.6). Due to the monodispersity of the droplet formed at day 0 for all samples, the polydispersity effects were excluded in determining the stability of the droplet and thus, variations in droplet size observed during static storage at 25°C was solely attributed to droplet composition.

The change in droplet stability was observed for five days of storage as a significant difference in droplet diameter ($P < 0.001$) and the effect of bacteria addition on droplet stability was clearly observed after five days storage. In general, the average droplet size for all the samples tested increased after five days of static storage at 25°C as shown in Table 3.1. Referring to the average diameter of the droplet in Table 3.1, a significant increase ($P < 0.001$) in droplet diameter was observed after one day of storage for all the control samples of empty droplet (empty DIW, LB broth and MRS broth). However, for samples containing bacteria (*E.coli*-GFP in DIW, *E.coli*-GFP in LB broth, *L.paracasei* in DIW and *L.paracasei* in MRS broth), a significant increase ($P < 0.001$) in droplet diameter was only observed after two days of storage. Comparing the overall diameter changes (%) between the empty droplet of DIW, LB and MRS broth shows that the addition of nutrient of both LB and MRS does not significantly affect the changes in droplet size as no significant difference ($P = 1.00$) was observed between the samples. Moreover, the addition of bacteria (both *E.coli*-GFP and *L.paracasei*) in DIW does not significantly affect ($P = 0.997$) the overall changes in droplet diameter as compared to the empty sample of DIW whereas the addition of *E.coli*-GFP in LB broth and *L.paracasei* in MRS broth resulted in a significant change ($P < 0.001$) of the overall droplet diameter when compared with the empty samples of LB and MRS broth.

As expected, the results obtained show that all samples remained monodispersed during five days of storage due to the presence of PGPR as surfactants in the continuous oil phase (refer to section 3.2.4 of bacteria encapsulation method). Although the monodispersity of samples was maintained during storage, an increase in CV value was observed during five days of storage for all the control samples of empty droplet with or without nutrients. Incorporating bacteria into the emulsion droplet helped in maintaining the CV value for example, with the presence of *E.coli*-GFP in LB broth, only 1.3% changes in CV value was observed after five days of storage with respect to day 0 while the control sample of empty LB broth show an increase in CV value (5.5%). The same result was also observed for *E.coli*-GFP in DIW whereby only a 3.2% increase in CV value was observed as compared to empty DIW droplet with an 8.7% increase in CV value. Comparing between *E.coli*-GFP and *L.paracasei*, samples containing *E.coli*-GFP shows a smaller change in CV value as compared to *L.paracasei* whereby sample containing *L.paracasei* in DIW shows a 5.5% increase in CV value as compared to *E.coli*-GFP with only 3.2% increase. This strongly suggests the role of bacteria in droplet stabilization in which the addition of *E. coli*-GFP showing better stability as compared to samples containing *L. paracasei*. Comparing droplet of bacteria with and without nutrient, it shows that droplet of bacteria encapsulated with nutrient had better stability compared to the droplet of bacteria encapsulated without nutrient for both *E. coli*-GFP and *L. paracasei*. The increase in average droplet size and CV value for control samples of empty droplet after five days of storage indicates instability due to the occurrence of emulsion breakage and coalescence during storage which was minimized in samples containing bacterial cells.

It has been reported previously that bacterial cells may act as particles that help in the stabilization of O/W emulsions (Dorobantu *et al.*, 2004; Wongkongkatep *et al.*, 2012; Firoozmand and Rousseau, 2016) which explains the stability of the droplet incorporated with

bacteria. The encapsulated bacteria in W/O droplet may act as particles that aid in maintaining the stability of the droplet in a similar way as it was observed in the stabilization of O/W emulsions droplet incorporated with bacteria. The stabilization effect of bacteria particles in the emulsion is probably due to the formation of an emulsion system known as Pickering emulsions whereby the adherence of bacterial cells onto the interface helps in reducing the interfacial tension. Furthermore, the addition of nutrients that promotes the growth of bacterial cells also plays an important role in droplet stabilization as the encapsulation of bacteria with nutrients increases the number of cells in the droplet that act as particles that improve bacterial coverage on the interface of the droplet. In addition, the presence of proteins such as tryptone (in LB broth) and peptone (in MRS broth) may also act as a stabilizer in maintaining the stability of droplet (Damodaran 2005).

Although the results strongly suggest the role of bacterial cells in stabilizing the droplet, it only showed its ability to minimize the change in droplet stability and does not offer total stabilization effects as droplet size was still increased after five days of storage. This may be attributed to the active coarsening that occurs between droplet containing bacteria and empty droplet within the same system. This has been observed in the previous studies done on the encapsulation of bacteria in single W/O emulsion droplet (Boitard *et al.*, 2012; Chang *et al.*, 2015). In a single emulsion system containing bacteria as the aqueous phase, active coarsening of the droplet is driven by the osmotic imbalances between droplet containing bacteria and empty droplet within the same emulsion system. Nutrient depletion due to bacterial bioactivity reduces the overall solute concentration within the droplet causing osmotically driven water flux from droplet containing bacteria to neighbouring empty droplet. This causes the droplet containing bacteria to shrink while the empty droplet swell (Boitard *et al.*, 2012; Chang *et al.*, 2015). Although the microfluidic encapsulation of bacteria enables the control of the size of the

droplet during droplet formation, it is impossible to precisely control the number of bacterial cells encapsulated within each droplet especially when encapsulating a large number of bacteria in a fairly large-sized droplet. This may cause the production of empty droplets containing only DIW or LB broth within the same system that creates an osmotically imbalanced environment between droplet. Therefore, these effects may cause a shift in droplet distribution towards the larger-sized droplet (Figure 3.6). In conclusion, although the results clearly show the ability of bacteria in emulsion stabilization, further investigations are needed in order to fully understand the mechanism of W/O droplet stability by bacterial cells.

3.3.3 The viability of encapsulated bacteria during storage

The viability of bacterial cells was determined in order to study the effect of encapsulation on bacterial growth as presented in Figure 3.7. Samples of encapsulated bacteria with nutrient (LB broth for *E. coli*-GFP and MRS for *L. paracasei*) or DIW were prepared together with control samples of free bacterial cells suspended in nutrient (LB or MRS broth) or DIW.

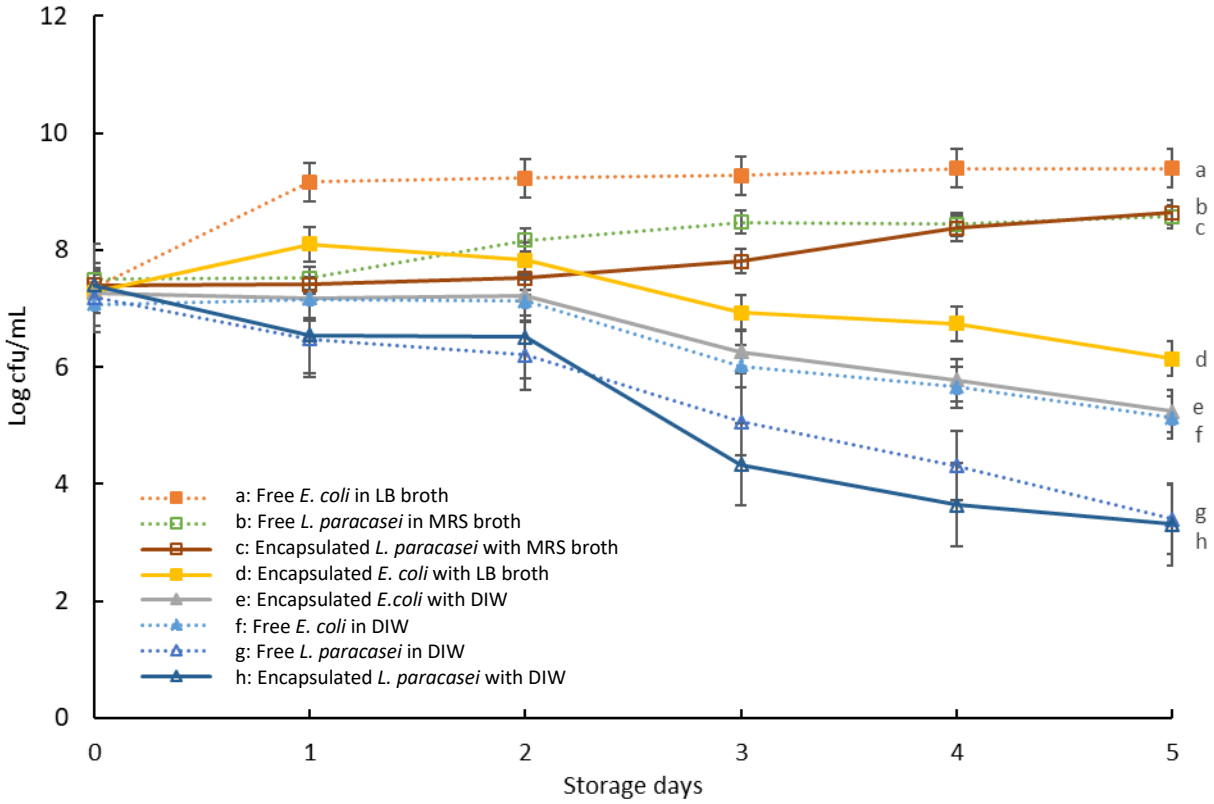

Figure 3.7 Bacterial growth during five days of storage for free bacterial cells and encapsulated bacterial cells in W/O droplet with or without nutrients. Bars represent mean ± SEM taken from 3 independent experiments (N=3) with 30 µl of sample tested with Miles and Misra technique for each experiment.

Figure 3.7 shows a comparison in the viability of bacteria for encapsulated and unencapsulated samples. As expected, a decrease in viable cells was observed for all samples suspended in DIW for both *E. coli*-GFP and *L. paracasei*. Encapsulation in W/O droplet with DIW did not improve the viability of bacterial cells as a decrease in viable cells was also observed for samples of encapsulated bacterial cells whereby the lack of nutrient had caused the cells to enter death phase. Referring to samples of *E. coli*-GFP suspended in LB broth, an increase in the growth of bacterial cells was observed for free *E. coli*-GFP cells during storage while an increase in the growth of *E. coli*-GFP cells encapsulated in W/O droplet was only observed on the first day of storage before decreasing. This shows that the growth of *E. coli*-GFP in W/O droplet was suspended and that encapsulation inhibited the growth of *E. coli*-GFP cells. Nevertheless, samples of *L. paracasei* suspended in MRS broth shows contradictory results whereby a slow but ongoing increase in viable cells was observed for both free and encapsulated samples.

The difference in viability between *E. coli*-GFP and *L. paracasei* may be attributed to the difference in growth rate as *E. coli*-GFP has a higher growth rate as compared to *L. paracasei*. The generation time in which the amount of time required by a bacteria cells to double in number during a designated time is reported to be around 20 minutes for free *E. coli*-GFP cells in LB broth under optimum conditions (Sezonov, Joseleau-Petit and D'Ari, 2007) and one hour for *lactobacilli* (Brizuela, Serrano and Ferez, 2001; de Mesquita *et al.*, 2017; Rezvani, Ardestani and Najafpour, 2017). The rapid growth of *E. coli*-GFP cells during the first day of storage speeds up nutrient depletion in each W/O droplet resulting in a decrease in bacterial viability after one day due to its inability to support the growth of bacteria in the droplet. This is in contrast with samples containing *L. paracasei* whereby slower growth rate had caused slower depletion in nutrients and therefore helps in maintaining the growth of *L.*

paracasei during five days of storage. Encapsulation limits the availability of nutrients and space for bacterial growth that lowers the bacterial growth rate and yield. Similar behaviour has been previously reported in the study of bacterial growth in O/W emulsion whereby inclusion of bacteria in the crowded environment of oil droplet reduced the growth rate and yield of bacterial cells (Parker *et al.*, 1995). In that study, the growth of bacteria was inhibited from planktonic to clustering that resulted in a reduced growth rate. In addition, the accumulation of bacterial metabolic end product may also inhibit the growth of encapsulated bacteria. Moreover, mineral oil has lower oxygen permeability as compared to water which limits the diffusivity of oxygen for maximum bacterial growth.

Nevertheless, referring to droplet size distribution results in section 3.3.2, the stability of the droplet was highly maintained for droplet containing bacteria even though the bacterial viability test showed a decrease in bacterial viability during storage. This was also true for bacteria encapsulated in DIW whereby inclusion of bacteria in DIW improved the stability of droplet although a decrease in cell viability was observed. The decrease in bacterial viability indicates the presence of dead cells within the droplet. Therefore, the stability of droplet with reduced cell viability indicates the role of dead cells in droplet stabilization. Dead cells may act as particles that adhere to the interface of W/O droplet and aid in droplet stability.

3.3.4 Microscopic observation of bacteria response in water-in-oil droplet

Following the results obtained from droplet stability and bacterial viability tests, it was hypothesized that the inclusion of bacterial cells in the W/O droplet promotes droplet stability during storage. In addition, droplet stability was also attributed to the presence of dead cells within the droplet during five days of storage. In order to provide a clear explanation of the mechanism of droplet stability due to bacteria, a microscopic observation was done daily during

storage to distinguish the growth of bacteria and the presence of dead cells within the droplet. However, photomicrographs of the samples presented in Figure 3.8 and Figure 3.9 only includes samples before storage (day zero), after one day and five days of storage as changes in bacterial growth were clearly observed during these periods. In addition, photomicrographs of the control sample of free (unencapsulated) bacteria with or without nutrient were also presented in figure 3.9.

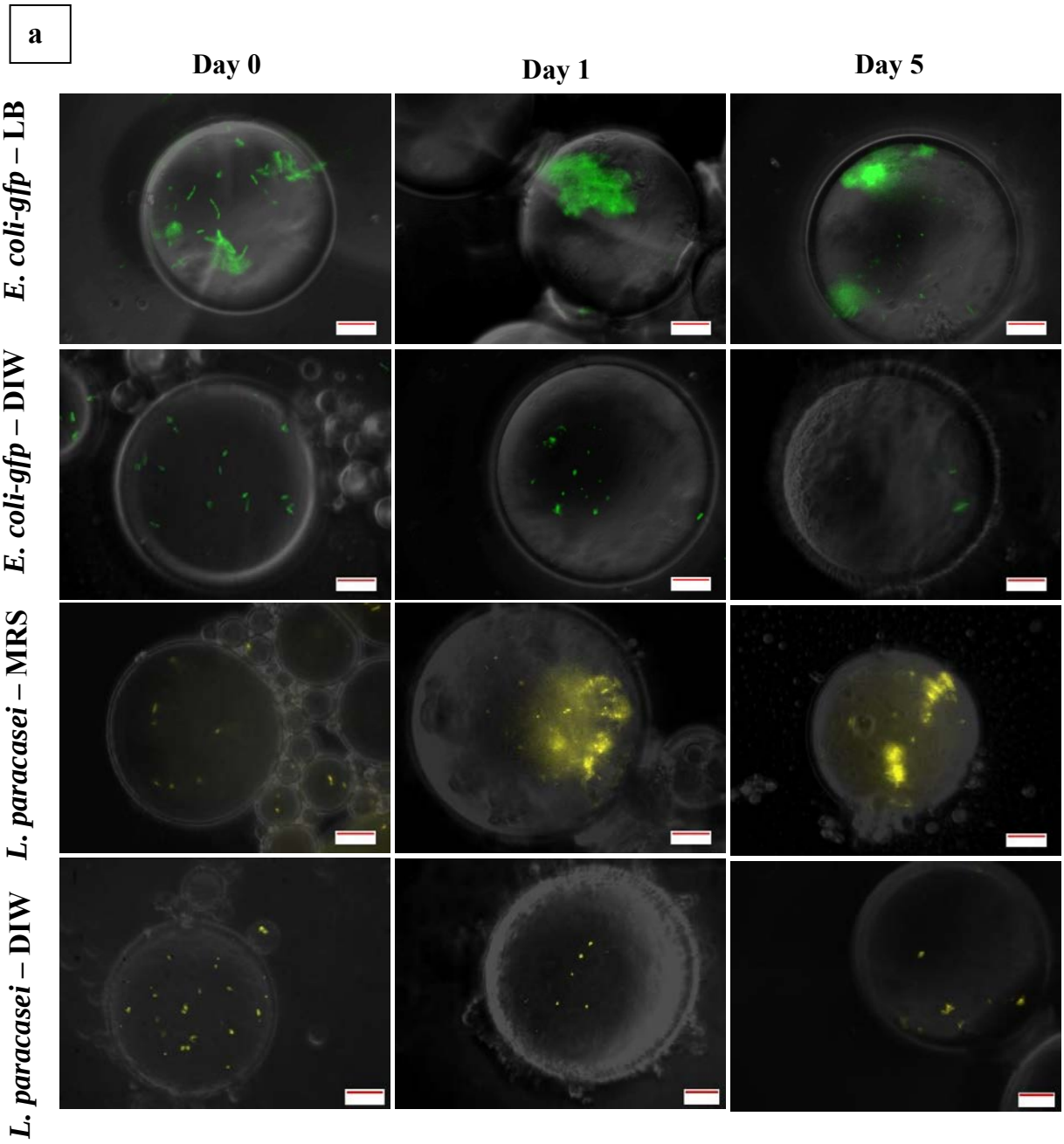
a
Day 0
Day 1
Day 5
E. coli-gfp – LB
E. coli-gfp – DIW
L. paracasei – MRS
L. paracasei – DIW

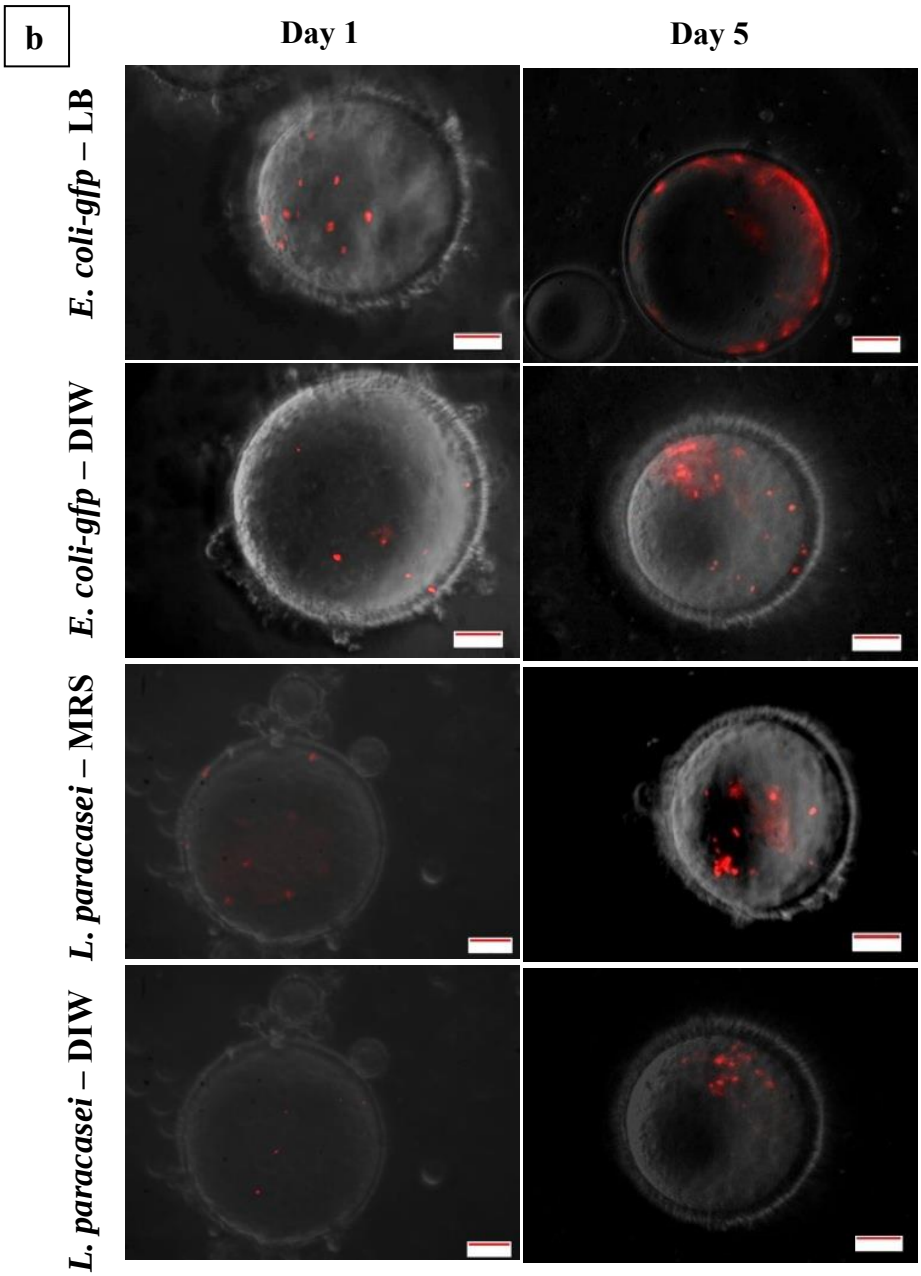

Figure 3.8 Photomicrographs of bacterial cells encapsulated in W/O droplets during storage showing (a) live cells and (b) dead cells. Bacterial clusters were observed during storage for samples encapsulated with nutrient. Presence of dead cells were also observed after one day of storage for all samples of bacteria encapsulated with or without nutrient. Colour codes were described as, Green: Live *E. coli*-GFP cells, yellow: Live *L. paracasei* cells and red: Dead cells. Scale bar: 10 μm

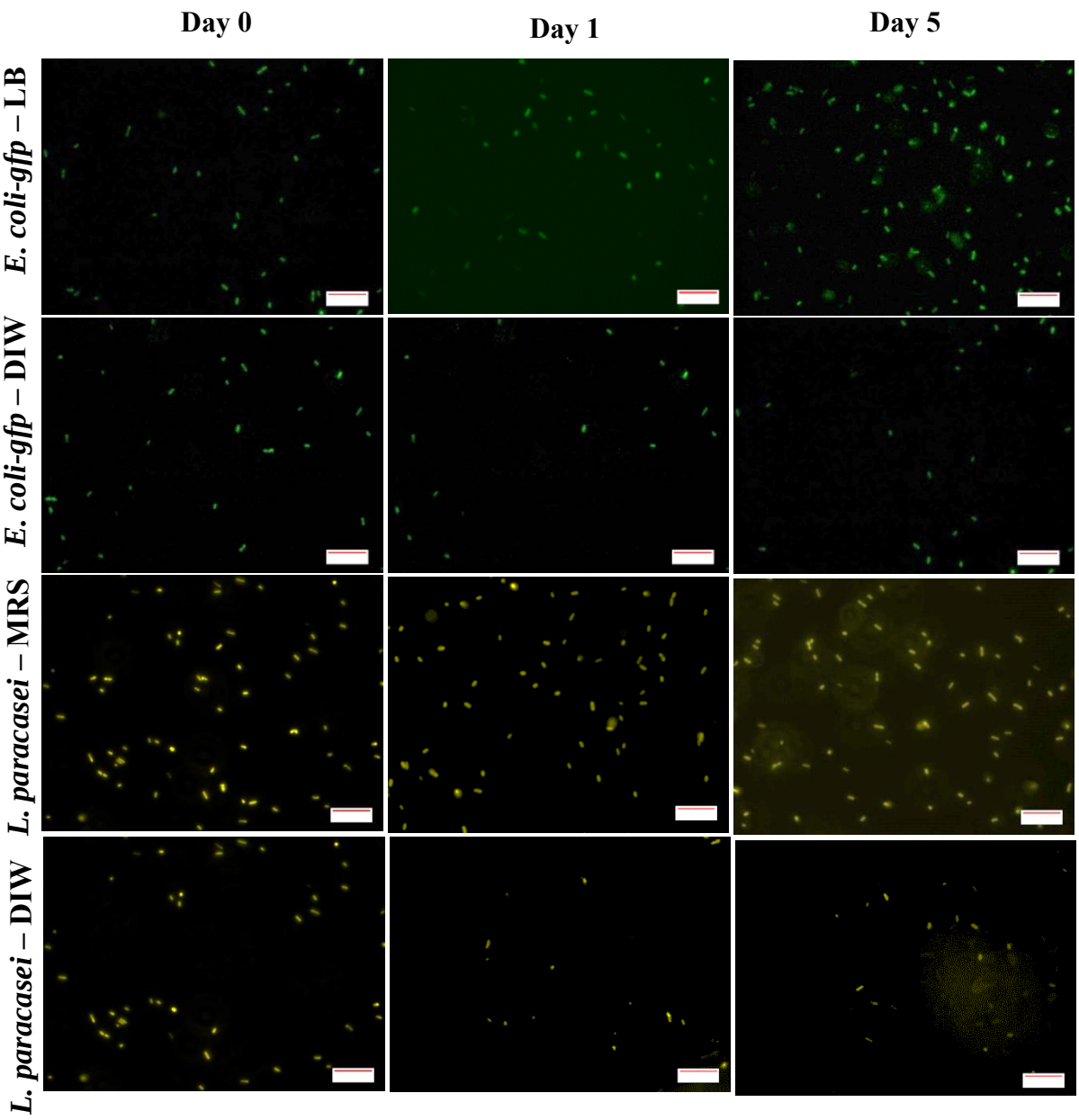

Figure 3.9 Photomicrographs of free (unencapsulated) bacterial cells suspended in LB broth (for *E. coli*- GFP, shown by green coloured cells) and MRS broth (for *L. paracasei,* shown by yellow coloured cells). No bacterial clusters were observed during five days of storage. Scale bar: 10 µm.

From the photomicrographs of fluorescence microscopy for encapsulated *E. coli*-GFP samples (Figure 3.8a), ropey-like structures were observed after two hours (at day 0) of bacterial encapsulation in LB broth that leads to the formation of bacterial clustering after one day of storage. The formation of bacterial clustering was only observed for bacteria encapsulated with LB broth while droplet containing bacteria in DIW and unencapsulated samples in DIW or LB broth (Figure 3.9) remained planktonic. For *L. paracasei* samples, the presence of bacterial clusters was only observed after five days of storage for samples encapsulated with nutrient and no bacterial clusters were observed for samples encapsulated with DIW or unencapsulated samples in DIW or MRS broth (Figure 3.9). This is in agreement with studies done by Chang *et al*. (2015) and Barlow *et al*. (2017) whereby clusters of bacteria was observed when biofilm-forming bacteria *Bacillus subtilis* was encapsulated in single W/O emulsion and in the inner phase of double $W_1/O/W_2$ emulsion. As expected, the presence of dead cells was observed after one day of storage which can be seen mostly on the interface (Figure 3.8b).

In the study done by Chang *et al*. (2015) on the growth of biofilm in a microfluidic-generated droplet, clumps of bacteria were observed in W/O droplet containing *Bacillus subtilis*. However, due to the absence of surface-like surfactants, the bacterial biofilm was not formed on the interface of the droplet but was seen floating in the aqueous phase similar to the results obtained by Barlow *et al.* (2017). It was reported that with a continuous supply of nutrients from the outer aqueous phase of double $W_1/O/W_2$ emulsion, rapid formation of biofilm was observed as early as four hours of *Bacillus subtilis* encapsulation with the formation of ropey like structures (Barlow *et al.*, 2017). In this study, the onset of biofilm formation by *E. coli*-GFP in W/O droplet was demonstrated with the formation of ropey-like structures after two hours of encapsulation that grew into distinct bacterial clusters after one day of storage. This is mainly due to the high growth rate of *E. coli*-GFP. Environmental stress such as nutrient

depletion, lack of oxygen and space for growth leads to several morphological and physiological changes in microorganisms. In such conditions, *E. coli* responded by ceasing all metabolic activity and growth in order to prolong their survival (Chung, Bang and Drake, 2006). Stress-induced enzymes were produced along with the accumulation of several storage compounds such as glycogen and polyphosphate. In addition, changes in cell size and shape were also observed which may lead to the formation of bacterial biofilms (Chung, Bang and Drake, 2006; Rowlett *et al.*, 2017). However, as observed in this study and reported previously, the formation of bacterial clusters and biofilms for lactobacilli strains is less distinct as the limitation in growth due to environmental stress such as lack of nutrients was not sufficient to induce the formation of biofilm (Lebeer *et al.*, 2007).

In order to get a clear view of the formation of bacterial clusters, the percentage and size of bacterial clustering with respect to the area of the droplet was quantified by analysing fluorescence photomicrographs with ImageJ (Figure 3.10). In addition, confocal microscopy of the encapsulated *E. coli*-GFP was also done after one day of storage as presented in Figure 3.11.

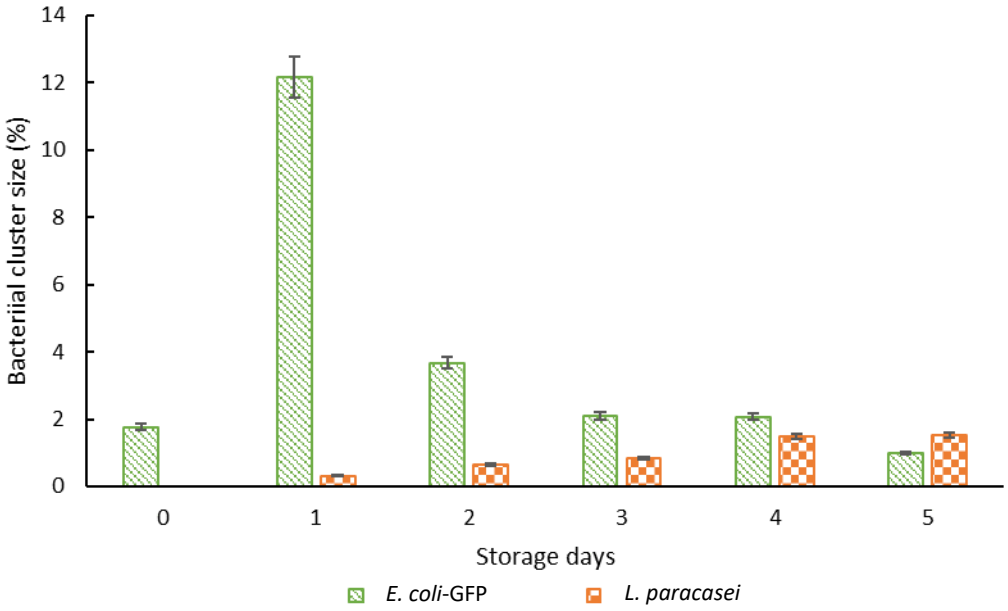

Figure 3.10 Cluster size with respect to storage days. Bars represent mean ± SEM taken from 3 independent experiments. A total of 10 droplets were measured for each experiment (N=10)

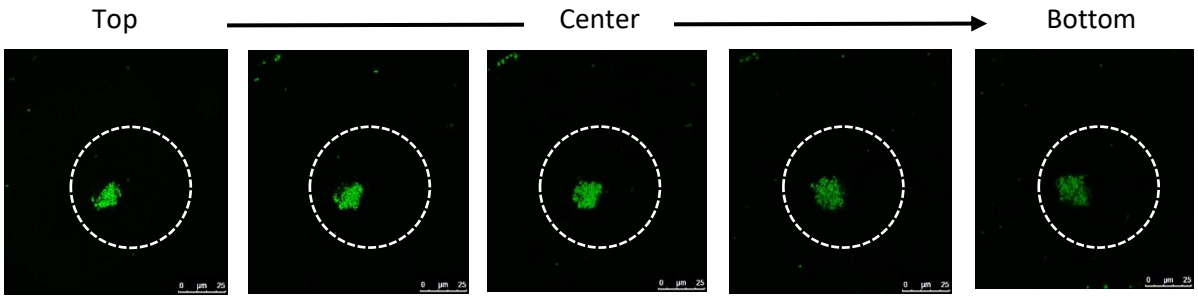

Figure 3.11 Cross-sectional images of *E. coli*-GFP clustering cells taken using a confocal microscope at day one of storage. Scale bar: 25 µm.

For *E. coli*- GFP, a large percentage of the bacterial cluster was observed on day one which started to decrease after one day of storage as opposed to *L. paracasei* whereby smaller cluster size was formed throughout the storage period. Day 0 shows a relatively small percentage of bacterial clustering for *E. coli*-GFP due to the formation of ropey-like structures at the beginning of the storage period. The decrease in size after 1 day of storage is attributed to the decrease in nutrients that caused a reduction in bacterial clusters as bacterial cells were detached from the clusters (Stoodley *et al.*, 2001). In addition, the lack of surface for attachment eases the process of cell detachment. The presence of planktonic dead cells was observed after 1 day of storage with the majority seen on the interface indicating the ability of dead bacterial cells as Pickering particles for droplet stabilization (Figure 3.6b). Due to distinct bacterial clusters formed after one day of storage, confocal microscopy was done on samples containing *E. coli*-GFP that produces a 3D image of the droplet (Figure 3.8). Cross-sectional images of bacterial clustering show the formation of bacterial clustering that extends from the top to the bottom of the droplet.

3.3.5 Characterisation of bacterial hydrophobicity and affinity towards the oil phase

The determination of bacterial hydrophobicity and affinity towards the oil phase was done in order to determine the surface-active characteristics of bacterial cells that aid in maintaining the stability of W/O droplet during storage. This involves the determination of bacterial hydrophobicity through the bacterial adherence to hydrocarbons assay (BATH) as presented in Figure 3.12 and the interfacial tension test of bacterial suspension against the oil phase as presented in Figure 3.13.

3.3.5.1 Bacterial hydrophobicity

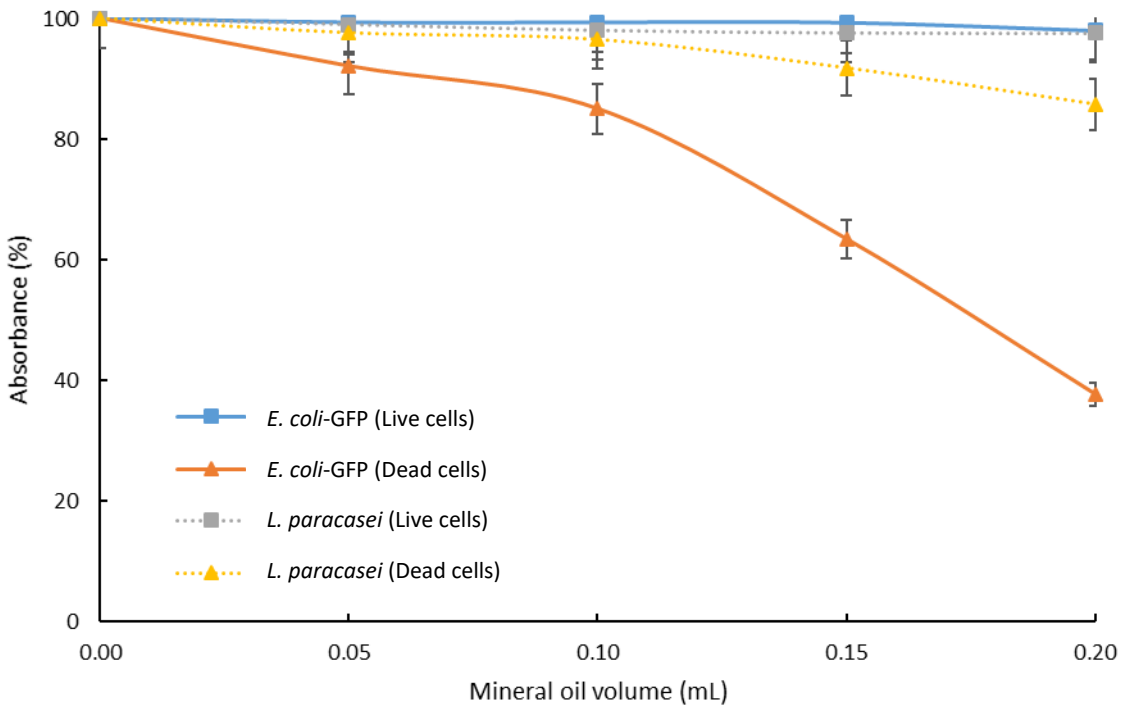

Figure 3.12 Bacterial adherence to mineral oil for live and dead cells at different mineral oil volume. The absorbance of bacterial suspension taken from each sample was measured against mineral oil volume. Bar represents mean ± SEM for 3 independent experiments (N=3).

The BATH assay was conducted according to Rosenberg *et al*. (1980). The test was done on both live and dead cells to determine the adherence ability of bacterial cells onto mineral oil. Figure 3.12 shows a decrease in absorbance with an increase in mineral oil volume for dead cells while no changes in absorbance were observed with the presence of live cells. The decrease in absorbance with an increase in mineral oil volume indicates an increase in the overall hydrophobicity as more dead bacterial cells adhere to the mineral oil. Transition in the wettability of bacterial cells was observed when the bacteria undergo death phase. This explains the observed affinity towards the interface for dead cells under the fluorescence microscope. Comparing between *E. coli*-GFP and *L. paracasei*, it was observed that dead *E. coli*-GFP cells exhibited better affinity towards mineral oil compared to dead *L. paracasei*. This is due to the difference in lipid and lipoprotein content of the bacteria whereby the Gram-negative *E. coli* has higher lipid content as compared to the Gram-positive *L. paracasei* due to the presence of the outer membrane in the Gram-negative bacteria (Seltmann and Holst, 2013).

The results obtained provide an idea on the stabilization mechanism of bacterial cells incorporated in W/O emulsion droplet. At the beginning of the storage time, an increase in bacterial cells occurred that leads to the formation of bacterial clustering. During this time, droplet stability was mainly maintained by the presence of surfactants on the interface as live cells with weak hydrophobicity prefer to stay in the aqueous phase rather than at the interface. After one day of storage, the presence of dead cells with high affinity towards the oil phase was observed that aided in maintaining droplet stability. It has been reported previously that thermally-inactivated microbial cells may act as particles in stabilizing Pickering oil-in-water emulsions via hydrophobic interactions whereby the denaturation of proteins in the bacterial cell wall caused the exposure of hydrophobic groups (Firoozmand and Rousseau, 2016). The ability of bacteria to adsorb onto the water-oil interface depends on several factors such as cell

surface characteristics, size and bacterial concentration. Nevertheless, changes in bacterial characteristics such as cell size and shape as it becomes smaller and rounder along with changes in the fatty acid and protein composition of the bacterial membrane due to other environmental stress such as starvation (Chung, Bang and Drake, 2006) may contribute to the increase in bacterial affinity towards the interface. As the cell becomes smaller and rounder, the cells can be easily embedded within the interface. In addition, the existence of pili on the bacteria which is known to assist its attachment onto surfaces and formation of biofilm may also play a role in the adsorption of bacteria onto the interface (Firoozmand and Rousseau, 2016).

3.3.5.2 Interfacial tension

In order to further understand the surface-active characteristics of bacterial cells, the interfacial tension test was done by adding bacterial suspension into mineral oil with or without 1.5% w/v PGPR surfactant using the pendant drop method. The results were as presented in Figure 3.13.

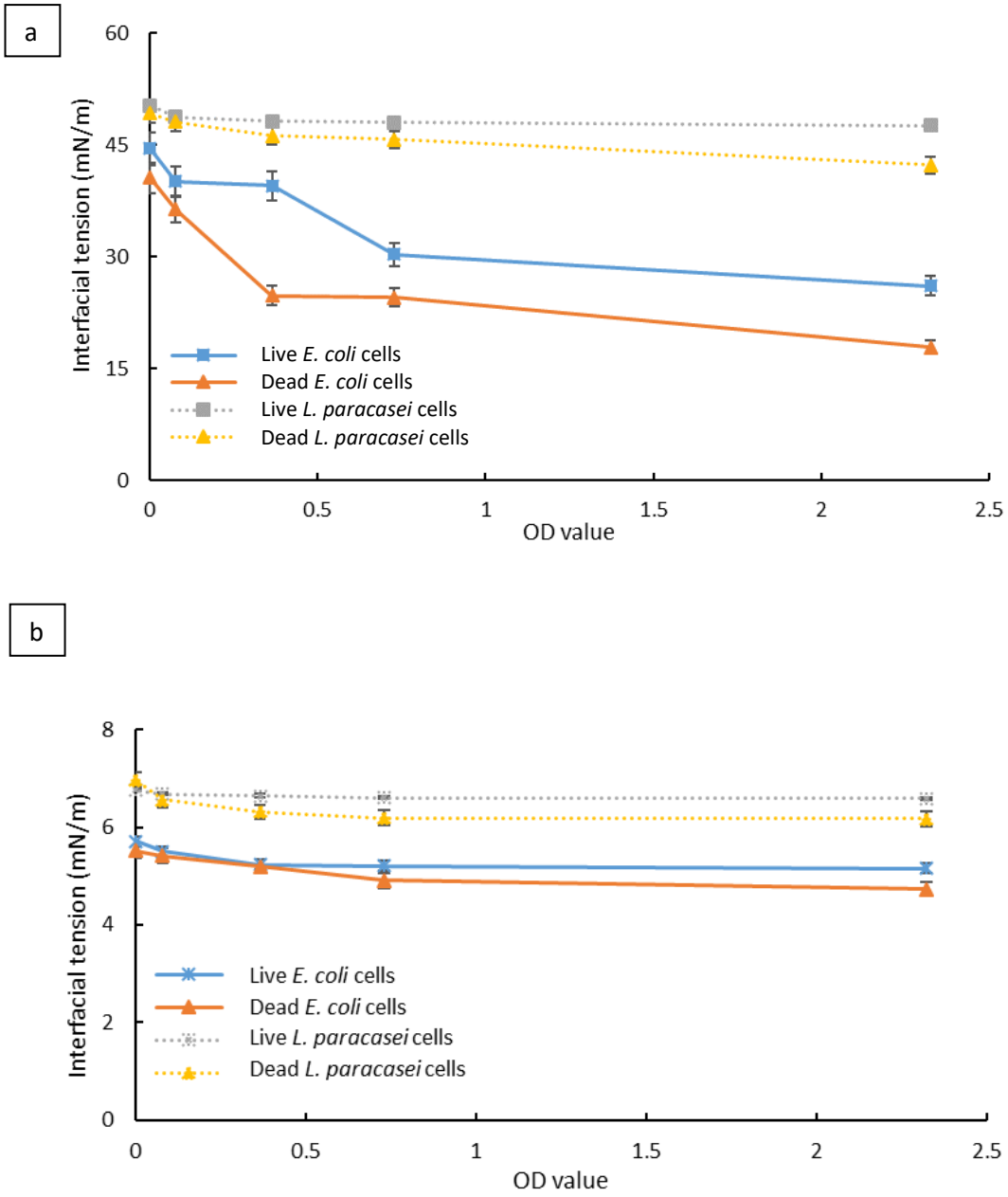

Figure 3.13 Interfacial tension of bacterial suspension at different concentration against mineral oil with (a) samples without PGPR in the oil phase (b) samples with PGPR in the oil phase. Bar represents mean ± SEM from 3 independent experiments (N=3).

The interfacial tension of bacterial cells suspended in DIW at different concentration against mineral oil was measured in mN/m by the attension software. From Figure 3.13, it was determined that the interfacial tension was reduced with the addition of bacteria even at low concentration for both samples with or without PGPR whereby greater reduction interfacial tension was observed in the absence of PGPR (Figure 3.13 a) as compared to samples with PGPR (Figure 3.13 b). In addition, it was also shown that the interfacial tension was affected by the bacterial concentration for both *E. coli*-GFP and *L. paracasei* samples whereby a reduction in interfacial tension was observed with an increase in bacterial concentration. The interfacial tension was better reduced in the presence of *E. coli*-GFP cells as compared to *L. paracasei* cells for both samples of live and dead cells with or without PGPR surfactant. As an example, referring to Figure 3.13 a for samples without PGPR surfactant, a reduction in interfacial tension was observed from 44.5 mN/m to 39.5 mN/m (5 mN/m reduction) as the OD reading for live *E. coli*-GFP cells increased from 0 to 0.4 whereas the interfacial tension was only reduced from 50.3 Mn/m to 48.2 Mn/m (2.1 mN/m reduction) with the same increase in bacterial concentration for live *L. paracasei* cells. When comparing between live and dead cells, it was determined that the addition of dead cells showed a better reduction in interfacial tension as compared to live cells for both samples of *E. coli*-GFP and *L. paracasei* which may be attributed to the hydrophobic characteristic of the dead cells. The addition of dead *E. coli*-GFP cells resulted in a better reduction of the interfacial tension as compared to dead *L. paracasei* cells which may be attributed to the difference in lipid content between the two bacterial strains.

a

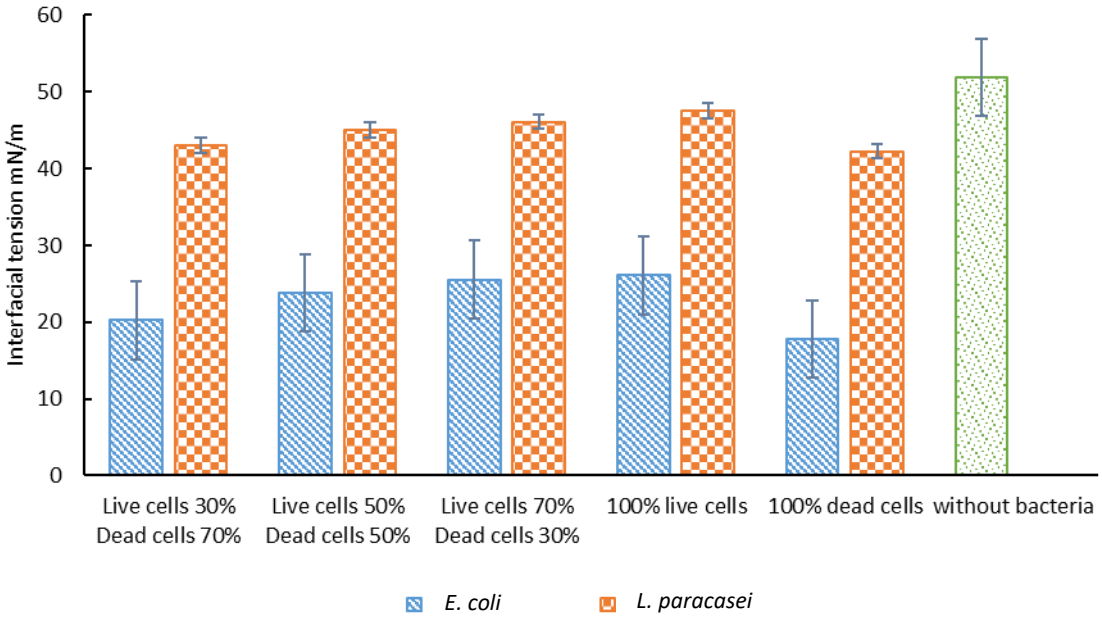

b

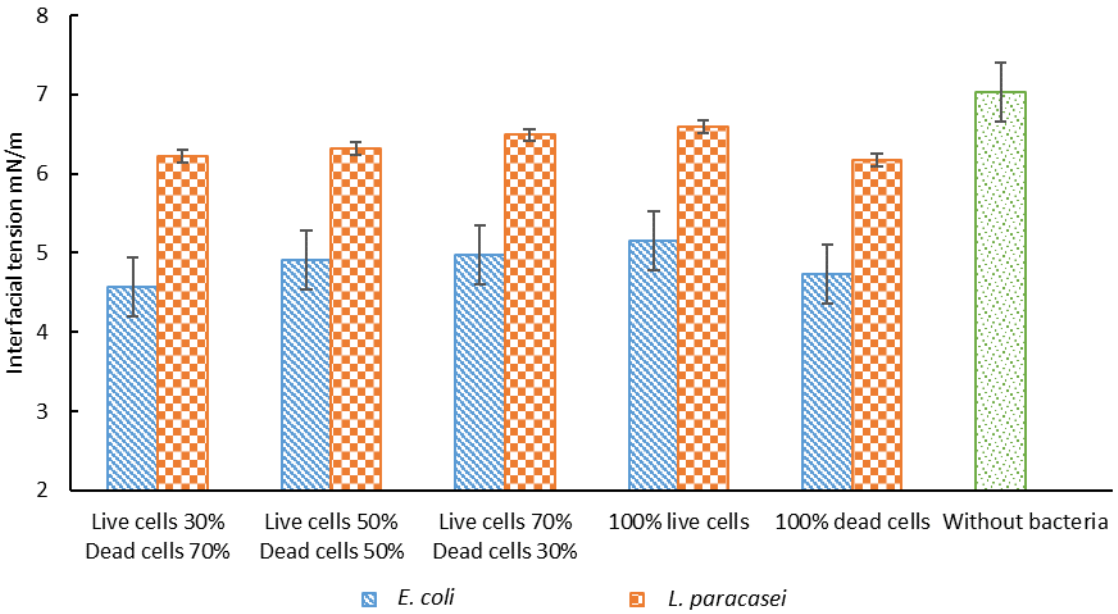

Figure 3.14 Changes in interfacial tension with the addition of samples containing live and dead cells at a different ratio with (a) without PGPR in the oil phase (b) with PGPR in the oil phase. Bars represent mean ± SEM taken from 3 independent experiments (N=3).

The surface-active effect of samples containing a mixture of both live and dead cells at different ratios (L:D, 30:70, 50:50, and 70:30) was also determined as shown in Figure 3.14 which clearly shows the effect of dead cells in reducing interfacial tension. From the results obtained, reduction in interfacial tension was affected by the ratio of dead and live cells in the sample with samples containing a higher ratio of dead cells shows better surface-active characteristics as it resulted in better interfacial tension reduction as compared to samples containing lower dead cells concentration. A similar trend was observed in both systems with or without PGPR surfactant. This shows that dead cells play a major role in reducing the interfacial tension compared to live cells.

The effect of bacteria in reducing interfacial tension between water and oil phase has been reported previously by Chen and Wang (2016) whereby *E. coli* cells were shown to have a better effect on interfacial tension reduction as compared to *Chlorella Vulgaris* (*C. vulgaris*) cells and polystyrene microparticles due to their higher affinity towards the hydrophobic interface. The ability of bacteria in improving emulsion stability is mostly attributed to bacterial surface properties whereby the wettability, bacterial size, shape and concentration play a major role in ensuring the effectiveness of the bacteria (Dorobantu *et al.*, 2004; Firoozmand and Rousseau, 2016). As discussed before in section 3.3.5.1, changes in bacterial affinity towards the oil phase were observed when bacteria were in the dead phase due to rheological and physiological changes that occur in the cell membrane (Chung, Bang and Drake, 2006). Changes in bacterial wettability, when bacteria were in the death phase as reported in section 3.3.5.1, caused the bacteria to become more adherent towards the oil-water interface due to changes in bacterial membrane conformation causing the hydrophobic groups to become more exposed. Moreover, environmental stress due to starvation caused the bacteria to become smaller and rounder that further improves its adherent ability towards the water-oil interface.

This explains the role of dead cells in reducing the interfacial tension. In addition, bacterial concentration is also important in ensuring effective coverage of the bacteria on the interface for stabilization. However, highly concentrated bacterial suspensions may cause the bacteria to cluster and diminish their ability to adhere to the interface. Therefore, further investigation into this matter may provide a better understanding on the mechanism of bacterial attachment onto the interface.

3.3.6 Changes in the zeta potential of bacteria

The zeta potential determination was done in order to determine the colloidal stability of samples containing bacterial cells in DIW or nutrient (LB or MRS broth) and the difference between live and dead cells. In addition, the interactions between live and dead cells were also determined by testing mixed samples containing different ratios of live and dead cells.

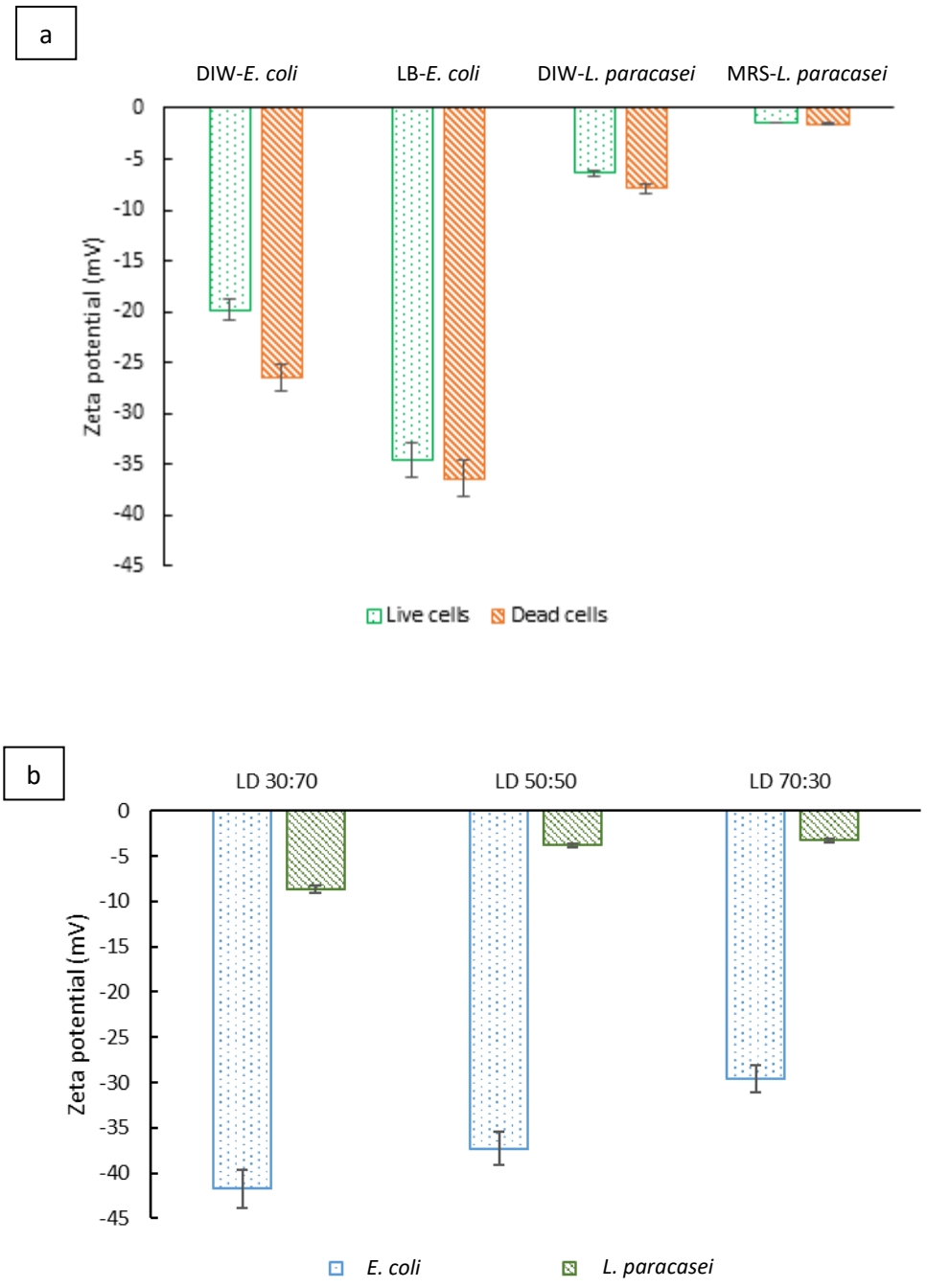

Figure 3.15 The zeta potential values of bacterial cells for (a) live or dead cells suspended in DIW or with nutrient, (b) mixed samples with Live:Dead cell ratio (L:D) of 30:70, 50:50 and 70:30. Bars represent mean ± SEM taken from 3 independent experiments (N=3).

The colloidal stability was determined by measuring the zeta potential of the bacterial suspension whereby values of more than +30 mV or less than -30 mV indicate an electrically stable colloid. Colloidal instability is perceived at values between -30mV to +30mV as solute particles tend to flocculate. From the results obtained, it was determined that bacterial samples suspended LB or MRS broth had better colloidal stability compared to samples in DIW. *E. coli*-GFP shows a reduction in zeta potential value from -19.8mV to -34.6mV for live cells and -26.48 to -36.36mV for dead cells when suspended in LB broth. In addition, dead *E. coli*-GFP cells show lower zeta potential values as compared to live cells and an increase in the number of dead cells in mixed samples also cause a reduction in the zeta potential value (Figure 3.12). This is in agreement with a study done by Beskok and Pillai (2008) whereby a reduction in zeta potential value was observed for *E. coli*-GFP samples grown in the rich medium as compared to starved cells. Changes in zeta potential were also observed when cells enter the death phase. This suggests that bacterial surface charge is affected by nutrient state and their viability. The suspension of bacteria in the LB or MRS broth along with changes in bacterial surface conformation as they enter the death phase also improve colloidal stability. For *L. paracasei*, the zeta potential value changed towards a positive value close to zero in MRS broth compared to in DIW. This is probably due to the interactions between *L. paracasei* cells and the environmental particles in the MRS broth whereby the presence of lactic acid due to fermentation of glucose in MRS broth lowered the pH and caused the carboxyl and phosphate group on the cell's surface to be protonated (Larsen *et al.*, 2018) and therefore improved colloidal stability. However, there is no difference observed in the zeta potential between live and dead *L. paracasei* samples and therefore indicates that change in bacterial cell surface as it enters the death phase does not affect the surface charge and colloidal stability. This is also

shown in samples containing mixed cells whereby an increase in dead cells amount does not affect changes in zeta potential (Figure 3.12b).

The results obtained provide an overview of the stability of bacterial suspensions before droplet formation. The colloidal stability of bacterial suspensions is mainly due to the availability of nutrient in the suspension in which the interaction of bacteria with particulate solutes in nutrient (LB or MRS broth) improves colloidal stability. Other than that, it also shows that for samples suspended in nutrient (LB or MRS broth), the colloidal stability of the samples indicates that the bacteria are more likely in the planktonic state rather than clustering. Therefore, this indicates that the clustering of cells observed under fluorescence microscopy was solely caused by the entrapment of bacteria in W/O droplet.

3.4 Conclusion

In conclusion, the inclusion of bacterial cells in W/O droplet affected the stability of droplet with the Gram-negative *E. coli*-GFP showed better stabilization effects compared to the Gram-positive *L. paracasei* due to the difference in lipid content. Further investigations revealed the ability of bacteria to act as particles in stabilizing the W/O droplet whereby better surface-active effects were shown by dead cells as compared to live cells. The inability of bacteria to survive in W/O droplet during storage indicated the presence of dead cells with high affinity towards the interface (due to hydrophobic nature) which aids in maintaining the stability of the droplet during storage. The effects of bacteria on droplet stability depended on several factors such as the type of bacteria, bacterial viability and bacterial concentration whereby these factors play a major role in ensuring the effectiveness of bacteria as particles in promoting droplet stability

Furthermore, the results obtained from this chapter provide an indication of the interrelationship between bacterial cells and W/O droplet microstructure that will be beneficial in understanding the stability of emulsion systems incorporated with bacteria. The proposed mechanism of bacterial stabilization effects in W/O droplet may be beneficial for the industrial application of emulsion systems with bacteria. In addition, it demonstrated the ability of droplet microfluidics in the development of model emulsion systems with controlled and monodispersed droplet size.

Chapter 4
Emulsion stability and release of bacteria from microfluidic-generated water-in-oil-in-water droplet

4.1 Introduction

Double emulsions are emulsions within an emulsion which can be divided into two types such as water-in-oil-in-water ($W_1/O/W_2$) and oil-in-water-in-oil ($O_1/W/O_2$). Some of the applications of such emulsions are in food where they are used in producing reduced-fat products and for the encapsulation of highly sensitive product such as flavours and bacteria (Muschiolik and Dickinson, 2017). Double emulsions have also been extensively used in pharmaceuticals for drug delivery (Dluska *et al.*, 2017) and cosmetics (Miyazawa and Yajima, 2000). $W_1/O/W_2$ emulsions are composed of two aqueous phases namely the inner and outer phases separated by a layer of oil in between. Depending on their application, they can be produced in a controlled manner with single inner core (Yan *et al.*, 2013) or with multiple inner cores for compartmentalization (Hou *et al.*, 2017) which can be produced through the microfluidics method.

Apart from being used as a means of encapsulation, there are also other interesting applications of double emulsions for example in the controlled release of the encapsulated materials/ cargo that benefited from the destabilization process of double emulsions. The controlled release of bacteria from double emulsions has been discussed for the first time by El Kadri *et al.* (2015) whereby the osmotic alterations of the outer aqueous phase leads to the

controlled release of bacteria into the outer aqueous phase that is dependent on the solute, surfactants and the inner phase (W_1) concentration. However, in that study, emulsion droplet was prepared by using two-stage homogenization process that produced double emulsion droplet with uneven numbers of the inner aqueous phase making it difficult to conduct a detailed investigation of the release mechanism.

Although studies have been done previously on the encapsulation and controlled release of bacteria in double emulsion droplet, further studies are still required to closely investigate the stability and destabilization process of the $W_1/O/W_2$ droplet in the presence of bacteria in order to permit their full utilisation in complex bacterial studies and at industrial level. The complex bacterial activity within the droplet may cause droplet instability as it changes the composition of the droplet. The metabolic activity of bacteria within the droplet may lead to continuous change in solute concentration due to nutrient depletion and the production of metabolic by-products. Furthermore, changes in bacterial activity may also affect the stability of the droplet in a similar or different way as it was discussed in the previous chapter while the addition of an outer aqueous phase may help in improving the viability of the bacteria. In addition, the application of droplet microfluidics allows for the controlled and monodispersed production of double emulsion droplet which is beneficial for close investigation on droplet stability and the mechanism behind the controlled release of bacteria.

Therefore, this chapter aimed to investigate the effect of microfluidic encapsulation in double $W_1/O/W_2$ emulsions on droplet stability and bacterial viability. The application of double $W_1/O/W_2$ droplet for the controlled release of bacteria, induced by osmotic alterations was also explored in detail by using microfluidic for droplet formation. *E. coli*-GFP, one of the most common bacteria used in various applications was encapsulated by using a two-junction

flow-focusing microfluidic device forming monodispersed double $W_1/O/W_2$ droplet in a controlled manner. The effect of nutrients and osmotic balance alterations on droplet stability, bacterial viability and controlled release was investigated in order to determine the potential use of $W_1/O/W_2$ for various bacterial study and industrial applications.

4.2 Materials and methods

4.2.1 Materials and bacterial cultures

Materials and bacterial cultures used were as described in section 3.2.1 with the addition of sodium chloride, NaCl (Fischer Scientific, United Kingdom), Poly(allylamine hydrochloride) (Mw ≈ 17500), Poly(sodium 4-styrenesulfonate) (Mw ≈ 70000) and water-soluble surfactant, polysorbate 80 (Tween 80) all purchased from Sigma-Aldrich (United Kingdom). For the bacterial study, tryptone and yeast extract were purchased from Oxoid Ltd. (United Kingdom). D (+) – glucose was purchased from Acros Organics (United Kingdom) and Nile red stain was purchased from Invitrogen™ (United Kingdom).

4.2.2 Microfluidic device fabrication

The microfluidic device used for generating double emulsion droplet was produced as described in section 3.2.2. A device with two flow-focusing channels with the dimensions of 100 µm (width before junction), 25 µm (width at junction) and 50 µm (width of exit channel) for the first junction and 50 µm (width before junction), 100 µm (width at junction), 200 µm (width of exit channel) at the second junction with 50 µm depth was used for one-step production of double $W_1/O/W_2$ droplet (Figure 4.1).

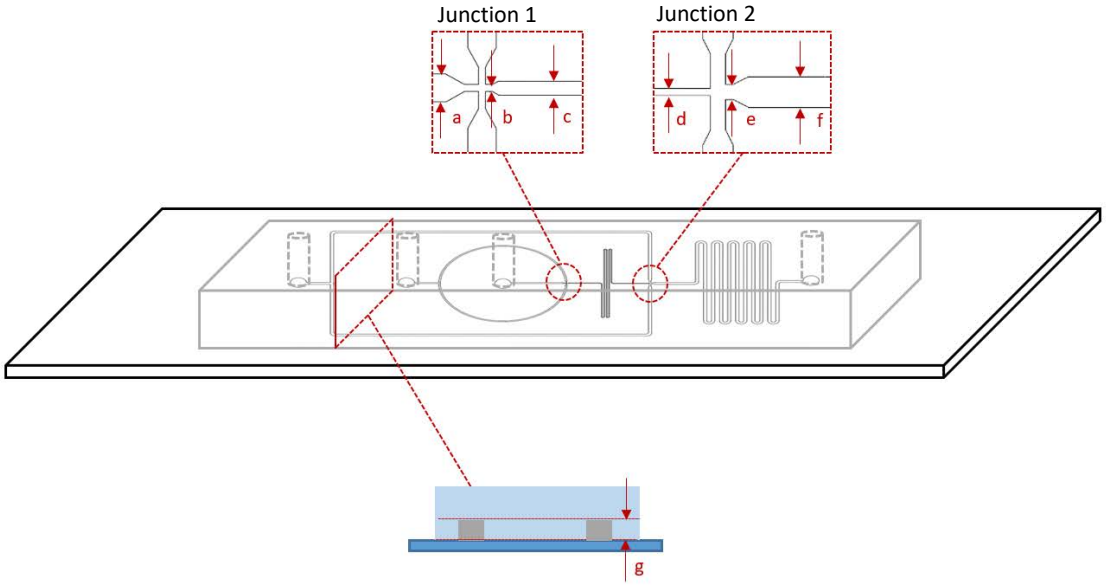

Figure 4.1 Flow-focusing microfluidic device with two junctions for one-step $W_1/O/W_2$ droplets generation. W/O droplets were first produced at junction 1 that were then flowed into junction 2 for further encapsulation into the second aqueous phase (W_2) forming $W_1/O/W_2$ droplet. The dimensions of the microfluidic device were, a: 100 µm, b: 25 µm, c: 50 µm, d: 50 µm, e: 100 µm, f: 200 µm for the widths of the channels while the depth of the channel is g: 50 µm.

4.2.3 Hydrophilic surface treatment for microfluidic device

Surface modification was conducted according to Bauer *et al.* (2010) whereby the layer-by-layer (LBL) method was employed to apply hydrophilic coatings of polyelectrolyte multilayer (PEM) onto the channel wall. The process was conducted as described in Figure 4.2 whereby the PEM sequence that was loaded into a polyethylene (PE) tube was flushed through the microfluidic device by using a syringe pump. The PEM was composed of poly(allylamine hydrochloride) (PAH) and poly(sodium 4-styrenesulfonate) (PSS) solutions in 0.5 M aqueous sodium chloride solution (0.1% w/v) with sodium chloride (NaCl) in deionized water (0.1M) as washing solution. The PE tube was alternatingly loaded with 5 cm segments of PAH and PSS with 2.5 cm long NaCl segments in between each segment by using a 5 mL syringe (BD, United Kingdom). All solution segments were separated from each other by 1 cm long air plugs (Figure 4.3).

The production of double $W_1/O/W_2$ emulsion droplet requires partial surface modification of the microfluidic device. The microfluidic device used for generating double emulsion droplet composed of an upper part with a smaller channel dimension of 50 µm wide and the lower part with a wider channel dimension of 200 µm (Figure 4.4). The upper and the lower part of the device were joined at the second flow-focusing junction whereby the wettability of the channel was changed from hydrophobic to hydrophilic in order to assist the encapsulation of the single W/O droplet into double $W_1/O/W_2$ droplet. Immediately after microfluidic device preparation, the prepared polyelectrolyte sequences loaded in the PE tube were injected into the lower part of the device (Figure 4.4) while the device was still in a hydrophilic state. The whole sequence of PEM was flushed through inlet D at a constant flow rate of 50 µl h^{-1} using syringe pump (AL-1000, World Precision Instruments, United States) and exited at outlet A. Inlet B was flushed with deionised water at 100 µl h^{-1} to block the

streaming of polyelectrolytes solution into the upper part of the device while inlet C was closed during the process. At the end of the process, the lower part of the microfluidic device was coated with a sequence of PAH-PSS-PAH-PSS-PAH-PSS polyelectrolyte multilayer (PEM) rendering hydrophilic channel walls.

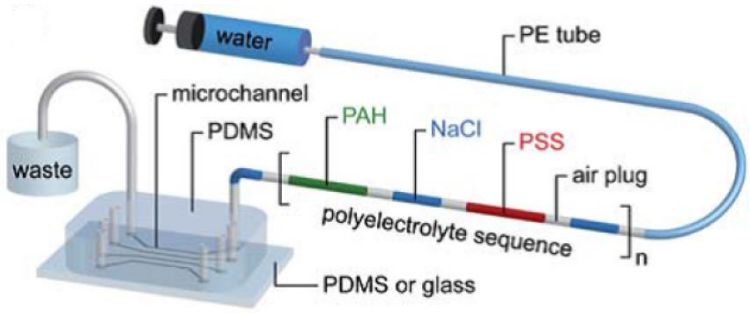

Figure 4.2 The schematic diagram of the hydrophilic treatment of the microfluidic device. The polyelectrolyte sequence (PEM) was flushed through the device by using a syringe pump at a constant flow rate of 50 µl h^{-1}, in order to apply a hydrophilic coating on the channel wall. Adapted from Bauer *et al*. (2010).

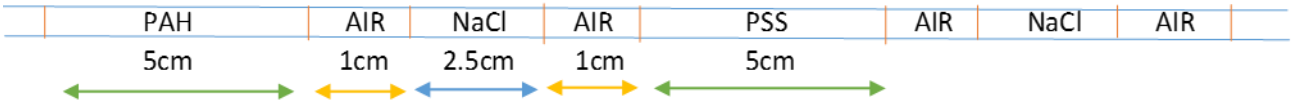

Figure 4.3 Polyelectrolyte multilayer (PEM) sequence in PE tube. The solutions were injected into the PE tube by using a syringe. Abbreviations, PAH: Poly(allylamine hydrochloride), NaCl: Sodium chloride, PSS: Poly(sodium 4-styrenesulfonate).

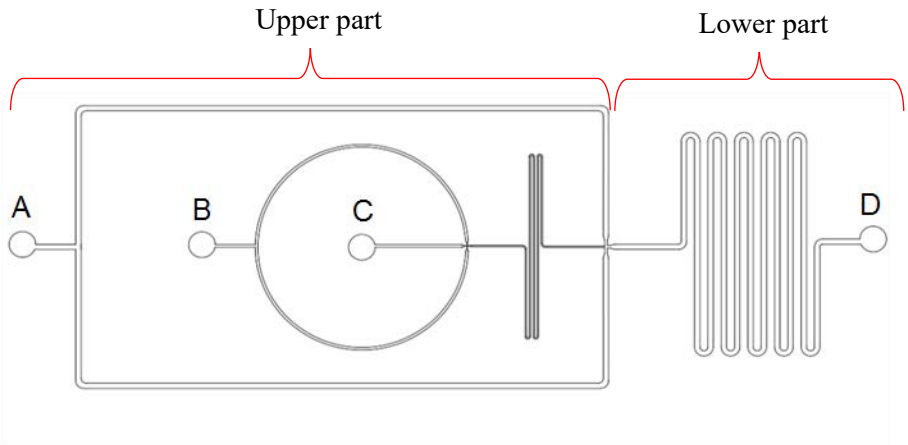

Figure 4.4 Hydrophilic treatment of $W_1/O/W_2$ droplet microfluidic device. The device was partially treated with PEM solutions that changed the lower part of the device from hydrophobic state to hydrophilic in order to ease the formation of $W_1/O/W_2$ droplet at the second junction. The partial hydrophilic treatment was conducted by flushing the PEM through inlet D and exited at outlet A. Inlet B was flushed with DIW to prevent the PEM from flowing through the upper part of the device while inlet C was closed.

4.2.4 Bacterial cell preparation

Bacterial culture was prepared for encapsulation in $W_1/O/W_2$ emulsion by culturing *Escherichia coli* strain SCC1 (MG1655-GFP mutation) expressing green fluorescent protein (*E. coli*-GFP) according to section 3.2.4.

4.2.5 Microfluidic encapsulation of *E. coli*-GFP in double $W_1/O/W_2$ droplet

Prepared culture of *E. coli*-GFP in LB broth or DI water was then used as the inner aqueous phase of $W_1/O/W_2$ droplet. The oil phase consisted of mineral oil with 1.5% w/v PGPR surfactant while the outer aqueous phase consisted of either LB broth or DI water with 1% w/v Tween 80 surfactant for samples used in the viability study. For the study that determined the effect of osmotic balance alterations on bacterial release and droplet stability, sodium chloride (NaCl) was added to either the inner W_1 phase (Hypo-osmotic) or outer W_2 phase (Hyper-osmotic) at 0.5%, 1.0% or 1.5% w/v with 1% or 5% w/v of Tween 80.

The bacterial encapsulation was done by using a double junction flow-focusing microfluidic device and a pressure controller (Elveflow, France) to produce a uniformed droplet of approximately 40-50 μm in diameter for inner aqueous phase (W_1) and approximately 100 μm in diameter for the oil globule (Figure 4.5). Pressure rates used were 300 mbar for the internal aqueous phase containing *E. coli*-GFP, 310 mbar for the middle oil phase and 330 mbar for the outer aqueous phase. For determining the effect of different pressure rates on droplet formation, the pressure rate for the inner aqueous phase was fixed to 300 mbar while the pressure rate for the middle oil phase and the outer aqueous phase was varied from 310 mbar to 330 mbar. The empty droplet of $W_1/O/W_2$ were also produced as controls to determine the effects of bacteria on droplet stability. All samples were kept statically in Eppendorf tubes at 25 °C.

a

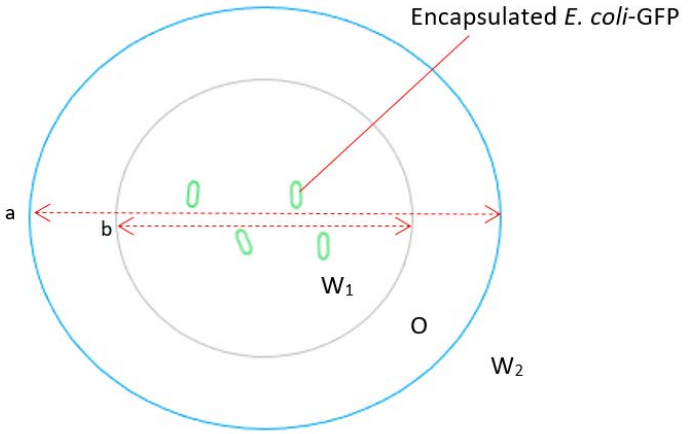

b

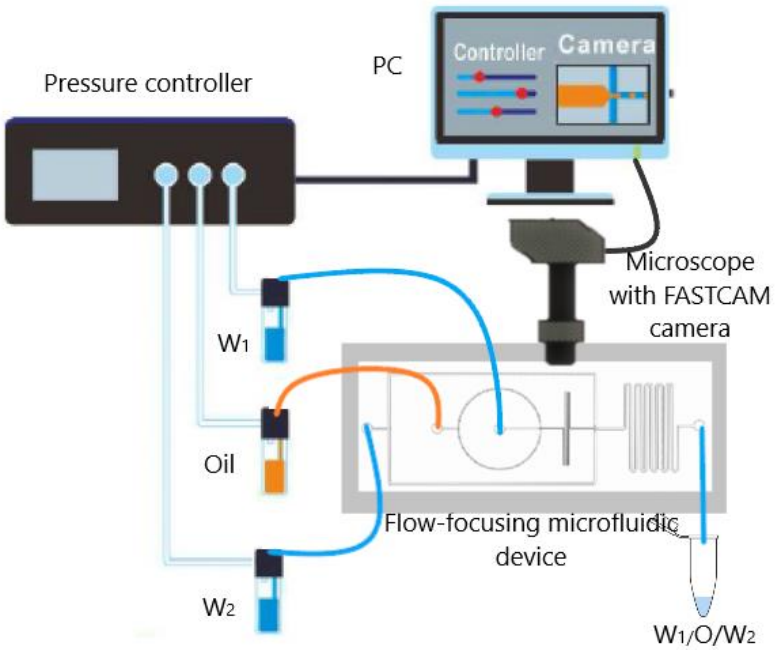

Figure 4.5 The microfluidic encapsulation process whereby (a) a schematic representation of the $W_1/O/W_2$ droplet containing *E. coli*-GFP. The diameter of the oil globule is given by a: 100 µm while the diameter of the inner aqueous phase is represented by b: 50 µm. The schematic representation of the microfluidic encapsulation was also represented in (b) whereby the different phases were flushed through the inlet by using a pressure controller and the produced $W_1/O/W_2$ droplet were collected continuously at the outlet. Droplet formation was monitored by using a microscope with FASTCAM camera.

4.2.6 Determining bacterial viability in different formulations of $W_1/O/W_2$

The viability of *E. coli*-GFP was determined for cells encapsulated in different formulations of $W_1/O/W_2$ as mentioned in section 4.2.5. Non-encapsulated bacteria dispersed in DIW or LB broth was prepared as controls. Serial dilutions of the sample were done using phosphate buffer saline (PBS) and viable cells were counted overtime for 24 hours using the Miles and Misra method (Miles and Misra, 1931) as described in section 3.2.5. In addition, the viability of bacteria in different components of LB broth was also determined. *E. coli*-GFP was suspended in 5g/L sodium chloride (NaCl), 10g/L tryptone and 5g/L yeast extract and the change in viable cell count were measured after 24 hours of incubation by using the Miles and Misra method.

4.2.7 Changes in metabolic activity

In order to determine the effect of encapsulation on the metabolic activity of bacteria, the change in glucose concentration in the presence of encapsulated and free *E. coli*-GFP cells was measured over time for 24 hours. Samples of encapsulated *E. coli*-GFP with DIW in both inner and aqueous phase was prepared along with samples of free *E. coli*-GFP suspended in DIW as non-encapsulated control. Non-bacterial controls were also prepared that included a sample with empty $W_1/O/W_2$ droplet. Approximately 2 ml of the prepared samples were transferred into LB broth supplemented with 0.6% w/v glucose and the change in glucose concentration was measured by using Accu-chek Aviva monitor with Accu-chek Aviva glucose test strips from Roche diagnostics (United Kingdom). The test was done according to the manufacturer instructions.

4.2.8 Fluorescence microscopy for bacterial observation

Fluorescence microscopy was done at room temperature for *E. coli*-GFP observation in $W_1/O/W_2$ emulsion droplet and to study the release of bacteria. The sample was prepared for microscopy by placing approximately 1 drop of sample onto the glass slide and covered with a

coverslip. In order to track the middle oil phase, the oil phase was stained with Nile red prior to sample preparation. The sample was then observed at 40X magnification and micrographs of the samples were acquired by using a Zeiss Axioplan microscope equipped with a 10-megapixel CMOS Motic Moticam digital colour camera system and Motic images plus software. The emission was observed at 509 nm for GFP and 640 nm for Nile red.

4.2.9 Measuring the encapsulation efficiency and release of bacteria from $W_1/O/W_2$ droplet

Encapsulation efficiency and the release of bacteria was determined by measuring the number of cells in the outer aqueous phase immediately after droplet preparation and over time for 3 hours for samples described in section 4.2.5. Samples were collected in Eppendorf tubes and kept statically upright at 25°C causing creaming or phase separation that divides the samples into a cream layer (oil globules) and serum phase (W_2) due to the difference in density between the two phases. Approximately 1 ml of serum phase was carefully withdrawn from the sample by using a pipette and serially diluted with PBS. Cell counts were done by plating on nutrient agar through Miles and Misra method (Miles and Misra, 1931).

As the serum phase does not contain oil globule, unencapsulated and released cells could be quantified according to the method described by El Kadri *et al.* (2015) with the following equation:

$$Encapsulation\ efficiency\ (\%) = \left((N_0 - N)/N_0\right) \times 100 \qquad (4.1)$$

$$Bacterial\ release = log_{10} N - log_{10} N_T \qquad (4.2)$$

Where N is the viable cell count for unencapsulated bacteria in W_2 immediately after emulsion preparation and N_0 is the total number of viable cell count before encapsulation into $W_1/O/W_2$. N_T is the number of viable cells in the W_2 phase at incubation time, T.

4.2.10 Determination of droplet size and phase separation

The effect of different pressure ratios on the production of monodispersed $W_1/O/W_2$ droplet was determined by measuring the size of the droplet immediately after formation. In addition, changes in the diameter of the inner aqueous phase (W_1) and the oil globule was also measured overtime for 3 hours at 25°C. Optical microscopy and image analysis were done according to section 3.2.6.

Droplet stability was also determined by measuring changes in creaming behaviour of the $W_1/O/W_2$ with or without the presence of *E. coli*-GFP. Creaming behaviour measurement was done by collecting 1 ml of sample into graduated syringes immediately after droplet preparation. The samples were left upright for 1 hour at 25 °C to allow the formation of a cream layer. The cream thickness was then measured immediately after creaming and during incubation time at 30, 60 and 180 minutes. The creaming volume was measured as follows:

$$Change\ in\ creaming\ volume\ (\%) = \frac{(C_0 - C_T)}{C_0} \times 100 \qquad (4.3)$$

Where C_0 is the creaming height at time 0 while C_T is the creaming height at incubation time, T.

4.2.11 Statistical analysis

The data obtained from the experiments were analysed according to section 3.2.12

4.3 Results and discussion

4.3.1 One-step generation of $W_1/O/W_2$ droplet incorporated with bacteria

Water-in-oil-in-water ($W_1/O/W_2$) double emulsion droplet were produced by using a single PDMS microfluidic chip (Figure 4.6) which consisted of two flow-focusing junctions that allowed for continuous one-step generation of double emulsion droplet in a high-throughput manner. The parameters used for droplet generation was tested in order to produce highly monodispersed droplet for bacterial encapsulation. By tuning the pressure introduced for the oil phase (P_{oil}) and the outer aqueous phase (P_{w2}), the size of the internal aqueous phase and the oil globule can be controlled which also allowed the production of droplet with single or multiple internal aqueous phase (Okushima *et al.*, 2004). The effect of different pressure rates on the formation of $W_1/O/W_2$ was presented in Figure 4.7 and Figure 4.8.

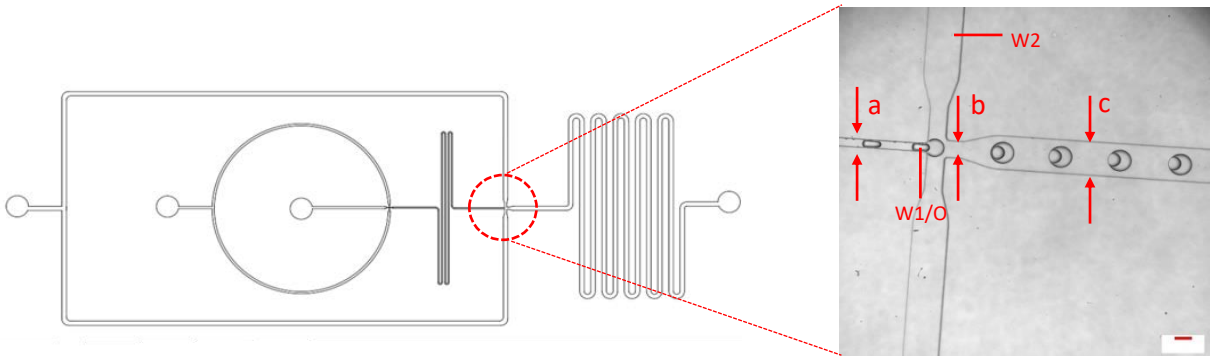

Figure 4.6 Monodispersed $W_1/O/W_2$ droplet formation with 2-junctions flow focusing device with (a) 50 µm (b) 100 µm and (c) 200 µm. Scale bar represents 100 µm.

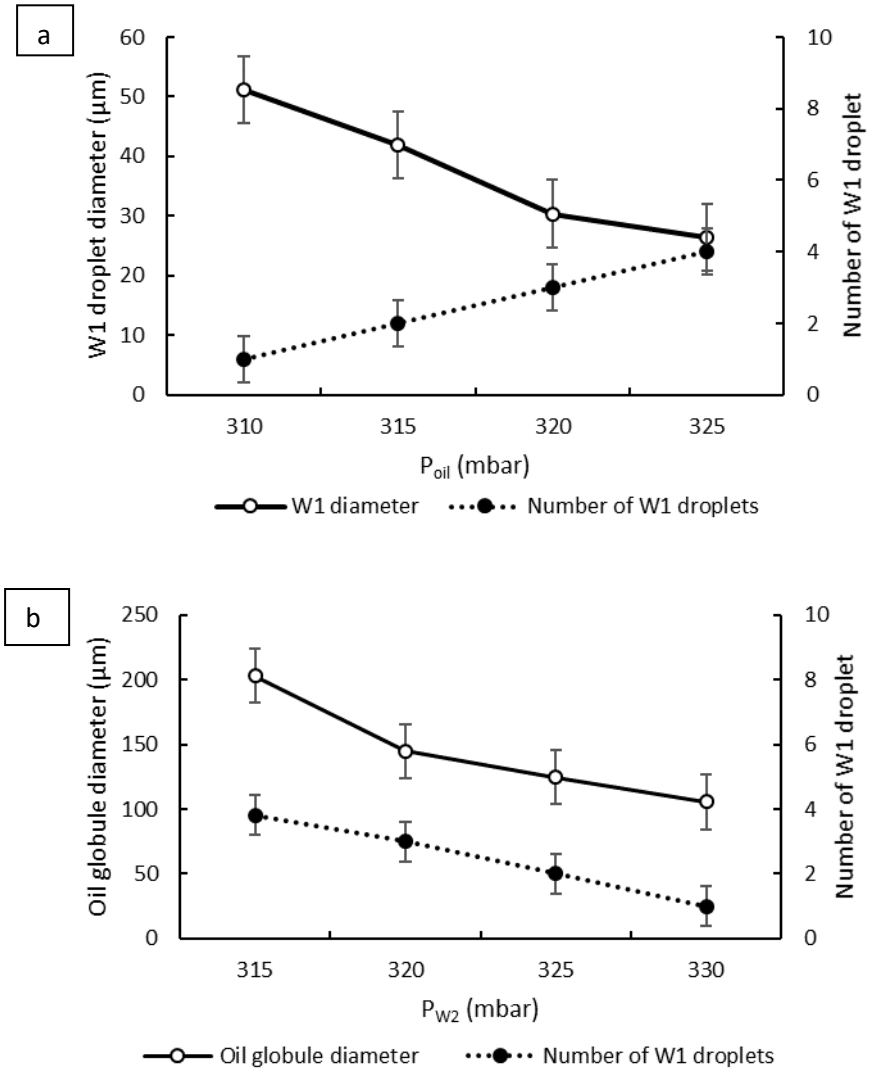

Figure 4.7 The effect of different pressure rates on the formation of $W_1/O/W_2$ emulsion droplet: (a) The effect of different oil phase pressure rates (P_{oil}) on the internal aqueous droplet (W_1) diameter and the number of internal aqueous droplet and (b) the effect of different outer aqueous phase pressure rate (P_{W2}) on the size of the oil globule and number of internal aqueous droplet. Bars represent mean ± SD from 10 independent experiments (N=10).

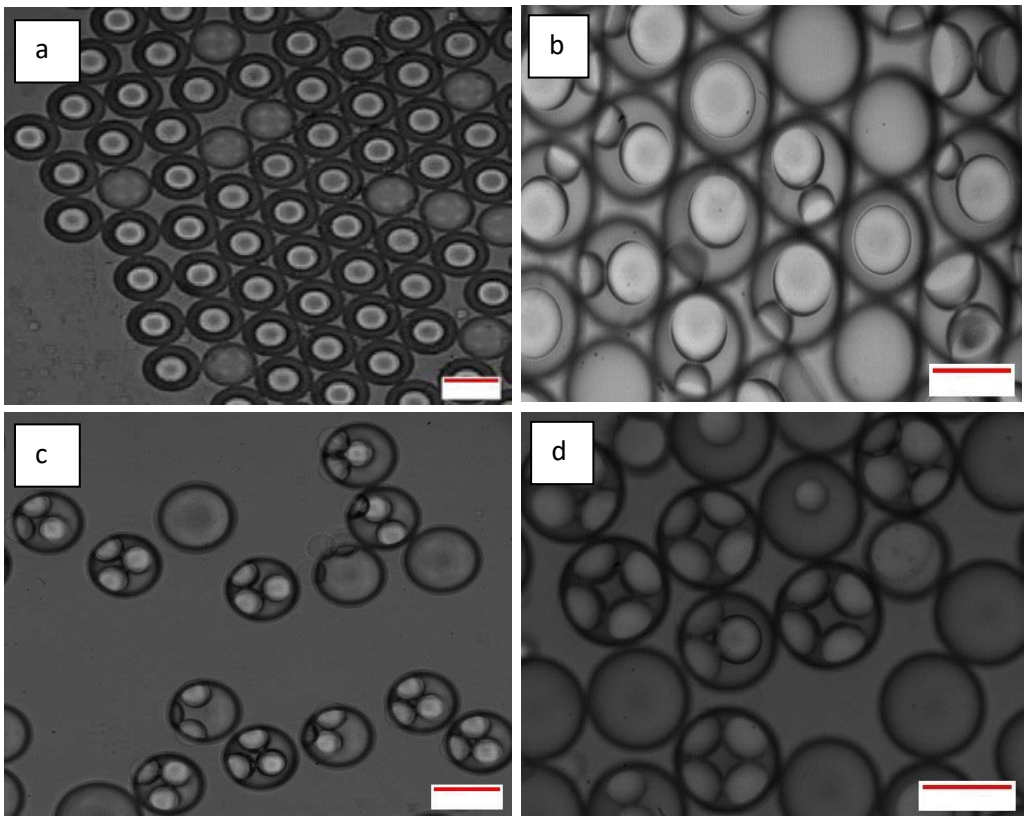

Figure 4.8 $W_1/O/W_2$ droplet with different configuration produced at a fixed pressure rate of 300 mbar for W_1 and 330 mbar for W_2. Droplet were produced at different oil phase pressure rates of: (a) 310 mbar, (b) 315 mbar, (c) 320 mbar and (d) 325 mbar. Scale bar represents 100 µm.

Figures 4.7 (a) and 4.8 show the effects of different oil phase pressure rates (P_{oil}) on the average diameter of the internal aqueous droplet (W_1) and the number of internal aqueous droplet enclosed in the oil globule at a fixed pressure rate of 300 mbar for the internal aqueous phase and 330 mbar for the outer aqueous phase. From the graph, it was observed that by increasing the pressure rate for the oil phase from 310 mbar to 325 mbar, the size of the W_1 droplet formed at the first junction decreased from approximately 50 μm to 25 μm in diameter. As the pressure rate for the internal aqueous phase was fixed at 300 mbar, the reduction in droplet size is due to the increase in shear rate causing the droplet to break easily at the first junction. On the other hand, an increase in the oil phase pressure rate causes a reduction in the shear rate at the second junction as it increases the overall pressure of the W/O droplet that travels from the first junction to the second junction. The closer the pressure rate value of the oil phase to the fixed pressure rate of 330 mbar set for the outer aqueous phase, the harder for the droplet to break at the junction due to low shear rate. The oil globule tends to elongate before breaking forming $W_1/O/W_2$ droplet with multiple internal aqueous phases.

Different format of $W_1/O/W_2$ droplet can also be produced by tuning the pressure rate of the outer aqueous phase (P_{w2}). From Figure 4.7 (b), it was determined that at a fixed pressure of 300 mbar for the internal aqueous phase and 310 mbar for the oil phase, an increase in the pressure rate of the outer aqueous phase caused a decrease in the oil globule diameter that resulted in a decrease in the number of internal aqueous droplet. An increase in the outer aqueous phase pressure rate increases the shear rate that allows the droplet to be able to break easily at the junction forming smaller droplet with less number of the internal aqueous phase. As the pressure rate increases from 315 mbar to 330 mbar, the oil globule size decreases from approximately 200 μm to 100 μm in diameter while the number of the internal aqueous phase decreases from 4 to 1 droplet per oil globule.

From the results obtained, it was determined that by tuning the pressure rate of the oil and outer aqueous phase, $W_1/O/W_2$ droplet with different configuration can be produced in a controllable manner with high monodispersity (droplet CV value of 4 to 6%). In order to study the emulsion stability and release of bacteria from the double emulsion microstructure, $W_1/O/W_2$ droplet with single internal core are deemed suitable as it may allow a close observation on the emulsion behaviour. Therefore, a set of pressure rate that allows for the formation of $W_1/O/W_2$ droplet with single-core was chosen for this study which consists of 300 mbar for the internal aqueous phase, 310 mbar for the oil phase and 330 mbar for the outer aqueous phase.

4.3.2 Encapsulation efficiency

The determination of encapsulation efficiency was done by measuring the number of viable free cells before and after the microfluidic encapsulation process. The results obtained show a high encapsulation efficiency indicating successful encapsulation of *E. coli*-GFP in $W_1/O/W_2$ droplet with approximately 99.9% of encapsulated viable cells as presented in Table A1 (Appendix 2).

4.3.3 The viability and metabolic activity of bacteria encapsulated in $W_1/O/W_2$ droplet

To understand the effect of encapsulation on the growth and metabolic activity of *E. coli*-GFP, the viability and rate of glucose consumption of the bacteria were determined by Miles and Misra method (Miles and Misra, 1931) and measuring the change in glucose concentration respectively. Samples of *E. coli*-GFP encapsulated in $W_1/O/W_2$ droplet with or without the presence of LB broth in the internal and outer aqueous phase was prepared and bacterial viability was determined as described in section 4.2.6. Samples of non-encapsulated bacteria suspended in DIW or LB broth was also prepared as controls. For bacterial metabolic activity determination, approximately 2 mL of encapsulated and non-encapsulated *E. coli*-GFP

suspended in DI water was transferred into LB broth supplemented with 0.6% w/v glucose and the change in glucose concentration was measured over time for 24 hours by using Accu-chek Aviva glucose monitor as described in section 4.2.7. The effect of different $W_1/O/W_2$ formulation on bacterial viability was presented in Figure 4.9 while the changes in the metabolic activity of the bacteria are presented in Figure 4.10.

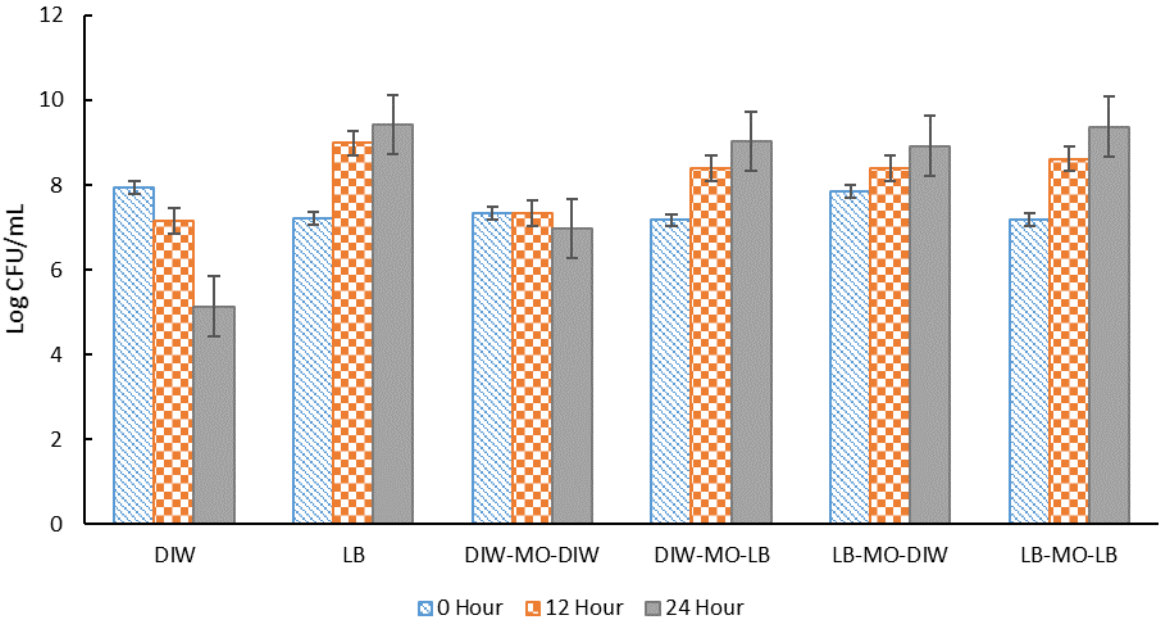

Figure 4.9 The effect of different $W_1/O/W_2$ formulations on the viability of *E. coli*-GFP cells. Free cells in DIW and LB broth were tested as controls against samples of bacteria encapsulated in $W_1/O/W_2$. Log CFU/mL of the samples were determined at 0, 12 and 24 hours of incubation. Bars represent mean ± SEM taken from 3 independent experiments with 3 replicates for each experiment (N=3). Abbreviations, DIW: Deionised water, MO: Mineral oil with 1.5% PGPR, LB: LB broth.

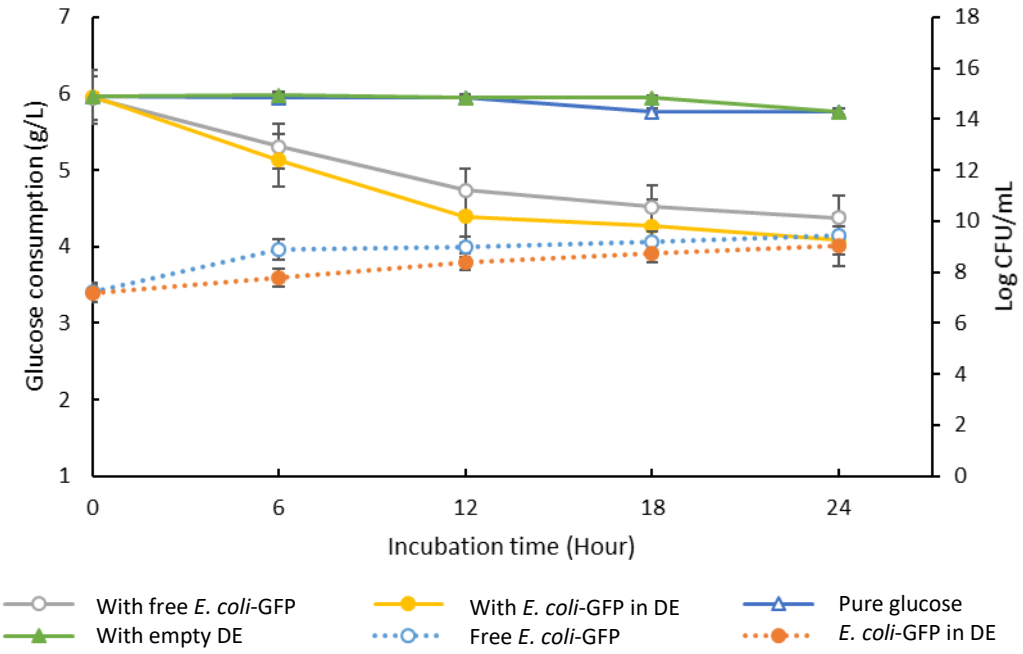

Figure 4.10 Changes in glucose concentration in the presence of encapsulated and free *E. coli*-GFP cells. The solid lines represent data for glucose consumption for samples containing free *E. coli*-GFP and encapsulated *E. coli*-GFP in DE against control samples containing empty DE and pure glucose (without the addition of free bacteria, encapsulated bacteria in DE or empty DE). The dotted lines represent changes in log CFU/ml for free (unencapsulated) bacterial cells and encapsulated cells in DE. All of the prepared samples are transferred into LB broth supplemented with 0.6% w/v glucose. Bars represent mean ± SEM taken from 3 independent experiments with 3 replicates for each experiment (N=3). Abbreviation, DE: Double emulsion.

Figure 4.9 shows the viability of *E. coli*-GFP encapsulated in the different formulation of $W_1/O/W_2$ emulsion droplet. As expected, the absence of LB broth caused a reduction in bacterial viability for both encapsulated and non-encapsulated samples whereby a greater reduction in bacterial viability was observed for free *E. coli*-GFP cells as compared to encapsulated cells. In the absence of nutrient (samples of *E. coli*-GFP in DIW only), the sample of free *E. coli*-GFP cell in DIW show a reduction in viable cell count from 7.94 log CFU/mL at 0 hour to 5.13 log CFU/mL at 24 hour of incubation time (a 2.81 log CFU/mL reduction) while for encapsulated sample in $W_1/O/W_2$ (DIW-MO-DIW), the viable cell count reduced from 7.33 log CFU/mL to 6.97 log CFU/mL (a 0.33 log CFU/ML reduction). In the presence of LB broth, the log CFU/mL of *E. coli*-GFP increased over time (from 0 hours to 24 hours) for all formulations. A better increase in log CFU/mL was observed for free *E. coli*-GFP suspended in LB broth and encapsulated with the presence of LB broth in both internal and outer aqueous phase compared to cells encapsulated with LB broth in either inner or outer aqueous phase. Referring to samples with LB broth in either inner or outer aqueous phase, samples prepared with LB broth in outer aqueous phase show better increase in log CFU/mL compared to samples with LB broth in inner aqueous phase only.

In addition, the encapsulation of bacteria also caused changes in the metabolic activity of the *E. coli*-GFP as shown in Figure 4.10. From the results obtained, it was observed that the reduction in glucose concentration was faster for samples containing encapsulated *E. coli*-GFP cells as compared to samples with free cells although free *E. coli*-GFP cells show a better increase in log CFU/mL compared to encapsulated samples in $W_1/O/W_2$ droplet. Samples containing encapsulated *E. coli*-GFP resulted in 31.42% of reduction in glucose concentration after 24 hours of incubation compared to samples containing free *E. coli*-GFP cells that show 26.36% reduction. These results suggested that encapsulation in $W_1/O/W_2$ improve bacterial

viability and the presence of LB broth promotes bacterial growth especially in samples with nutrients in the outer aqueous phase. Moreover, the encapsulation of bacteria also caused changes in the metabolic activity of the bacteria as the encapsulated bacteria shows higher activity in terms of glucose consumption compared to non-encapsulated samples.

The ability of double emulsion system in improving the viability of bacterial cells during storage, processing and against harsh processing conditions has been reported previously in various studies (Shima *et al.*, 2006; Pimentel-Gonzalez *et al.*, 2009; Rodríguez-Huezo *et al.*, 2014; Lalou, Kadri and Gkatzionis, 2017; Devanthi *et al.*, 2018). The protective effect of the double emulsion is mainly attributed to its role as a buffer against harsh environmental conditions (Pimentel-Gonzalez *et al.*, 2009). However, in order to maintain the viability of the encapsulated bacteria especially during long term storage, the presence of nutrient is equally important whereby a continuous supply of nutrient is required in order to support bacterial growth in emulsion droplet.

As discussed previously in section 3.3.3, the growth of *E. coli*-GFP, encapsulated in single W/O droplet was suspended due to an inadequate supply of nutrient to support bacterial growth. Therefore, by encapsulating bacteria in double $W_1/O/W_2$ emulsion droplet, continuous supply of nutrient can be made possible by nutrient replenishment from the outer aqueous phase. It has been reported previously that the middle oil phase of the $W_1/O/W_2$ acts as a selective barrier that modulates the transport of molecules, allowing the diffusion of nutrients and small inducer molecules through the interface (Chan *et al.*, 2013, 2017; Zhang *et al.*, 2013). This creates a programmable microenvironment whereby $W_1/O/W_2$ emulsion droplet serve as micro-incubator that helps in sustaining the growth of bacteria. Other than that, the presence of the outer aqueous phase also improves oxygen permeability through the interface and prevents desiccation caused by the evaporation of the oil phase (Zhang *et al.*, 2013). Furthermore, the

immobilization of bacteria in $W_1/O/W_2$ droplet may cause morphological and physiological changes (Zur, Wojcieszyńska and Guzik, 2016).

The effect of immobilization on the metabolic activity of *E. coli* cells have been described in previous studies including an increase in the metabolic activity of *E. coli* cells due to their adhesion onto a glass surface (Hong and Brown, 2009), an increase in oxidized glucose metabolites (Zur, Wojcieszyńska and Guzik, 2016) and the entrapment of *E. coli* cells that resulted in better enzymatic activity and reduced degradation of RNA (Lyngberg *et al.*, 1999). The effect of encapsulation in $W_1/O/W_2$ droplet on the metabolic activity *Z. rouxii* has also been reported previously whereby the entrapment of *Z. rouxii* resulted in accelerated glucose consumption (Devanthi, El Kadri, *et al.*, 2018). The change in metabolic activity may be attributed to the change in microenvironment conditions such as a reduction in the water activity and oxygen supply which usually occurs in an immobilized microenvironment (Zur, Wojcieszyńska and Guzik, 2016). These changes not only affect the metabolic activity of microorganism but also make it less susceptible to environmental stresses. Nevertheless, further studies are still required in order to understand the effect of $W_1/O/W_2$ droplet on the metabolic activity of bacteria as well as understanding the mechanism behind the change in metabolic activity of the encapsulated bacteria.

Although the encapsulation of bacteria in $W_1/O/W_2$ droplet with the presence of nutrient helps in improving the viability and promotes bacterial growth, the effectiveness of the system depended on the stability of the droplet. Therefore, further study is required to understand the stability of $W_1/O/W_2$ droplet in these conditions.

4.3.4 The release of bacteria by osmotic balance alterations

As discussed previously in section 4.3.3, the encapsulation of bacteria in $W_1/O/W_2$ droplet improves bacterial viability and promotes the growth of bacteria with the presence of nutrient in the outer aqueous phase. However, the addition of nutrients in the outer aqueous phase may cause osmotic imbalances that lead to the release of the encapsulated bacteria. This may affect the long term storage of samples and thus, it is important to understand the effect of osmotic imbalances towards droplet stability and the release of bacteria. In addition, other than protecting the bacteria against harsh conditions, the controlled release of bacteria is also one of the most interesting applications of $W_1/O/W_2$. Therefore, the study of the release of bacteria not only provides an insight on droplet stability but also provides interesting information on the application of $W_1/O/W_2$ in controlled release of bacteria that may be beneficial for various industrial applications.

To study the effect of osmotic alterations on droplet stability and bacterial release, it is important to ensure that the solute used is not able to support bacterial growth as it may affect the accuracy of the results. LB broth consists of 10 g/L of tryptone, 5 g/L of yeast extract and 5g/L of sodium chloride. Each of these ingredients was tested for its ability to support bacterial growth (Table A2, Appendix 3). The results obtained show that sodium chloride (NaCl) does not support the growth of *E. coli*-GFP as approximately 1.48% of reduction in viable cell counts was observed after 24 hours incubation at 37 °C. However, it is crucial to take into account the effect of different NaCl concentration on the viability of the bacteria and to determine the tolerable level of NaCl for the bacteria as it may affect the accuracy of the results obtained. In a study conducted by Roeßler, Sewald and Müller (2003), a significant effect on the growth of *E. coli* was only observed at high NaCl concentration of 1.2 M (7.0 % w/v) while at lower NaCl concentration, no significant ($P > 0.05$) changes in the final OD_{578} was observed between

samples with 0.1 M of NaCl (0.58% w/v) and 0.8 M of NaCl (4.67% w/v). Therefore, only NaCl was used in this study at a low concentration concentration of 0.5% w/v (similar to that found in LB broth), 1.5% w/v and 2.0% w/v. The effects of NaCl addition in the inner aqueous phase and the outer aqueous phase was studied that creates hypo-osmotic and hyper-osmotic conditions respectively.

The release of *E. coli*-GFP into the outer W2 phase of the $W_1/O/W_2$ emulsion prepared with different formulations are presented in Figures 4.11 and 4.12. From the results obtained, it was observed that osmotic balance alterations due to the addition of NaCl in W_1 or W_2 phases resulted in a significant increase ($P < 0.001$) in viable cell count in the outer aqueous phase (W_2). The rate of increase in log CFU/mL dependent on NaCl concentration and the Tween 80 concentration in W_2 whereby a better increase in viable cell count was observed for samples with higher NaCl concentration and lower Tween 80 concentration as compared to samples containing lower NaCl concentration and higher Tween 80 concentration. Comparing between hypo-osmotic (NaCl in W_1) and hyper-osmotic condition (NaCl in W_2), a higher increase in log CFU/ mL was observed for samples in hyper-osmotic condition as compared to samples in the hypo-osmotic condition during the three hours of the incubation period. For example, referring to Figure 4.11 a for samples with 1% w/v of Tween 80 in the W_2 phase, the presence of 2.0% w/v NaCl in the W_2 phase (hyper-osmotic) resulted in 4.86 log CFU/mL increase of bacterial cell count in W2 phase at 180 minute (3 hours) of incubation period as compared to only 3.69 log CFU/mL increase for sample with 2.0% of NaCl in the W1 phase (hypo-osmotic). The results obtained show that the release of bacteria into the outer W_2 phase is dependent on the concentration of NaCl added in either inner or outer aqueous phase as it creates osmotic pressure imbalances (Figure 4.11). This, in turn, caused emulsion destabilization with changes in droplet diameter that leads to the release of bacteria into the outer W_2 phase (Figure 4.12).

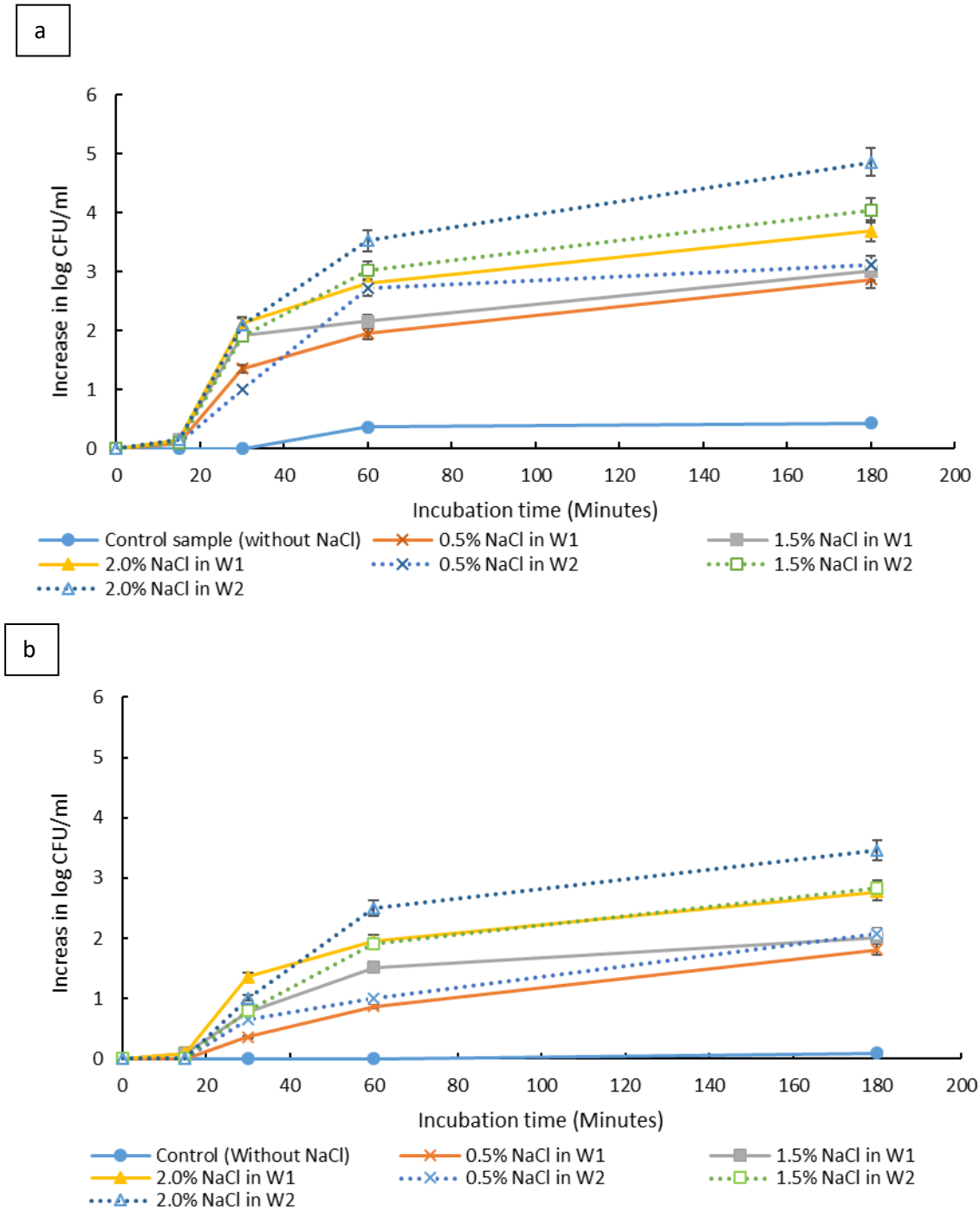

Figure 4.11 The release of *E. coli*-GFP into the outer aqueous phase (W_2) of $W_1/O/W_2$ droplet at 15, 30, 60 and 180 minutes of incubation at 25°C. Samples were prepared with different sodium chloride concentration in either inner (W_1) or outer aqueous phase (W_2). Tween 80 concentration in W_2 was also differentiated with (a) 1% w/v and (b) 5% w/v. Bars represent mean ± SEM taken from 3 independent experiments with 3 replicates for each experiment (N=3).

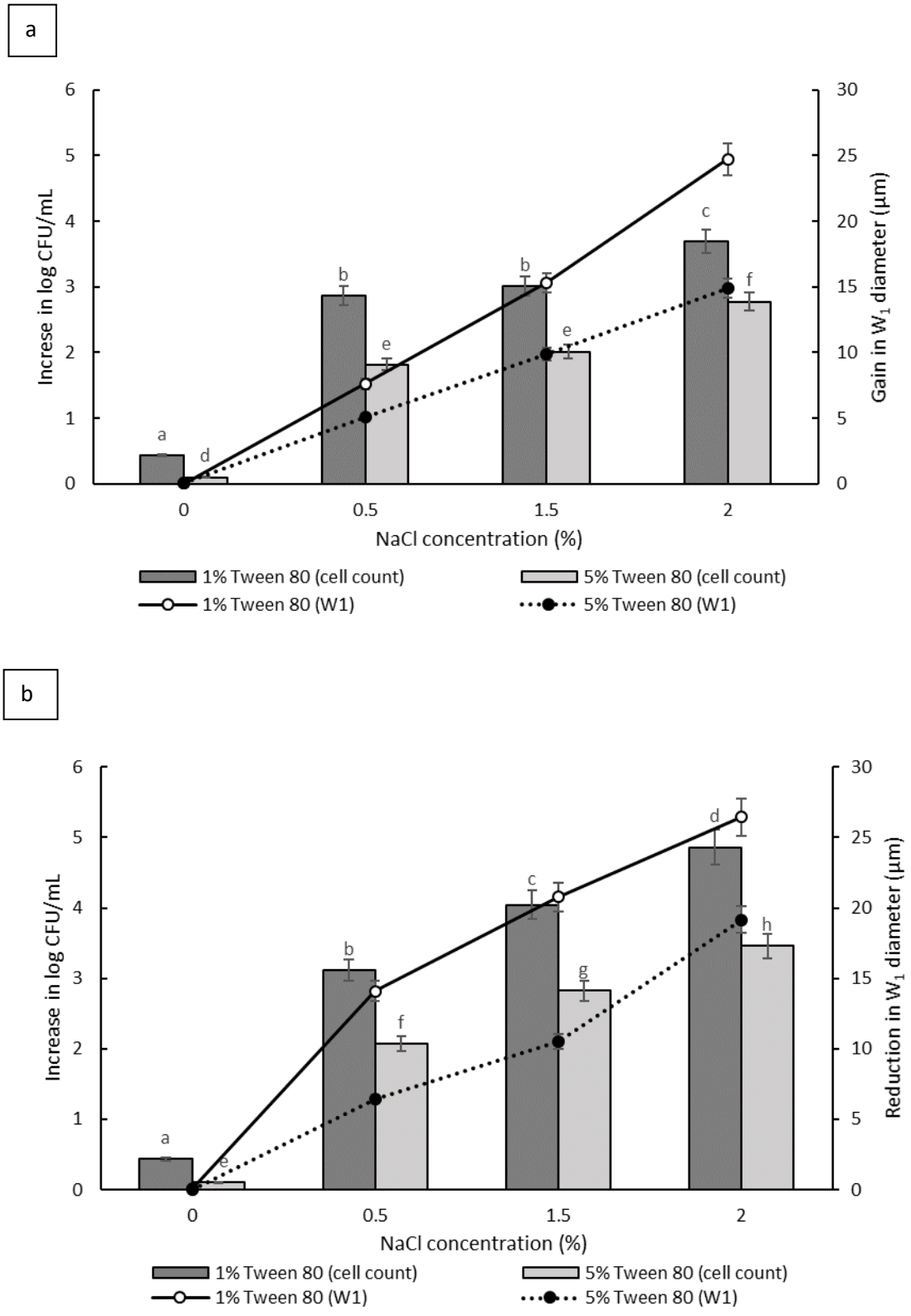

Figure 4.12 Increase in viable cell count and changes in droplet diameter with different NaCl concentration of 0%, 0.5%, 1.5% and 2.0% w/v in inner W_1 phase (a) and outer W_2 phase (b) of $W_1/O/W_2$ emulsion droplet after 3 hours of incubation. Bar chart represents the data for the increase in viable cell count while the line graph represents the data for changes in droplet diameter. Bars represent mean ± SEM taken from 3 independent experiments with 3 replicates for each experiment (N=3). The data for the increase in viable cell count was analysed with one-way ANOVA. ^{abcdefgh}mean ± SEM with different letters is significantly different at $P < 0.05$.

Microscopic observation was done immediately after droplet formation. The oil phase was stained with Nile red in order to distinguish between the middle oil phase from the inner and outer aqueous phase (Figure 4.13c). Droplet observation reveals the splitting of $W_1/O/W_2$ droplet forming a secondary double emulsion containing bacteria enclosed by a very thin film during the first 30 minutes of observation (Figure 4.13a). No bacteria were observed in the outer W_2 phase during droplet splitting which was confirmed by bacterial cell count whereby no increase in log CFU/mL was observed for all samples during the first 15 minutes of incubation (detection limit: 10^3 CFU/mL). An increase in viable cell count was only observed at 30 minutes which occurs immediately after droplet separation and continues to increase during 3 hours of incubation (Figure 4.11, 4.13b).

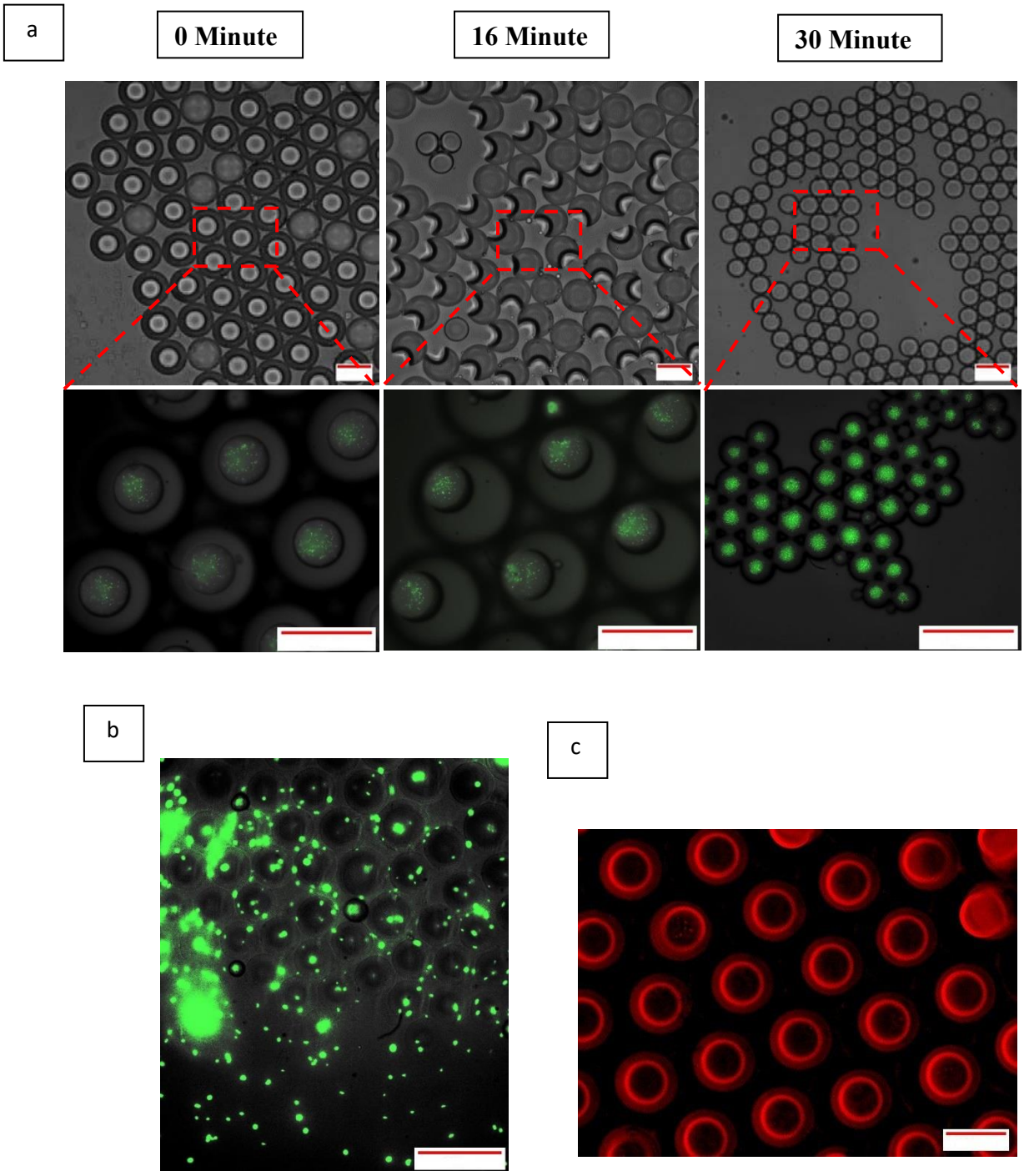

Figure 4.13 Optical and fluorescence photomicrographs of droplet splitting releasing inner W_1 phase (a) leading to release of bacteria from the released inner W_1 droplet after 3 hours of incubation (b). The oil phase was stained with nile red in order to distinguish between the aqueous and the oil phase (c). Droplet were prepared with 0.5% NaCl and 1% of Tween 80 in outer W_2 phase. Scale bar represents 100 µm.

Overall, the instability of $W_1/O/W_2$ induced by osmotic balance alterations leads to the release of bacteria. Droplet destabilization begins with the splitting of $W_1/O/W_2$ droplet producing secondary double emulsions with thin oil layer at the interface followed by changes in droplet size as a function of NaCl concentration that causes swelling of droplet with the addition of NaCl in the inner W_1 phase or shrinking of droplet with NaCl incorporated in the outer W_2 phase. Bacterial release occurs only after droplet splitting as shown in Figure 4.11 whereby a significant ($P < 0.001$) increase in viable cell count was observed after 30 minutes of incubation. Furthermore, the bacterial release also occurs for samples containing a similar concentration of NaCl in the LB broth (0.5% w/v) thus, increase in bacterial cell count in the presence of LB broth as mentioned in section 4.3.3 could be attributed to the release of bacteria into the W_2 phase. However, this process is highly complex and requires further investigation as with the presence of LB broth, the difference in osmotic balance does not only cause the migration of water but also nutrients through the interface.

The double emulsion system of $W_1/O/W_2$ is metastable in which the inner aqueous phase tends to escape into the continuous outer phase forming into a more stable and direct system of O/W. In a $W_1/O/W_2$ system, the difference in density between the oil and the aqueous phase caused the inner W_1 droplet to move towards the bottom of the oil globule and eventually escape into the outer W_2 phase forming a small oil globule that moves upwards leaving the inner W_1 water droplet immersed in the outer W_2 phase. The escaped water droplet persisted within the outer W_2 phase and are held by a thin film that consists of a complex mixture of oil and surfactants (González-Ochoa, Ibarra-Bracamontes and Arauz-Lara, 2003). Jiao, Rhodes and Burgess (2002) also reported on the formation of a dimpled structure caused by the inner droplet that was very close to the interface, separated by only a thin film from the outer aqueous phase. The formation of the dimpled structure was related to the strength of the thin film

surrounding the water droplet in which a film with high elasticity is required to maintain its stability. By increasing the NaCl concentration of the outer W_2 phase, the interfacial elasticity of the thin film decreases causing droplet instability. Rapid release of bacteria occurred immediately after the splitting process as the escaped droplet were only being held by a thin film, therefore, accelerating the migration of water between the aqueous phases that eventually leads to droplet destabilization. This consequently resulted in bacterial release into the W_2 phase. In a study done by Zhang *et al.* (2017), the intentional destabilization of the droplet by using an ultrathin layer of polymeric shells makes it highly susceptible to osmotic shock due to the rapid diffusion of water into the droplet. Therefore, an immediate burst of droplet releasing encapsulated cargo can be triggered easily by only adding a large amount of water in the outer phase causing the droplet to swell and burst instantly.

It has been reported previously that osmotic alterations in $W_1/O/W_2$ may cause droplet instability that leads to bacterial release (El Kadri *et al.*, 2015; 2016; Devanthi, *et al.*, 2018). El Kadri *et al.* (2015; 2016) reported that the released of bacteria from $W_1/O/W_2$ under hypo-osmotic and hyper-osmotic conditions was induced by changes in osmotic balance, the amount of W_1 phase and surfactant concentrations whereby a better increase in bacterial release was observed at high amount of NaCl and W_1 phase along with a low concentration of surfactants. In these studies, the release of bacteria in both hyper-osmotic and hypo-osmotic conditions is triggered by the bursting of $W_1/O/W_2$ droplet. Under hypo-osmotic conditions, the swelling of droplet caused the thinning of the interface resulted in film rupture that released the bacteria into the outer aqueous phase (Kadri *et al.*, 2016). However, the release of bacteria under hyper-osmotic conditions is not caused by the change in droplet size but due to the migration of surfactants desorbing from the interface as water migrates from the inner aqueous phase towards the outer aqueous phase of higher solute concentration (Kadri *et al.*, 2015). At higher

surfactant concentration, the replacement of surfactants in the gaps created by the swelling of the droplet under hypo-osmotic conditions and the loss of surfactants from the interface of the droplet under hyper-osmotic conditions is much faster compared to samples with lower surfactant concentration making it much more stable and delays bacterial release.

In addition, higher bacterial release was observed for samples prepared under hyper-osmotic conditions as compared to samples prepared under hypo-osmotic conditions which are attributed to the Laplace and osmotic pressure balance. The Laplace pressure resulted in the shrinkage of the droplet and is depended on its radius given by:

$$\Delta P = \frac{2\gamma}{r} \qquad (4.4)$$

Where γ is the interfacial tension and r is the droplet's radius (Walstra, 1993). As ΔP is inversely associated with the radius, the smaller radius will cause larger inward force that resulted in droplet shrinkage. However, with the presence of NaCl in the inner W_1 phase (hypo-osmotic), the osmotic pressure resulted in the swelling of the droplet that counterbalanced the Laplace pressure (Jiao, Rhodes and Burgess, 2002). The balance between the osmotic and Laplace pressure is given by the Walstra equation (Walstra, 1993):

$$2\gamma = 3mRT \qquad (4.5)$$

in which m is the molar concentration of NaCl, R is the universal gas constant and T is temperature. From this equation, it is shown that optimal NaCl concentration in the internal W_1 phase is required in order to reach equilibrium. Jiao, Rhodes and Burgess (2002) reported that the stability of double $W_1/O/W_2$ droplet is improved as the salt concentration is closer to the optimal value of 13.4 mol m^{-3} calculated from equation 4.5. Therefore, emulsions prepared under hypo-osmotic conditions are more stable as compared to emulsions under hyper-osmotic conditions resulting in a lower bacterial release.

The difference in density between the oil and the aqueous phase is mentioned in Table A3 (Appendix 4) whereby DIW has a higher density than mineral oil and the density increases with increase in NaCl concentration that caused the splitting of the $W_1/O/W_2$ droplet. As the W_1 water droplet escaped into the outer W_2 phase, the difference in osmotic pressure between the phases caused the diffusion of water through the thin film to be accelerated due to the decrease in interfacial strength. This eventually leads to the release of bacteria into the outer W_2 phase due to the swelling of the droplet (for samples under hypo-osmotic condition) and the loss of surfactants from the interface of the droplet, (for samples under hyper-osmotic condition) as water migrates through the interface causing film rupture. As the release of bacteria highly depended on the stability of the droplet, further study on the stability of droplet such as by measuring the change in the size of both W_1 phase and oil globule during osmotic balance alterations is important in order to further understand its effect on the release of *E. coli*-GFP.

4.3.5 The effect of different osmotic conditions on droplet size change

In this section, the stability of $W_1/O/W_2$ emulsion droplet incorporated with bacteria and the effect of osmotic balance alterations on droplet stability was investigated. $W_1/O/W_2$ droplet samples with or without *E. coli*-GFP in the internal aqueous phase were prepared with different osmotic conditions and Tween 80 concentrations as mentioned in section 4.2.5. Real-time observation on droplet behaviour was done microscopically and changes in the size of the droplet (for both internal W_1 phase and oil globule) was quantified in order to understand the effect of different formulation on the stability of the $W_1/O/W_2$ emulsions droplet.

The diameter of the W_1 phase and oil globule was measured by analysing the photomicrographs of the droplet with MATLAB software. Photomicrographs of the droplet were taken at every time interval that includes, immediately after droplet preparation (0

minutes), immediately after the release of the W_1 inner droplet (30 minutes) and followed by 1 to 3 hours after the separation process. The oil globule phase was distinguished from the inner W_1 droplet by staining the oil with Nile red prior to the encapsulation process. In addition, the inner W_1 phase was also identified with the presence of *E. coli*- GFP as the hydrophilic nature of the cells making it more likely to remain in the aqueous phase rather than the oil phase.

Table 4.1 summarizes the change in the diameter of the inner W_1 phase and oil globule during the 3 hours of the incubation period. From the results obtained, it was determined that osmotic alterations (by adding 1.5% w/v of NaCl) in either inner W_1 phase or outer W_2 phase caused significant ($P < 0.001$) changes in W_1 diameter whereby a gain in diameter was observed for samples prepared under hypo-osmotic (NaCl in W_1 phase) conditions whereas a reduction in diameter was observed for samples under hyper-osmotic (NaCl in W_2 phase) conditions. Change in droplet diameter was minimized at high concentration of Tween 80 (5%) compared to low concentration in Tween 80 (1%). Furthermore, a slight change in the diameter of the W_1 droplet was observed during the first 30 minutes of the incubation period that increased rapidly after one hour. No significant ($P = 1.00$) change in W_1 droplet size was observed for samples without NaCl.

Referring to results obtained from the oil globule measurements shows a significant ($P < 0.001$) reduction in droplet size at 30 minutes of the incubation period (approximately 22 μm reduction from time 0) for all samples. Oil globule size remains the same at 1 and 3 hours of incubation for samples containing 5% of Tween 80 while an increase in droplet size was observed for samples containing 1% of Tween 80 in samples with or without NaCl. As the release of bacteria depended on the stability of the inner W_1 droplet, the effect of different NaCl concentration on the gain and reduction of the inner W_1 droplet diameter was determined as presented in Figure 4.14. From the results, the gain (NaCl in inner W_1 phase) and reduction

(NaCl in outer W_2 phase) in the diameter of the droplet was significant ($P < 0.001$) at high NaCl concentration (2.0% w/v) and lower Tween 80 concentration (1% w/v). Overall, samples prepared under hypo-osmotic conditions were shown to have better stability compared to samples prepared under hyper-osmotic conditions as discussed previously in section 4.3.4. The presence of sodium chloride in the inner W_1 phase act as osmotic regulators that counterbalanced the Laplace pressure whereas the presence of NaCl in the W_2 phase resulted in the lack of osmotic pressure in the W_1 phase to withstand against Laplace curvature pressure (Jiao, Rhodes and Burgess, 2002). Moreover, the presence of bacteria does not affect droplet stability the way it was in single W/O emulsions droplet as discussed in the previous chapter (chapter three).

Table 4.1 Change in mean W_1 droplet and oil globule diameter (µm) at 30, 60 and 180 minutes with respect to 0 minutes of incubation. Samples were prepared in the presence or absence of *E. coli*-GFP in the W_1 phase, with or without 1.5% w/v of NaCl in either W_1 or W_2 phase. Surfactant concentration was set at either 1% w/v or 5% w/v for Tween 80 in W_2 phase. Data represent mean ± standard deviation from 3 independent experiments with N=900 droplet. The mean diameters were compared between samples within each incubation time (small letters) and between different incubation time within each sample (capital letters).

	$W_1/O/W_2$ samples	**30 Minutes (µm)**		**60 Minutes (µm)**		**180 Minutes (µm)**	
		W_1	Oil Globule	W_1	Oil globule	W_1	Oil Globule
With *E. coli*-GFP	No NaCl, 1% Tween 80	0.015^{aA} ± 0.001	-22.25^{aA} ± 1.10	0.036^{aA} ± 0.002	-22.23^{aA} ± 1.301	0.051^{aA} ± 0.002	-19.99^{aA} ± 1.241
	No NaCl, 5% Tween 80	0.017^{aA} ± 0.001	-22.26^{aA} ±0.802	0.027^{aA} ± 0.001	-22.25^{aA} ± 0.913	0.032^{aA} ± 0.002	-22.23^{aA} ± 0.921
	1.5% NaCl in W_1, 1% Tween 80	0.947^{bA} ± 0.10	-22.24^{aA} ± 1.406	9.085^{bB} ± 0.62	-22.23^{aA} ± 0.923	15.304^{bC} ± 1.08	-18.04^{bB} ± 1.01
	1.5% NaCl in W_1, 5% Tween 80	0.317^{cA} ± 0.03	-22.256^{aA} ± 1.302	5.316^{cB} ± 0.51	-22.232^{aA} ± 1.311	9.865^{cC} ± 1.16	-22.22^{aA} ± 1.409
	1.5% NaCl in W_2, 1% Tween 80	-0.813^{dA} ± 0.06	-22.23^{aA} ± 1.105	-15.388^{dB} ± 1.02	-22.16^{aA} ± 0.805	-20.758^{dC} ± 1.04	-16.12^{cB} ± 0.903
	1.5% NaCl in W_2, 5% Tween 80	-0.381^{eA} ± 0.02	-22.23^{aA} ± 1.007	-6.732^{eB} ± 0.82	-22.23^{aA} ± 1.106	-10.534^{eC} ± 1.47	-22.2^{aA} ± 1.202
Without *E. coli*-GFP	No NaCl, 1% Tween 80	0.03^{aA} ± 0.002	-22.23^{aA} ± 0.801	0.038^{aA} ± 0.001	-22.23^{aA} ± 0.821	0.065^{aA} ± 0.002	-17.76^{aB} ± 0.701
	No NaCl, 5% Tween 80	0.025^{aA} ± 0.003	-22.24^{aA} ± 0.935	0.04^{aA} ± 0.004	-22.23^{aA} ± 0.905	0.048^{aA} ± 0.01	-22.22^{bA} ± 1.408
	1.5% NaCl in W_1, 1% Tween 80	1.021^{bA} ± 0.02	-22.22^{aA} ± 1.401	10.242^{bB} ± 1.62	-22.23^{aA} ± 1.207	16.527^{bC} ± 1.62	-16.98^{cB} ± 1.301
	1.5% NaCl in W_1, 5% Tween 80	0.439^{cA} ± 0.06	-22.23^{aA} ± 1.611	5.837^{cB} ± 1.13	-22.23^{aA} ± 1.503	10.104^{cC} ± 1.16	-22.22^{bA} ± 1.371
	1.5% NaCl in W_2, 1% Tween 80	-0.92^{dA} ± 0.12	-22.23^{aA} ± 0.781	-13.323^{dB} ± 0.91	-22.13^{aA} ± 0.838	-18.906^{dC} ± 1.02	-15.28^{dB} ± 0.911
	1.5% NaCl in W_2, 5% Tween 80	-0.368^{eA} ± 0.05	-22.22^{aA} ± 1.108	-9.048^{eB} ± 0.56	-22.22^{aA} ± 1.265	-13.015^{eC} ± 1.14	-22.2^{bA} ± 1.153

Data were analysed with one-way ANOVA.
^{abcde}means ± standard deviation and ^{ABC}means ± standard deviation with different letters are significantly different at $P < 0.05$.

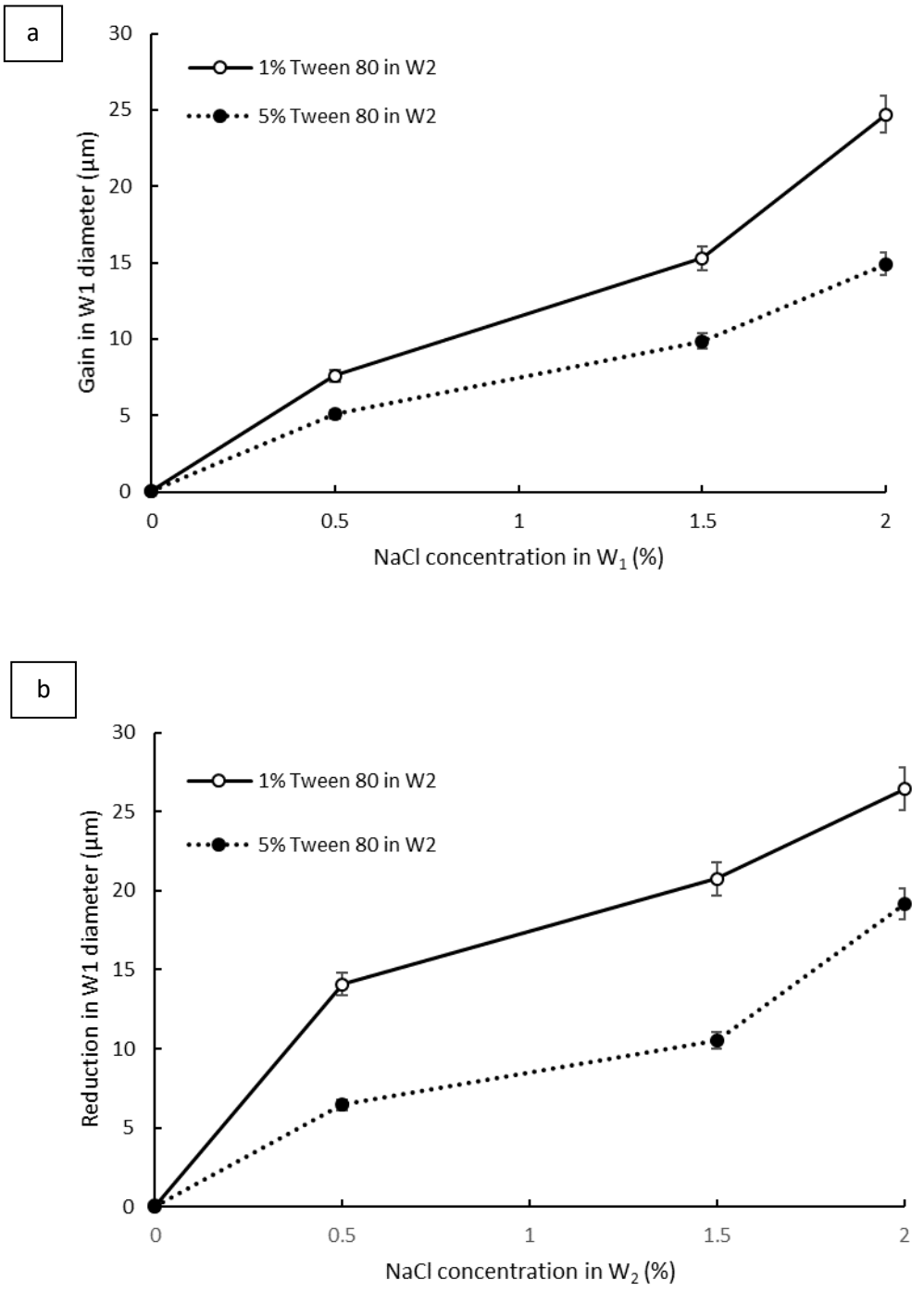

Figure 4.14 Changes in W_1 diameter at 180 minutes of incubation time due to the addition of NaCl at 0.5, 1.5 and 2% w/v in the inner W_1 phase (a) and outer W_2 phase (b). The emulsion was prepared with *E. coli*-GFP in the inner W_1 phase and stabilized with 1% w/v or 5% w/v of Tween 80 in the W_2 phase and 1.5% w/v PGPR in the oil phase. Bars represent mean ± SEM from 3 independent experiments with N=900 droplet.

The data from Table 4.1 reveal that no significant ($P = 1.00$) change in size was observed for both inner W_1 droplet and oil globule immediately after droplet formation with or without osmotic pressure alterations (during the first 30 minutes). A significant change ($P < 0.001$) in inner W_1 size was only observed immediately after the splitting of the $W_1/O/W_2$ droplet releasing inner W_1 droplet into the W_2 phase and forming smaller oil globule or O/W droplet. The change in the W_1 droplet occurs rapidly after droplet splitting as the escaped W_1 droplet was only enclosed by a very thin film. As the splitting caused the formation of smaller oil globule or O/W droplet, a significant reduction ($P < 0.001$) in oil globule size was observed immediately after the splitting process (at 30 minutes) that remains stable afterwards. The absence of inner W_1 phase in the oil globule after the splitting process caused the droplet to be relatively unaffected by the change in osmotic pressure. A slight increase in droplet size for oil globules in samples containing low Tween 80 concentration mainly due to the undesirable interactions between the Tween 80 and the NaCl that weakens the interfacial strength and caused coalescence between neighbouring droplet (Burgess and Yoon, 1995; Jiao, Rhodes and Burgess, 2002).

The stability of the $W_1/O/W_2$ droplet depended on the osmotic and Laplace pressure balance (Klojdová, Štětina and Horáčková, 2019) as discussed in section 4.3.5. Other factors that also influence the stability of the $W_1/O/W_2$ droplet as a whole are the interactions between the surfactants with high and low HLB value and also interactions between the solutes and emulsifier in the W_2 phase (Kanouni, Rosano and Naouli, 2002). The main cause for droplet destabilization is attributed to the diffusion of water between the aqueous phases of the $W_1/O/W_2$ due to osmotic imbalances as an extensive change in droplet size may cause bursting of the droplet releasing encapsulated contents into the outer continuous phase (Muschiolik and Dickinson, 2017). The stability of the droplet against bursting depended on the interfacial strength and thickness along with the characteristics of the continuous outer phase such as

viscosity (Schuster, 1996). The thin and complex film that enclosed the W_1 droplet as it escaped from the $W_1/O/W_2$ droplet making it more susceptible to rupture. Moreover, under hypo-osmotic conditions, the increase in NaCl concentration caused extensive swelling of the W_1 droplet leading to droplet rupture as the film that enclosed the W_1 droplet reaches its critical thickness (Schuster, 1996; Krebs, Schroen and Boom, 2012). Reduction in the thickness of the interfacial film also lowers the activation energy needed to form a hole that destabilizes the droplet (Schuster, 1996). Surfactant concentration also plays an important role in protecting the droplet against rupture and keeping the droplet apart. At high surfactant concentration, a multilayer arrangement of hydrophilic surfactants formed on the interface of the droplet that cause an increase in interfacial strength as the droplet is completely enclosed in these layers, protecting them against hole formation that leads to droplet rupture (Tadros, 2013). In addition, the swelling of the droplet also caused rearrangements of surfactants on the interface as the surfactant molecules were dragged along the interface during the swelling process leaving areas with more surfactant molecules and areas with less surfactant or gaps that are prone to hole formation (Kadri *et al.*, 2016). To ensure the stability of the droplet, these gaps had to be recovered quickly by the adsorption of excess surfactant molecules onto the interface (McClements, 1998). At high Tween 80 concentration, the adsorption of surfactants molecules to fill in the gaps created by the expansion of the droplet interface will occur more rapidly whereas, at low Tween 80 concentration, the adsorption of the surfactant on the interface will be much slower than the formation of the gaps on the interface causing it to destabilize at a much faster rate (El Kadri *et al.*, 2016).

The shrinkage of W_1 droplet suspended in hyper-osmotic conditions is due to the migration of water from the inner W_1 phase towards the outer W_2 phase. As the W_1 droplet size reduction was accelerated after the splitting of $W_1/O/W_2$ droplet, the destabilization effect may be attributed to the thin film enclosing the droplet after being released into the W_2 phase.

During the splitting process, the majority of the oil phase separated from the $W_1/O/W_2$ leaving the W_1 droplet suspended in W_2 phase enclosed by a very thin complex layer that may consist of a mixture of PGPR and Tween 80 surfactants with less oil phase. Moreover, due to the low amount of oil that exists on the interface, the thin film is most likely dominated by the hydrophilic surfactant, Tween 80 rather than PGPR. By altering the osmotic balance between the inner and outer phase, it triggers the water flux through the thin film that is assisted by the surfactant molecule. When the W_1 phase is closely in contact with the W_2 phase of high solute concentration and separated by a very thin film, water transport mainly occurs due to surfactant hydration (Wen and Papadopoulos, 2000). During this process, the surfactant molecule hydrates at an interface and migrated through the film to dehydrate at the other interface with higher solute concentration causing loss of surfactants molecules on the interface. As the thin layer of film was most likely consists of Tween 80 surfactant, the loss in Tween 80 creating gaps on the interface, may cause the droplet to be highly susceptible to bursting. At high concentration of Tween 80, the excess surfactant molecule is sufficient to replace the loss of surfactant molecules on the interface whereas, at lower concentration of Tween 80, the insufficient amount of surfactant molecule to fill the gaps left by the desorbing surfactants leads to droplet instability and bursting (El Kadri *et al.*, 2015). Moreover, during the shrinkage of W_1 droplet, the hydrophilic *E. coli*-GFP was retained in the droplet. Therefore, the bacterial release is more likely due to droplet bursting caused by the presence of NaCl that destabilizes the thin film which is in agreement with the study done by El Kadri *et al.* (2015).

Therefore, the stability of W_1 droplet and oil globules in both hypo-osmotic and hyper-osmotic conditions is highly dependent on the NaCl and Tween 80 concentrations as they affect the integrity of the interfacial film. The release of bacteria is highly dependent on the stability of the inner W_1 droplet whereby the presence of very thin film separating the inner W_1 phase from the W_2 phase after the splitting of $W_1/O/W_2$ droplet making it more susceptible to droplet

destabilization and bursting. Further study is required to confirm the composition of the thin film that may provide a further understanding of the behaviour of the escaped W_1 droplet in the W_2 phase.

4.3.6 The effect of osmotic imbalances on creaming behaviour

The thickness of the cream layer with difference in NaCl and Tween 80 concentration was measured for both samples under hypo-osmotic and hyper-osmotic conditions. As the presence of bacteria in the W_1 phase does not affect the change in droplet size, only samples containing bacteria were tested for creaming behaviour as presented in Figure 4.15.

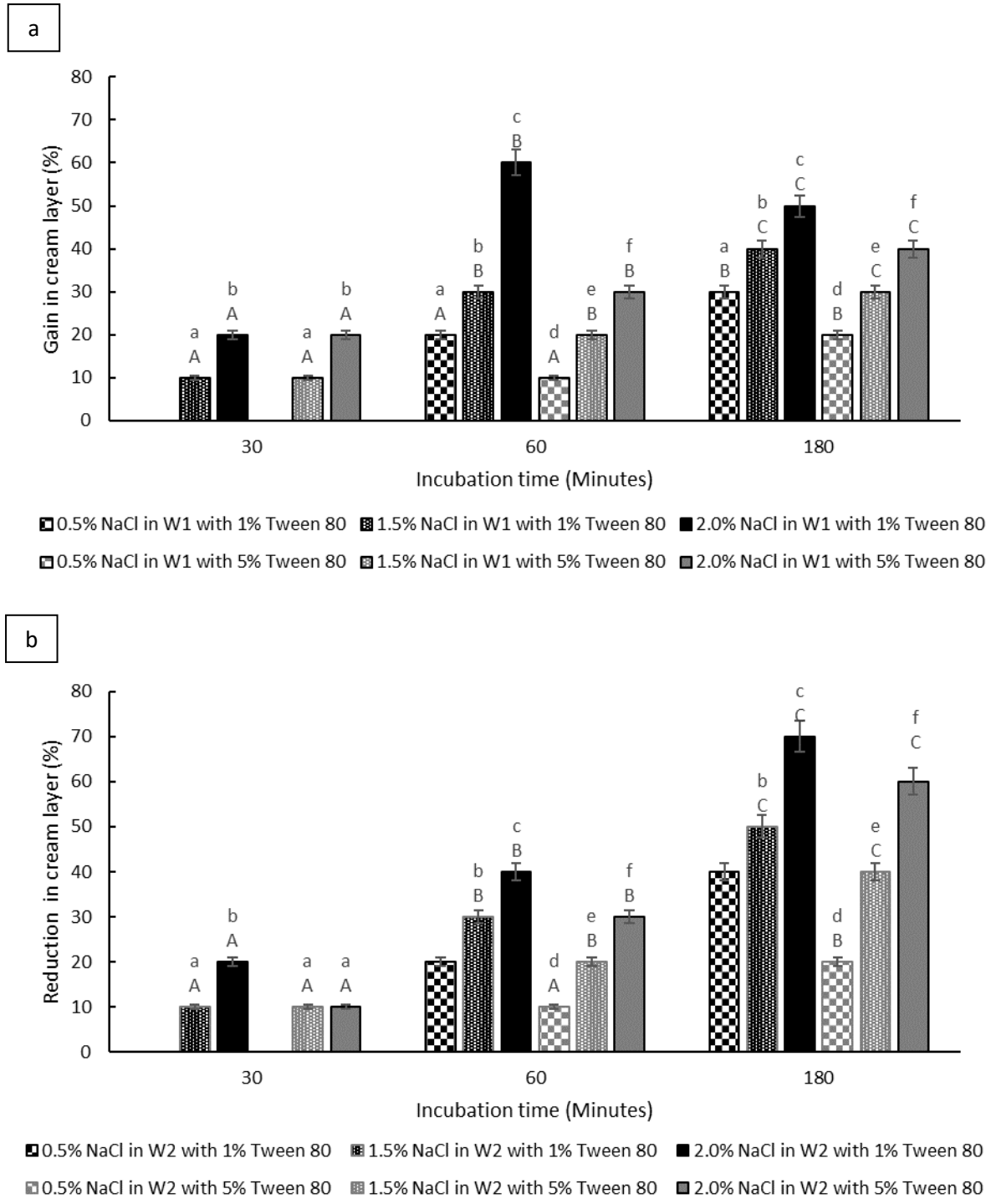

Figure 4.15 Change in creaming behaviour for samples under hypo-osmotic conditions (a) and hyper-osmotic conditions (b). Samples were prepared with *E. coli*-GFP in inner W_1 droplet at different Tween 80 concentration of 1% w/v and 5% w/v along with 1.5% w/v PGPR. Bars represent mean ± SEM taken from 3 independent experiments. Mean comparison with different small and capital letters indicate significant different ($P < 0.05$) between samples within each incubation time and between storage time within each sample respectively. Data were analysed with one-way ANOVA.

From the results obtained (Figure 4.15), it was determined that the change in creaming behaviour is dependent on the sodium chloride and Tween 80 concentrations whereby significant ($P < 0.001$) gain and reduction in creaming thickness was observed with samples containing a high concentration of NaCl and low concentration of Tween 80. As discussed in section 4.3.5, changes in the size of W_1 droplet occurred rapidly after the $W_1/O/W_2$ droplet breakup/split while significant ($P < 0.001$) change in the oil globule size was only observed immediately after the splitting process as the release of W_1 droplet from the $W_1/O/W_2$ droplet caused the formation of smaller oil globule. No significant ($P = 1.00$) change in oil globule size was observed after 1 to 3 hours of the splitting process for samples containing 5% Tween 80 and lower NaCl concentration while an increase in size was observed for samples with 1% Tween 80 and higher NaCl concentrations. According to previous studies (El Kadri *et al.*, 2015; 2016), under hypo-osmotic conditions, the gain in creaming thickness is attributed to the migration of water from W_2 to W1 phase whereby for samples under hyper-osmotic conditions, the reduction in creaming size is attributed to the loss in oil globule.

Referring to the data presented in Figure 4.15 (a) for samples under hypo-osmotic conditions, at high NaCl concentration (2%), a significant increase ($P < 0.001$) in creaming size was observed at 30 minutes to 1 hour of incubation. However, a decrease in creaming size was observed after 3 hours of the incubation period. Immediately after droplet splitting, the migration of water from W_2 to W_1 phase occurs rapidly that diminishes with a reduction in osmotic gradient. Droplet bursting due to extensive swelling especially with samples containing a higher concentration of NaCl resulting in loss of oil globule and a decrease in creaming size. In addition, the reduction in interfacial strength due to high NaCl concentration (Burgess and Yoon, 1995; Jiao, Rhodes and Burgess, 2002) caused coalescence between the oil globule that grows into a separated layer of oil on top of the samples and a decrease in the creaming volume. Under hyper-osmotic condition (Figure 4.13 b), the loss in the cream layer

is mainly attributed to the shrinkage of W_1 droplet that diminishes with a reduction in osmotic gradient. Further loss in cream layer occurred due to bursting of W1 droplet and coalescence between oil globules as undesirable interaction between NaCl and Tween 80 weakens the interfacial strength of the droplet.

4.4 Conclusion

In conclusion, the results obtained from this study provide important information on the applications of $W_1/O/W_2$ droplet for bacterial encapsulation that can be beneficial in various bacterial studies. Moreover, it also provides a better understanding of the application of $W_1/O/W_2$ droplet for controlled release of not only bacteria but also drugs, enzymes, flavours and other hydrophilic materials. As an example, $W_1/O/W_2$ droplet can be applied in the controlled release of the sensitive probiotics in food and during the digestion process whereby double emulsions serve as a mean of protection for bacteria against harsh conditions and the triggered destabilization of droplet may aid in the controlled release of these bacteria at a desirable time or region that maximizes their efficiency. The present study reveals that splitting or droplet breakup accelerates the release of bacteria with osmotic balance alterations. However, further studies are still required to further understand the controlled release of bacteria from $W_1/O/W_2$ droplet such as the nature and composition of the thin film that surrounds the droplet after the splitting process and the mechanism behind the droplet breakup/split in order to control this process. In addition, it is also worth investigating the effect of other factors that may induce the release of bacteria from $W_1/O/W_2$ droplet such as a change in temperature or pH on the droplet breakup/split in order to further improve and widen the applications of $W_1/O/W_2$ droplet in the encapsulation of bacteria.

Chapter 5
The stability of bacteria incorporated in emulsion droplet in cold temperature storage

5.1 Introduction

Emulsion droplet had been studied recently for the encapsulation of materials such as bacteria and drugs (Chavarri, Maranon and Carmen, 2012; Dluska *et al*., 2017; Devanthi *et al*., 2018). These materials usually require storage at low temperatures in order to maintain its stability, especially for long-term storage. The storage of bacteria in low temperatures is a common practice in bacterial preservation in order to maintain its viability, for example, lactic acid bacteria in the dairy industry and also for its application in various bacterial study in the laboratory. The freezing of cell to temperatures such as -20˚C and -80˚C help in maintaining not only its viability but also functionality over a long storage period (Fonseca, Béal and Corrieu, 2002; Wang *et al*., 2019).

The development of various cryoprotectant formulations helped in minimizing the detrimental effects of freezing on bacteria (Wang *et al*., 2019). Besides that, the encapsulation of bacteria in emulsion, especially food-based emulsions such as milk and ice cream has also been reported to improve bacterial viability during freezing depending on the nature of the emulsion (Goderska and Czarnecki, 2008; Dianawati, Mishra and Shah, 2013; Nurliyani, Suranindyah and Pretiwi, 2015; Farias *et al*., 2019). Nevertheless, further studies are still required in order to asses not only the viability of bacteria encapsulated in emulsion droplets but also to determine the effect of bacteria on the emulsion stability during storage in cold temperatures.

The successful application of emulsion droplet for bacterial encapsulation depended on their stability. The stability of emulsion during cold temperature storage depended on the changes in the phase behaviour of the oil and aqueous phase as reported in many related studies (Vanapalli, Palanuwech and Coupland, 2002; Cramp *et al*., 2004; Ghosh and Rousseau, 2009; Tippetts and Martini, 2009). The crystallization of the oil phase followed by the aqueous phase in oil-in-water (O/W) emulsions may cause partial coalescence of the oil droplets whereby in loosely packed emulsions sample, the collision between the still-liquid oil droplets and crystallized oil droplets with protruding crystals may cause membrane rupture that resulted in the droplets with still-liquid oil to flow out forming a linkage between the two droplets as it freezes. This mechanism will cause droplets flocculation that eventually leads to complete coalescence and oiling-off upon thawing (Vanapalli, Palanuwech and Coupland, 2002; Lin *et al*., 2007).

Another mechanism involved in emulsion destabilization during freezing is the flow-induced coalescence whereby the crystallization of the continuous phase prior to the dispersed phase forces the still-liquid droplets to be concentrated in the still-liquid region of the continuous phase as it gradually crystallizes. This resulted in the droplets to be pushed closer together thus promoting droplets flocculation, coalescence and eventually phase separation (Ghosh and Coupland, 2008; Degner *et al*., 2013, 2014). A different destabilization mechanism for multiple emulsions namely water-in-oil-in-water ($W_1/O/W_2$) emulsion has been proposed which involves the external coalescence of the inner W_1 phase with the outer W_2 phase that occurred during the thawing process while the W_1 inner phase remains intact during the freezing process (Rojas and Papadopoulos, 2007; Rojas *et al*., 2008).

Although emulsion destabilization is unfavourable for food emulsions as it may affect product quality, it is highly beneficial in emulsions extraction and oil recovery process for example during the Emulsion Liquid Membrane processing (ELM) and also for the processing

of unwanted emulsions such as oil sludge (He and Chen, 2002; Lin *et al*., 2007, 2008). Moreover, the application of the freeze-thaw technique for the controlled and immediate release of materials from double emulsion droplets has also been explored previously (Rojas and Papadopoulos, 2007; Rojas *et al*., 2008). That study shows an interesting application of the freeze-thaw process for the controlled release in which will be further explored in this chapter by using live bacterial cells as the encapsulated material.

This chapter focused on the application of emulsion droplet for bacterial encapsulation under cold temperature storage. It is crucial to understand the flexibility of the emulsion droplet to be used as an alternative for bacterial encapsulation and their stability during storage not only in ambient temperature as discussed previously in chapter three but also in cold temperature. The detrimental effects of cold temperature on bacterial viability and droplet destabilization during storage remains a challenge. Therefore, the experiments conducted in this chapter were important and may provide valuable information on the effects of encapsulation on bacterial viability and droplet stability in cold temperature storage. In this study, *E. coli*-GFP which is one of the most widely studied bacteria and commonly subjected to cold temperature storage was used. As cold temperature storage is mostly related to the food-based emulsion, soybean oil was used as the oil phase of the emulsion prepared in this chapter. Moreover, in order to focus on the industrial application of the emulsion as compared to a general study on emulsion by using mineral oil as the oil phase in the previous chapters (chapter three and four), the soybean oil was chosen to replace mineral oil in this study whereby soybean oil is one of the most common types of oil used in the food industry with various nutritional benefits such as omega-3 and omega-6 fatty acids (List, 2016).

5.2 Materials and methods

5.2.1 Materials and bacterial cultures

Materials and bacterial cultures used are as described in section 4.2.1. Soybean oil (Alfa Aesar, United Kingdom) was used as the oil phase for both single water-in-oil (W/O) and double water-in-oil-in-water ($W_1/O/W_2$) emulsion droplet.

5.2.2 Bacterial cells preparation

Bacterial culture was prepared for encapsulation in water-in-oil (W/O) and water-in-oil-in-water ($W_1/O/W_2$) as described in section 4.2.4 and was re-suspended into sterilised deionised water (DIW).

5.2.3 Microfluidic encapsulation of *E. coli*-GFP in W/O and $W_1/O/W_2$ droplet

The prepared culture of *E. coli*-GFP in deionised water (DIW) was then used as the aqueous phase of W/O and the inner aqueous phase of $W_1/O/W_2$ droplet. The oil phase for both types of emulsion consists of soybean oil with 1.5% w/v PGPR surfactant while for $W_1/O/W_2$, the outer aqueous phase consists of DIW with 1% w/v Tween 80 surfactant. The bacterial encapsulation into W/O droplet was conducted according to section 3.2.5 while the encapsulation into $W_1/O/W_2$ was done according to section 4.2.5. The microfluidic devices used for droplet generation were prepared according to section 3.2.2 for single emulsion droplet and section 4.2.2 for double emulsion droplet. As part of microfluidic device preparation, partial hydrophilic surface treatment was done on double emulsion droplet devices as mentioned in section 4.2.3.

5.2.4 Storage of samples in different temperature

The prepared samples of emulsion droplet incorporated with or without *E. coli*-GFP was stored in different storage temperature of 25°C (control), 5°C (refrigeration temperature), -20°C (freezing temperature) and -80°C (freezing temperature) in laboratory-based refrigerator and

freezers whereby the temperature was monitored throughout the storage period. Samples were stored for 24 hours and were thawed at 25°C for one hour prior to further tests. Samples of *E. coli*-GFP suspended in sterilised deionised water (DIW) were also prepared and kept at the designated temperature as non-encapsulated control.

5.2.5 Bacterial viability determination

The viability of *E. coli*-GFP was determined before and after the thawing process of samples stored in different temperatures as mentioned in section 5.2.4. Serial dilutions of the samples were done using Phosphate buffer saline (PBS) and viable cells were counted immediately after samples preparation and storage by using the Miles and Misra method (Miles and Misra, 1931) as described in section 3.2.6.

5.2.6 Microscopic observation of droplet destabilization.

Droplet destabilization was observed with respect to changes in temperature as described in Figure 5.1. The samples were prepared for microscopy by placing approximately one drop of sample onto the glass slide. The prepared glass slide was then placed on a Peltier temperature-controlled stage (Model PE-120, LINKAM scientific instruments, United Kingdom) where the temperature of the stage was controlled by using Link software. Eheim circulation pump (ECP) was used for water circulation through the stage in order to keep the temperature-controlled stage at the desired temperature. The temperature-controlled stage was fitted on a Nikon Eclipse Ti microscope equipped with Pco. Edge 5.5 sCMOS camera where the samples were cooled and thawed on the microscope stage while photomicrographs of the samples were acquired. The sample was prepared at an initial temperature of 25°C and was cooled down to -25°C as it was the minimum reachable temperature of the stage (temperature range of the Peltier temperature-controlled stage: 120°C to -25°C). The sample was then thawed back to the initial temperature of 25°C. For fluorescence microscopy, the encapsulated *E. coli*-GFP was observed at 509 nm emission.

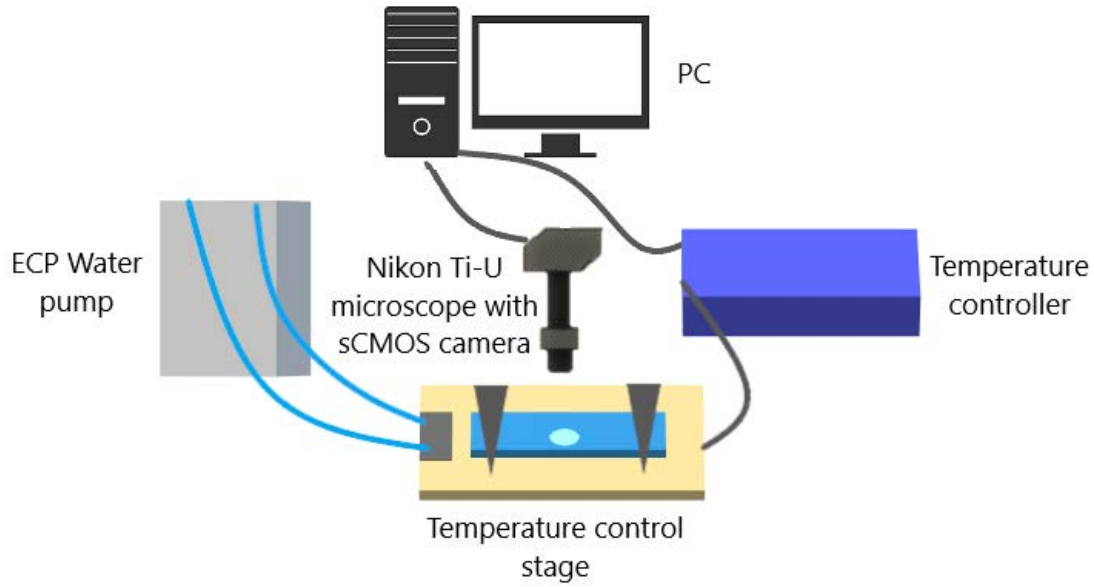

Figure 5.1 Microscopic observation of emulsion destabilization with the change in temperature. Sample of the emulsion was placed on a glass slide and placed on a temperature-controlled stage at 25˚C. The temperature of the stage was then reduced to -25°C that freezes the sample and was kept at that temperature for 10 minutes. The temperature of the stage was then increased to 25°C in order to thaw the sample. Photomicrographs of the sample were taken with every temperature change, from 25°C (initial) to -25°C (cooling), 5°C (heating) and back to 25°C (thawed). The temperature of the stage was maintained with ECP water pump.

5.2.7 Determination of droplet size and phase separation

The effect of different storage temperature on droplet size was determined by measuring the diameter of the droplet immediately after sample preparation and after the thawing process at 25°C. Approximately one mL of double and single emulsion samples with or without *E. coli*-GFP were prepared at 25°C and stored in cold temperatures as described in section 5.2.4. Photomicrographs of the droplet were taken before and after the storage period and changes in the size of the dispersed aqueous phase for single emulsion droplet and oil globule size for double emulsion droplet were measured by using the MATLAB software according to section 3.2.3.

Droplet stability was also determined by measuring the amount of free water (for W/O emulsion) and free oil (for $W_1/O/W_2$ emulsion) with or without the presence of *E. coli*-GFP. Phase separation measurement was done by collecting 1 mL of sample into graduated syringes immediately after droplet preparation. The samples were then stored at different temperatures in an upright position for 24 hours. The volume of the free water and oil were measured from the graduated syringe immediately after the thawing process and the percentage of free water and oil were determined as follows:

$$Percentage\ of\ separated\ water/oil\ (\%) = \frac{V_{water/oil}}{V_{emulsion}} \times 100 \quad (5.1)$$

Where $V_{water/oil}$ is the volume of separated water or oil at time 0 as measured from the graduated syringe while $V_{emulsion}$ is the total volume of the emulsion sample.

5.2.8 Measuring the release of bacteria from $W_1/O/W_2$ droplet.

The release of bacteria was determined by measuring the number of cells in the outer aqueous phase immediately after droplet preparation and after the thawing process for double emulsion samples described in section 5.2.3. The release of bacteria was determined as described in section 4.2.9.

5.2.9 Differential scanning calorimetry

Differential scanning calorimetry (DSC) was done in order to determine the thermal properties of emulsions samples and bulk aqueous solutions. The crystallization and melting behaviour were characterised by using a differential scanning calorimeter (Mettler Toledo, model 822e, Mettler Scientific Instruments, Germany) with liquid nitrogen as the cooling substance. Approximately 5 mg of sample was weighted and hermetically sealed in aluminium pans together with an empty pan as reference. Samples were then cooled from 25°C to -70°C and were held at -70°C for 5 minutes before heated back to 25°C at 1°C/min. The cooling and heating curves were obtained from the Star e software (Mettler Toledo, Mettler Scientific Instruments, Germany) whereby positive curves resulted from exothermic reaction while the endothermic reaction in the sample creates negative curves. The crystallization and melting points of the tested samples were determined from the peak onset temperatures of the curves by using the same software.

5.2.10 Statistical analysis

The data obtained from the experiments conducted in this chapter were analysed according to section 3.2.12.

5.3 Results and discussion

5.3.1 The effect of storage on droplet size change

The stability of the prepared emulsions stored at different temperatures for 24 hours was determined by measuring changes in droplet size as described in section 5.2.7. Photomicrographs of emulsion destabilization were also acquired in order to obtain a clear view of the destabilization process and were done according to section 5.2.6. Changes in the dispersed droplet diameter for W/O emulsion were presented in Figure 5.2 A, B, C, D while changes in the oil globule diameter of $W_1/O/W_2$ emulsion were presented in Figure 5.2 E, F, G, H. The results obtained were summarized in Table 5.1 and photomicrographs of droplet destabilization with the change in temperature were presented in Figure 5.3.

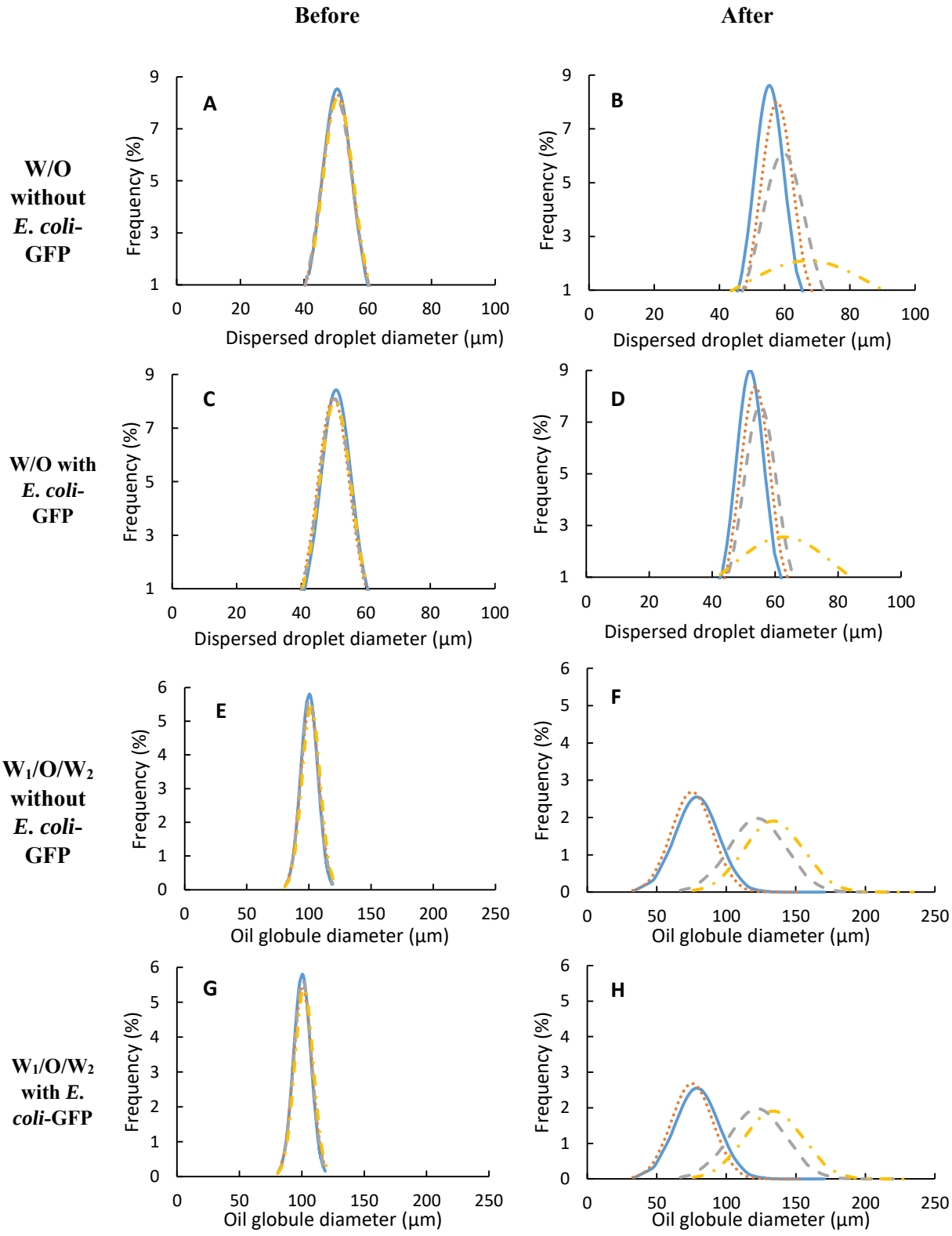

Figure 5.2 Droplet size distribution for single W/O and double $W_1/O/W_2$ emulsions stored in 25 °C (—), 5°C (⋯), -20°C (----), -80°C (- · -). Graph A-D represent the data for single W/O emulsion while graph E-H represent the data for double $W_1/O/W_2$ whereby droplet size distribution was compared between sample containing *E. coli*-GFP and without *E. coli*-GFP, before and after storage for 24 hours.

Table 5.1 Summary of droplet size and distribution measured before and after 24 hours of storage. Samples were prepared with or without *E.coli*-GFP for W/O and $W_1/O/W_2$ droplets. Data represent mean ± standard deviation taken from 3 independent experiments with N=900 droplet. The coefficient of variation (%) was measured by dividing standard deviation with mean droplet diameter. Mean comparison with small letters and capital letters indicate significant different ($P < 0.05$) between temperatures within each sample and between before and after storage within each temperature respectively. Data were analysed with one-way ANOVA and students' T-test.

Samples	Temperature (°C)	Average droplet diameter (µm)		Coefficient of variation (%)	
		Before	After	Before	After
W/O without *E. coli*-GFP	25	$50.4^{aA} \pm 4.7$	$55.3^{aA} \pm 5.2$	9.3	9.4
	5	$50.4^{aA} + \pm 4.8$	$57.7^{aA} \pm 5.6$	9.5	9.7
	-20	$50.3^{aA} \pm 4.9$	$59.6^{cB} \pm 6.6$	9.7	11.1
	-80	$50.7^{aA} \pm 4.8$	$67.2^{dB} \pm 19.0$	9.6	28.3
W/O with *E. coli*-GFP	25	$50.8^{aA} \pm 4.7$	$52.1^{aA} \pm 4.9$	9.3	9.4
	5	$50.0^{aA} \pm 4.9$	$53.7^{aA} \pm 5.3$	9.8	9.9
	-20	$50.4^{aA} \pm 4.9$	$55.3^{bB} \pm 5.4$	9.7	9.8
	-80	$50.5^{aA} \pm 5.0$	$62.8^{cB} \pm 15.6$	9.9	24.8
$W_1/O/W_2$ without *E. coli*-GFP	25	$100.3^{aA} \pm 6.9$	$79.0^{aB} \pm 15.6$	6.9	19.7
	5	$100.7^{aA} \pm 7.3$	$75.4^{bB} \pm 14.9$	7.2	19.8
	-20	$100.6^{aA} \pm 7.1$	$122.3^{cB} \pm 20.2$	7.1	16.5
	-80	$101.8^{aA} \pm 7.4$	$133.8^{dB} \pm 20.9$	7.3	15.6
$W_1/O/W_2$ with *E. coli*-GFP	25	$100.9^{aA} \pm 7.1$	$79.4^{aB} \pm 15.6$	7.0	19.6
	5	$100.3^{aA} \pm 7.7$	$76.3^{bB} \pm 14.7$	7.7	19.3
	-20	$100.4^{aA} \pm 7.1$	$116.7^{cB} \pm 18.5$	7.1	15.9
	-80	$100.4^{aA} \pm 7.4$	$126.3^{dB} \pm 18.9$	7.4	14.9

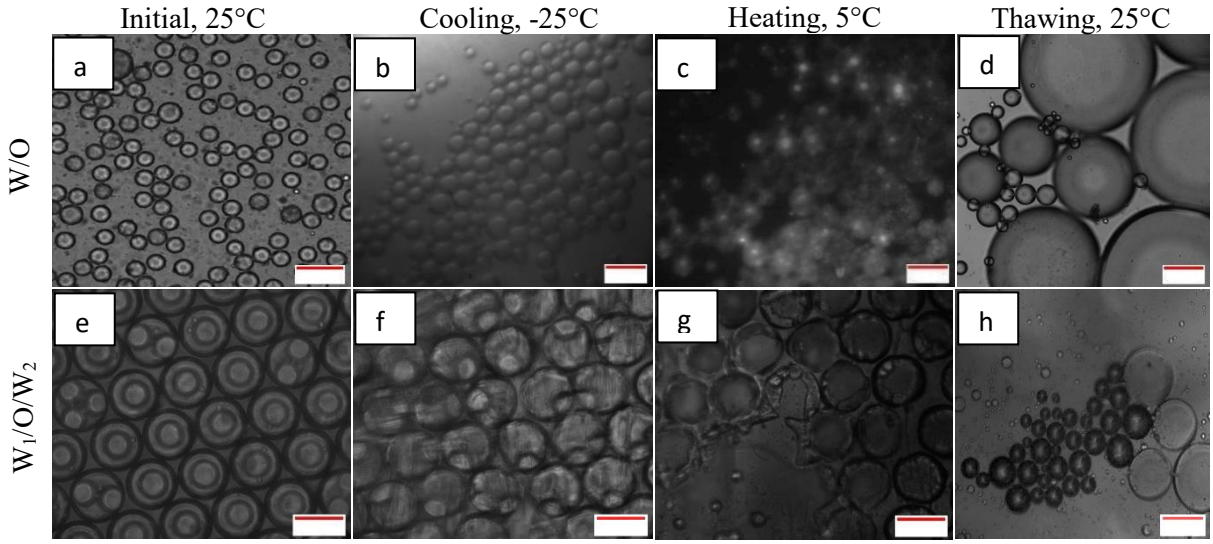

Figure 5.3 Photomicrographs of W/O and $W_1/O/W_2$ emulsion droplet with change in temperature. The cooling and thawing processes were conducted on the microscope stage. Scale bar represents 100 µm.

From Figure 5.2 (A, C, E, G) and Table 5.1, monodispersed droplet for both single and double emulsion droplet were observed for all samples with or without *E. coli*-GFP with a CV value of approximately 9% for single emulsion droplet and 7% for double emulsion droplet prior to the storage test. These indicate the ability of the flow-focussing microfluidic devices in producing highly monodispersed droplet and that the presence of *E. coli*-GFP does not affect droplet formation. For samples of single emulsion droplet, no significant change in droplet size was observed after storage at 25°C ($P = 0.24$) and 5°C ($P = 0.07$) (Table 5.1) for both samples with and without bacteria. The droplet remains monodispersed with only 0.1-0.2% change in the value of the coefficient of variation (CV). However, a significant change ($P < 0.001$) in droplet size and distribution were observed after 24 hours of storage for samples stored at freezing temperatures of -20°C and -80 °C for both sample with and without bacteria. Samples stored at -80°C show the highest increase in CV value whereby the value increases from 9.6% to 28.3% for samples without *E. coli*-GFP indicating a polydispersed distribution of droplet (CV values of higher than 25% are regarded as polydispersed). Comparing samples with or without *E. coli*-GFP, change in droplet stability was minimized with the presence of *E. coli*-GFP whereby a smaller change in average droplet size and CV was observed with samples containing *E. coli*-GFP as compared to samples without *E. coli*-GFP.

Samples of double $W_1/O/W_2$ emulsion droplet show a significant change ($P < 0.001$) in the size of oil globule after storage for 24 hours for all the samples tested. A decrease in average oil globule size was observed for samples stored at 25°C and 5°C along with presence of large droplet with tails that extend towards 170 μm in droplet size distribution graphs (Figure 5.2 F, H) while for samples stored at freezing temperatures of -20°C and -80°C, an increase in droplet size was observed (Table 5.1). Samples containing *E. coli*-GFP show better droplet stability as compared to samples without *E. coli*-GFP indicating the ability of bacterial cells in maintaining droplet stability during cold temperature storage. The size of the inner aqueous phase (W1) was

not measured in this study due to complete external coalescence between the inner W1 droplet with the outer W2 phase after 24 hours of storage forming single oil-in-water (O/W) emulsion.

The storage of single W/O samples at -20°C caused the solidification of the aqueous phase and partial crystallization of the oil phase whereas storing the samples at -80 °C completely solidifies the emulsions. With broad crystallization temperature as opposed to pure water that exhibits a sharp crystallization curve, it is quite difficult to determine the exact crystallization temperature of the soybean oil due to presence lipids and a mixture of molecules. It has been reported previously that soybean oil is partially crystallized at a temperature between -10°C to approximately -20°C whereby below this temperature, the soybean oil is most likely to become solid (Tieko Nassu and Gonçalves, 1999; Harada and Yokomizo, 2000; Mezzenga, Folmer and Hughes, 2004; Ishibashi, Hondoh and Ueno, 2016). Several destabilization mechanisms of single W/O emulsions during the freeze-thaw process have been proposed depending on the droplet arrangements in the emulsion (Aronson and Petko, 1993; Aronson *et al.*, 1994; He and Chen, 2002; Chen and He, 2003; Lin *et al.*, 2007). The destabilization of loosely packed W/O emulsion droplet is due to the collision-mediated coalescence (Lin *et al.*, 2007). This process is triggered by the uneven crystallization of the polydispersed water droplet in the emulsion whereby the collision between the smaller still-liquid water droplet with protruding ice crystals of the larger frozen droplet punctures the membrane surrounding the smaller still-liquid water droplet. This leads to the heterogeneous nucleation and crystallization of the smaller water droplet that coalesces forming larger droplet upon thawing (Lin *et al.*, 2007; Ghosh and Rousseau, 2009b). However, this may not be the case for single W/O droplet generated by the microfluidic device as it is highly monodispersed and therefore, minimizes the heterogeneous crystallization of the water droplet and the effect of collision-mediated coalescence.

Although the effect of collision-mediated coalescence was minimized, the destabilization of W/O droplet was still observed and is mainly attributed to the static and upright storage of the samples during freezing that caused the inevitable sedimentation of the water droplet making them closely packed. For densely packed emulsions, the destabilization mechanism is induced by the direct breakage of interfacial films and emulsion inversion (Aronson and Petko, 1993; Aronson *et al.*, 1994). The direct breakage of the droplet interfacial film occurred as neighbouring droplet crystallizes and expands causing destabilization. Droplet expansion pressed the droplet closely together while crystallized droplet punctured the interfacial film of neighbouring still-liquid droplet leading to droplet rupture (Ghosh and Coupland, 2008). This caused the content of the ruptured droplet to flow out and formed a link between the two frozen droplets resulting in flocculation as observed in this study in Figure 5.3 b (van Boekel and Walstra, 1981). During the thawing process, the crystal network collapsed and the two partially coalesced droplet merged together forming larger droplet (complete coalescence) as observed in Figure 5.3 d (Vanapalli, Palanuwech and Coupland, 2002). Droplet crystallization and expansion also resulted in the thinning of the oil and surfactant layer around the aqueous phase that accelerates droplet coalescence during the melting process (Ghosh and Rousseau, 2009b). Emulsion inversion, as reported by Aronson and Petko (1993) involves the rearrangement of ice crystals and the still-liquid oil that leads to the presence of distinct oil droplet within the ice structure. However, this may not be the case for samples tested in this study as it occurs mainly in densely packed emulsions containing distinctively high volume fraction of the dispersed phase (Vanapalli, Palanuwech and Coupland, 2002)

It has been reported previously that the stability of water-in-oil droplet during the freeze-thaw process depended on the freezing sequence of the oil and aqueous phases and also the type of surfactants used (Ghosh and Rousseau, 2009b). The freezing sequence between the oil and aqueous phase may depend on the type of oil used as some oils may have a lower

freezing point or higher freezing point than the aqueous phase. Ghosh and Rousseau (2009) reported that for single water-in-oil emulsions, instability is mostly evident in samples with the oil phase that crystallizes first prior to the aqueous phase and when the emulsifier is in liquid-state during the freezing process. For emulsion droplet containing soybean oil, the oil phase crystallizes at a much lower temperature than the aqueous phase in which droplet destabilization should be minimized. However, significant changes ($P < 0.001$) in droplet size distribution were observed for samples stored at -80°C. At -80°C, the gradual crystallization of the oil phase due to difference in the melting fraction of fats in soybean oil as the high-melting fraction crystallizes first followed by the low-melting fraction (Ishibashi, Hondoh and Ueno, 2016) resulted in the ice crystals to be forced into the still-liquid oil phase forming a region with highly concentrated ice crystals. These occurred in the same way as the solidification of the continuous aqueous phase forcing the oil droplet to be concentrated in the region of the still-liquid continuous phase during the freezing of O/W emulsions (Ghosh and Coupland, 2008; Degner *et al.*, 2013). During thawing, as the oil melts, the ice crystals will immediately coalesce as a further increase in temperature caused the aqueous droplet to melt and fuse together (Degner *et al.*, 2014).

As mentioned in section 4.3.4, the difference in density between the aqueous and oil phases in double emulsions caused the separation of the W_1 phase from the double emulsion droplet that retained in the W_2 phase supported by a very thin and complex layer of oil and surfactants. This also caused the reduction in oil globule size as the W_1 phase escaped into the W_2 phase leaving the oil globule with smaller size. Similar behaviour was also seen for samples of double emulsion kept in a lower temperature of 5°C. However, for double emulsion samples kept in a much lower temperature of -20°C and -80°C, significant ($P < 0.001$) increase in the average oil globule size and change in size distribution was observed. The inner W_1 phase

remains intact in the $W_1/O/W_2$ during the freezing process as shown in Figure 5.3 f and droplet separation process was not observed.

The destabilization mechanism of the double emulsion droplet is mainly attributed to the coalescence between the inner W_1 phase and the outer W_2 phase which is termed as external coalescence (Magdassi and Garti, 1987; Rojas and Papadopoulos, 2007). In contrast with single emulsions droplet whereby the droplet destabilization process occurred throughout the freeze and thawing processes, the external coalescence of double emulsion occurred during the thawing process of the emulsions while the inner W_1 phase remains intact during the freezing process (Rojas and Papadopoulos, 2007). The thawing process caused deformation of the inner W_1 phase followed by the complete burst of droplet due to external coalescence and is mainly affected by the size of the inner W_1 phase and surfactant concentration. According to Rojas and Papadopoulos (2007), the determined threshold of the W_1 inner aqueous phase size to the oil globule size ratio is 0.3 in which above, resulting in coalescence upon thawing. In addition, emulsion droplet with thick surfactant layers creates a repulsive force between the W_1 inner phase and the O/W_2 interface that improves droplet stability against external coalescence (Wangqi Hou and Papadopoulos, 1996). A similar mechanism was observed in this study whereby the inner W_1 droplet remain intact during the freezing process and rapid freezing prevents the droplet from splitting (Figure 5.3 e-f). Emulsions destabilization only occurred during the thawing process for both samples kept at -20°C and -80°C. As the frozen oil melts at a lower temperature during the thawing process of samples kept at freezing temperatures, the liquid oil flows through the cracks and gaps created by the gradual thawing of the aqueous phase (Figure 5.3 g) leading to absence of the oil layer that separates the inner W_1 phase from the outer W_2 phase. This accelerates the external coalescence of the aqueous phase as it melts completely with increase in temperature. Moreover, the droplet distribution graph that tails towards the larger droplet size with sharp distribution at the smaller droplet size region shows

evidence of oil globule coalescence after the thawing process that is in contrast to droplet instability that was induced by Ostwald ripening. Ostwald ripening, as mentioned in section 2.1 is a droplet destabilization process whereby it occurred as a result of mutual solubility between immiscible liquids causing droplet with smaller size to solubilise into larger droplet. Thus, with Ostwald ripening, it tends to form sharp droplet distribution at the larger size region with tailing at smaller droplet size region (Aronson and Petko, 1993).

The presence of bacteria also affected droplet stability, especially for single emulsion droplet. As the PGPR surfactant remained liquid during the freezing process (Ghosh and Rousseau, 2009), it is most likely retained in the oil phase and withdrawn from the ice crystals as the aqueous phase freezes. These accelerate the coalescence process of the aqueous phase as the emulsions warmed up. However, the presence of *E. coli*-GFP on the interface minimizes the droplet coalescence during the thawing process as they are most likely crystallized on the interface. The *E. coli*-GFP was observed to have a high affinity towards the soybean oil as determined by the BATH assay (Figure A2, Appendix 5). Changes in bacterial characteristics due to storage in freezing temperatures ease the attachment of the bacteria onto the interface making the droplet less susceptible to rupture. The stabilization effect of bacteria may be similar to emulsion stabilization due to surfactant crystallization and presence of particles on the droplet interface forming Pickering emulsion as reported previously by Ghosh and Rousseau (2009) and Zhu *et al.* (2017). The crystallization of glycerol monostearate (GMS) at 25°C creates a crystalline shell around the water droplet that helps in preventing crystallization damage between the adjacent water droplet and coalescence during the thawing process which is in contrast to emulsions containing molten PGPR (Ghosh and Rousseau, 2009). According to Zhu *et al.* (2017), the addition of heated soy and whey protein in emulsions improves droplet stability against freeze/thaw cycling due to Pickering stearic stabilization. However, further study is still required to confirm the effect of bacteria on droplet stability in freezing conditions.

5.3.2 The effect of storage on phase separation of emulsions

The percentage of free water, separated from W/O samples (Figure 5.4 a) and free oil which is separated from the $W_1/O/W_2$ samples (Figure 5.4 b) was measured in order to further understand the effect of storage conditions and presence of bacteria on emulsion stability. The percentage of free water was measured for W/O sample as droplet destabilization resulted in the presence of a free water layer due to droplet coalescence while the destabilization of $W_1/O/W_2$ droplet lead to the presence of a free oil layer due to the external coalescence between the inner and outer aqueous phase (forming O/W emulsion) and coalescence between large oil droplets that resulted in the presence of an oil layer on top of the sample as discussed in section 5.3.1. Samples were prepared as described in section 5.2.7.

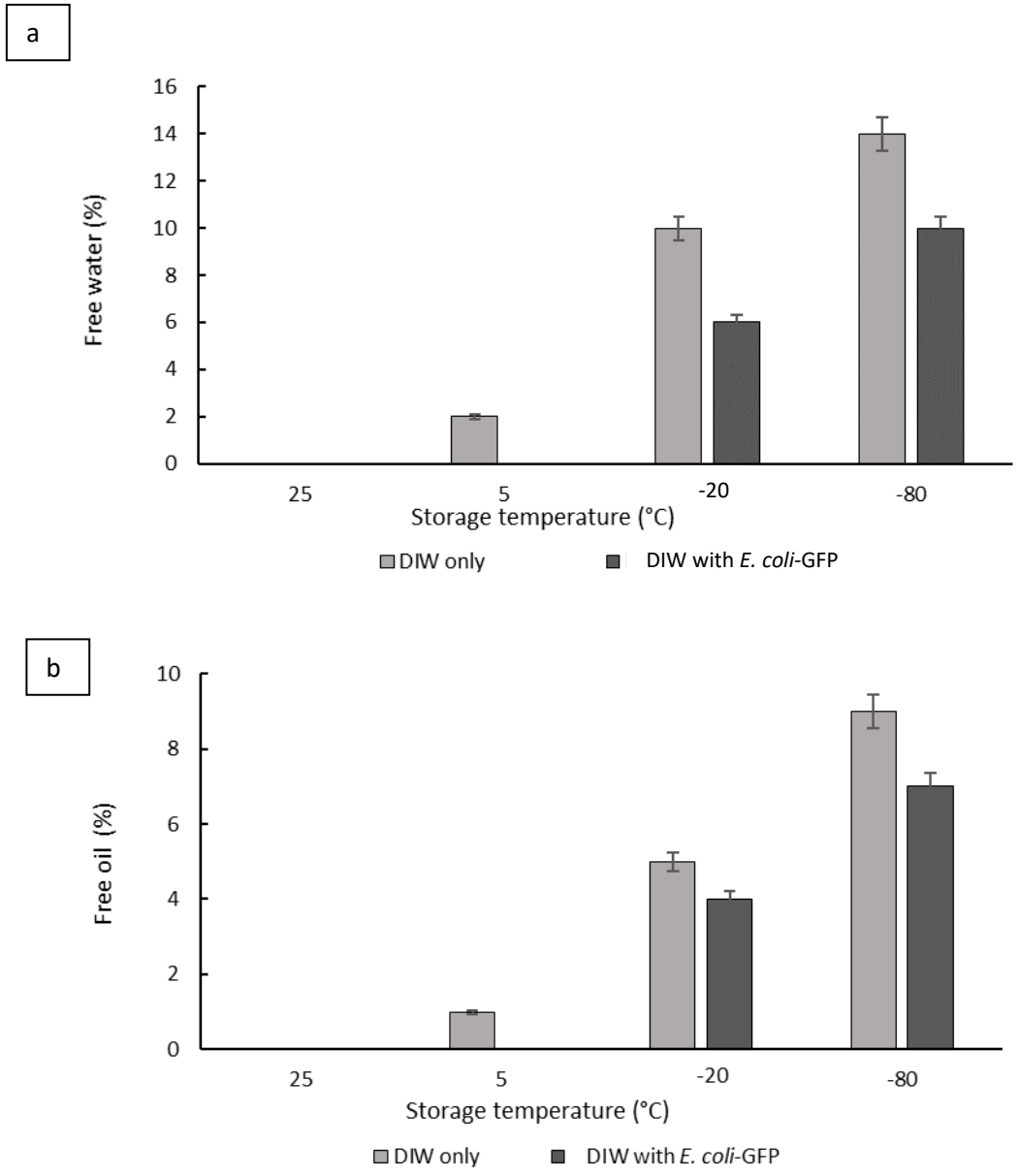

Figure 5.4 The percentage of (a) free water measured for W/O samples and (b) free oil for $W_1/O/W_2$ samples. The volume of free water and free oil was measured with respect to the total volume of the emulsion after 24 hours of storage at different temperature. Bars represent mean ± SEM taken from 3 independent experiments (N=3).

Figure 5.4 shows the percentage ratio of free water and oil measured after 24 hours of storage with respect to the total emulsion. From the results obtained it was determined that phase separation occurred for samples of both single and double emulsions kept in -20°C and -80°C with the highest amount of free water and free oil observed for samples kept at -80°C. Emulsion stability for samples stored at 25°C was maintained during the storage period as there were no observable free water or oil after the thawing process. However, a small percentage of free water and oil (approximately 2%) were observed for samples without *E. coli*-GFP at 5°C and is mainly attributed to the closely packed water droplet during storage and the absence of *E. coli*-GFP that helps in improving droplet stability. Overall comparison between samples with or without the presence of *E. coli*-GFP shows that phase separation was minimized with the presence of *E. coli*-GFP indicating the role of bacterial cells in preventing phase separation.

As discussed previously, droplet destabilization for W/O emulsions kept at -20°C and -80°C occurred due to partial coalescence of the droplet as the crystallization of the dispersed phase resulted in film rupture that connects neighbouring droplet leading to complete coalescence upon thawing (Boode, Walstra and de Groot-Mostert, 1993; Vanapalli, Palanuwech and Coupland, 2002). This eventually leads to bulk water separation that is minimized with the presence of *E. coli*-GFP in the inner W_1 phase. During the crystallization process of the oil phase, the dispersed ice crystals were forced to the still-liquid region of the oil phase and as the temperature decreases, crystallized oil will be withdrawn from this region. Combination of these processes leads to complete aqueous droplet coalescence and extensive bulk water separation from the emulsion during the thawing process (Degner *et al.*, 2013, 2014). The partially crystallized oil phase of samples stored in -20°C prevented the complete withdrawal oil phase as some region within the emulsion may contain liquid oil thus minimizes extensive droplet coalescence. Moreover, the direct destabilization process of the double emulsion droplet that occurs immediately upon the thawing process also leads to bulk oil

separation and the external coalescence of the inner W_1 phase and W_2 phase. As shown in Figure 5.3 g, the movement of liquid oil through the cracks of the outer aqueous phase during the thawing process immediately separates the oil and aqueous phase forming bulk oil layer due to coalescence of bigger oil droplet and a layer of O/W emulsion. The unfrozen W_1 phase will remain in the W_2 phase and eventually be infused into the W_2 phase as it melts (Figure 5.3 h). This process leads to complete release of the W_1 phase into the W_2 phase and extensive separation of the oil phase from the emulsion. Complete $W_1/O/W_2$ emulsion destabilization due to external coalescence during the thawing phase of the oil layer was also reported previously by Rojas and Papadopoulos (2007) whereby it leads to the complete release of the W_1 phase into the W_2 phase forming O/W emulsions.

The presence of crystallized surfactants and Pickering particles has been reported to improve droplet stability as it minimizes droplet coalescence during the thawing process by creating a protective layer that prevents droplet fusion (Ghosh and Coupland, 2008; Marefati *et al.*, 2013; Zhu *et al.*, 2017). A similar stabilization effect may occur with the presence of *E. coli*-GFP on the interfacial layer. Under the freezing condition, *E. coli*-GFP undergo changes in membrane conformation and cell shrinkage (Souzu, 1980) making it easily embedded in the interfacial layer. As discussed previously in section 3.3.2, the presence of *E. coli*-GFP in single W/O emulsions droplet helps in maintaining the stability of the droplet during five days of storage at 25°C whereby the presence of *E. coli*-GFP particularly dead cells helps in reducing interfacial tension due to its attachment on the interfacial layer. The bacterial affinity towards the interface is due to its hydrophobic nature as the dead *E. coli*-GFP cells exhibit higher affinity towards the oil phase as compared to live cells. BATH assay of *E. coli*-GFP with soybean oil reveals its affinity towards the oil phase (Figure A2, Appendix 5) thus may help in reducing the interfacial tension and creates a protective barrier that prevents extensive droplet coalescence during the thawing process. Moreover, the presence of bacteria in the W_2 phase

due to its release as the $W_1/O/W_2$ emulsion destabilizes may help in preventing coalescence between the oil droplet as reported previously by Firoozmand and Rousseau (2016) whereby the presence of bacterial cells in the aqueous phase of the O/W emulsions improves droplet stability due to the attachment of bacterial cells onto the oil droplet that creates a boundary layer thus protecting the droplet against coalescence and phase separation. Although the storage of samples under freezing temperature leads to the unfavourable bulk phase separation, the immediate destabilization of emulsions especially the $W_1/O/W_2$ triggered by the thawing process may be beneficial for the controlled release of bacteria in which will be explained in detail in section 5.3.5.

5.3.3 Thermal properties of emulsions by Differential Scanning Calorimetry (DSC).

The thermal properties of the bulk aqueous solution (Figure 5.5) were characterised as opposed to emulsified samples of single and double emulsions in soybean oil (Figure 5.6). The freshly prepared samples of the bulk aqueous phase with or without *E. coli*-GFP and the emulsified samples in W/O and $W_1/O/W_2$ samples were prepared and scanned by using the differential scanning calorimeter as detailed in section 5.2.9.

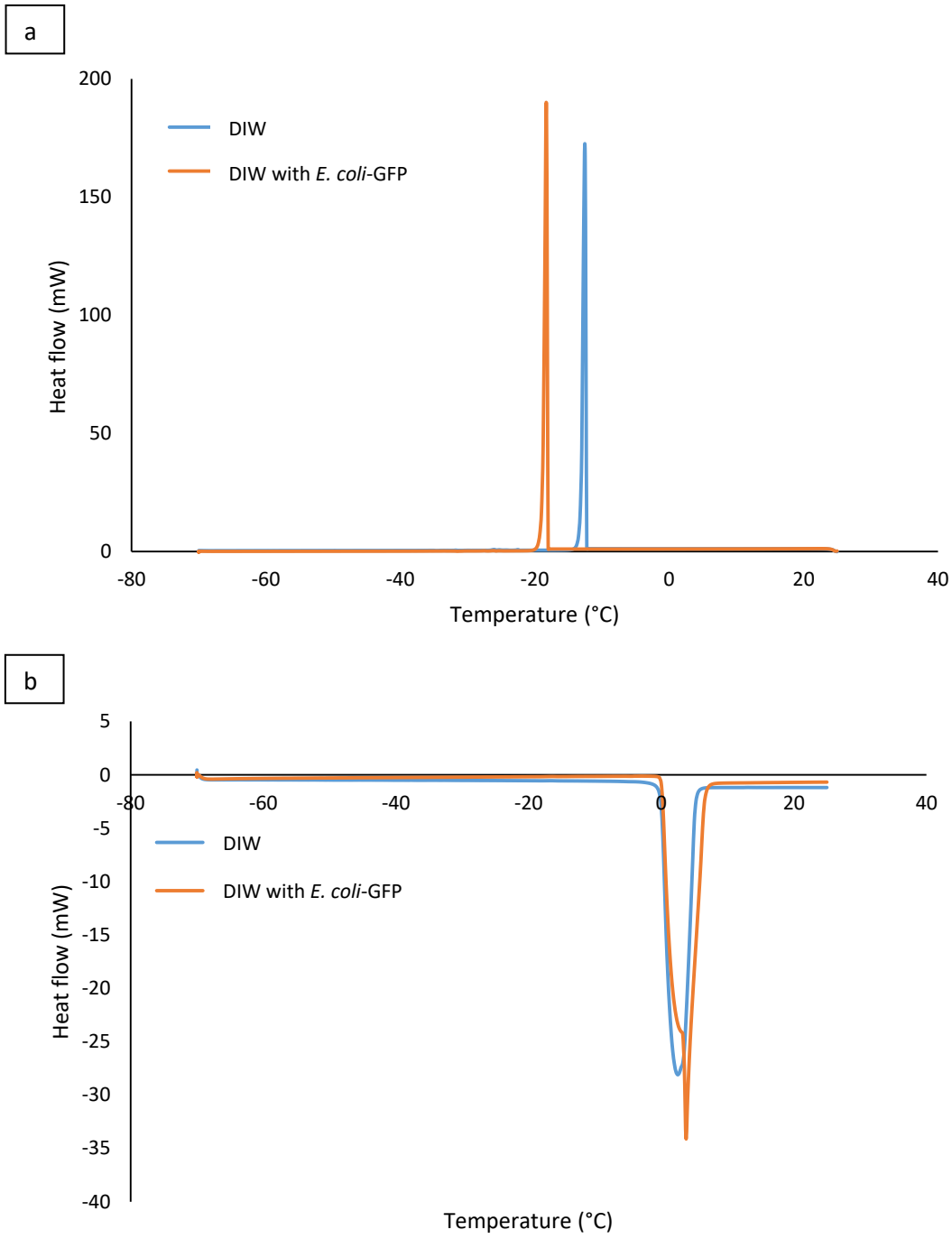

Figure 5.5 DSC thermograms showing the cooling curves (a) and heating curves (b) of bulk aqueous samples with or without *E. coli*-GFP. The samples were prepared at 25°C and were then cooled to -70°C and were held for 5 minutes at -70°C before being heated back to 25°C at 1°C/min. The crystallization and melting temperatures were determined from the onset temperature of the curves.

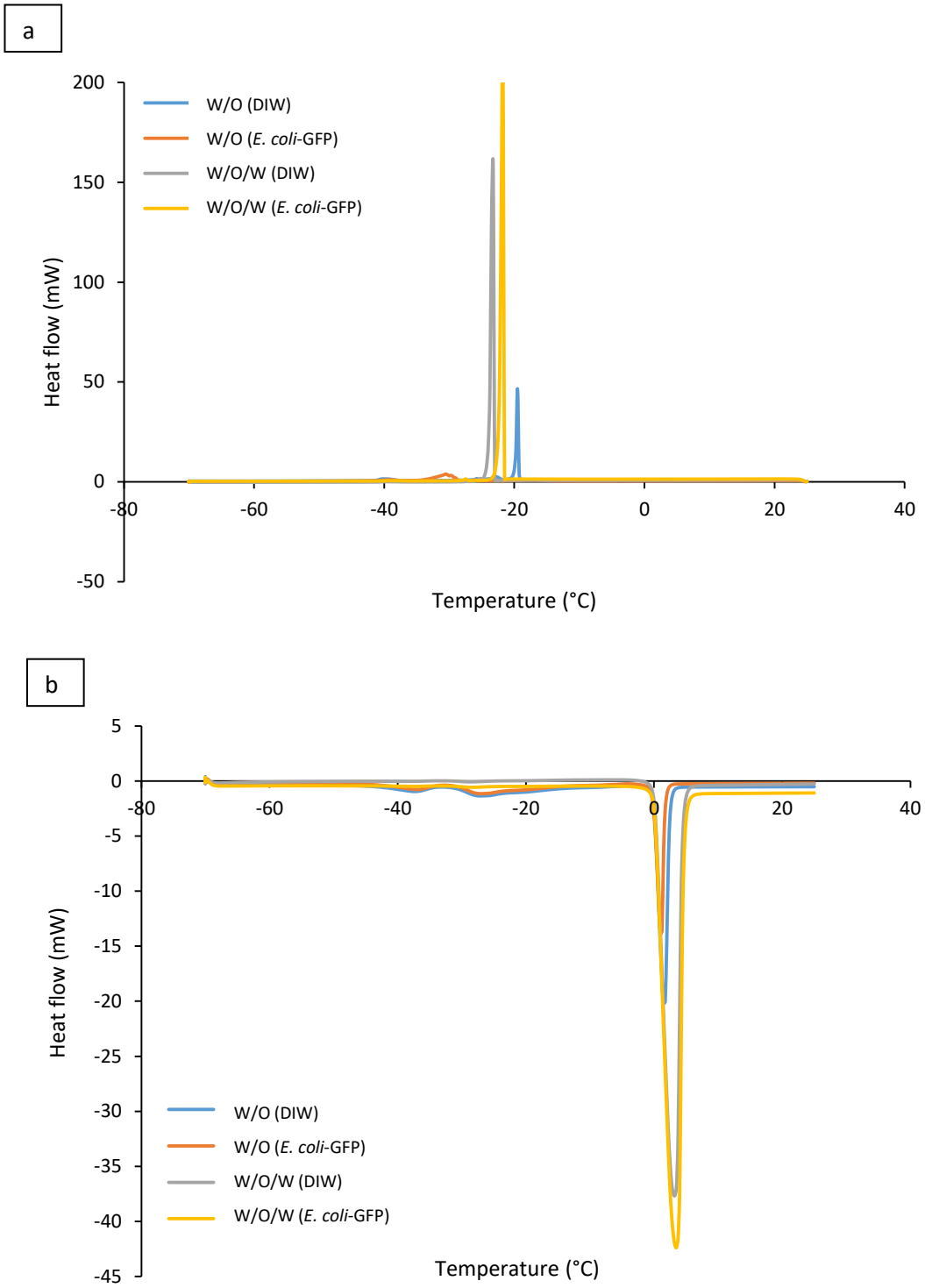

Figure 5.6 DSC thermograms of (a) cooling curves and (b) heating curves of emulsified samples with or without *E. coli*-GFP. The samples were prepared at 25°C and were then cooled to -70°C and were held for 5 minutes at -70°C before being heated back to 25°C at 1C/min. The crystallization and melting temperatures were determined from the onset temperature of the curves.

The cooling and heating curves of bulk aqueous samples are presented in Figure 5.5. In this study, the crystallization temperature of the samples was determined from the onset temperature of the crystallization peaks in which the temperature was recorded at the beginning of the crystallite formation. The onset temperature was determined by using the Star e software (Mettler Toledo, Mettler Scientific Instruments, Germany). Referring to the crystallization peaks in Figure 5.4 a, it was determined that the crystallization of *E. coli*-GFP suspension in DIW occurred at a lower temperature as compared to pure DIW. The pure DIW crystallizes at -12°C and melted at 0°C which is around the same temperature as reported previously in several studies (Cramp *et al.*, 2004; Clausse *et al.*, 2005; Ghosh and Rousseau, 2009b). For the *E. coli*-GFP suspension, the crystallization temperature was recorded at -17°C while the melting of the *E. coli*-GFP suspension occurred around the same temperature as the pure DIW. The reduction in the crystallization temperature with the presence of *E. coli*-GFP is due to the freezing point depression whereby the presence of solute in water or solvent tend to lower the freezing point. The decrease in freezing temperature is due to the presence of the non-volatile solute that reduces the vapour pressure of the solvent. The freezing point of a solution is referred to as a point of equilibrium between the solid and liquid phase as shown in the phase diagram (Figure 2.9). An increase in the solute concentration resulted in a shift in the equilibrium point towards the lower temperature as a reduction in temperature is required for the solid and solution to reach equilibrium (Reger, Goode and Ball, 2009).

Figure 5.6 describes the freezing and cooling curves of the emulsified samples in single W/O emulsions and double $W_1/O/W_2$ emulsions. From the results obtained, it was determined that the emulsified samples freeze at a much lower temperature compared to pure solutions. A broader crystallization curve was observed for samples of W/O emulsions as compared to $W_1/O/W_2$ emulsions. This is mostly attributed to the presence of a large percentage of oil in the continuous phase as compared the aqueous phase. The presence of long chains of lipids

together with a mixture of other molecules in vegetable oils such as soybean oil resulted in broader crystallization temperature as opposed to pure water making it difficult to determine the exact freezing point of the soybean oil. It has been reported that pure soybean oil crystallizes at approximately -10°C to -20°C whereby it is most likely to solidify below these temperatures while soybean oil emulsions solidify at a much lower temperature than the pure oil (Harada and Yokomizo, 2000; Ishibashi, Hondoh and Ueno, 2016). In this study, the single W/O emulsion crystallizes at -20°C for samples without *E. coli*-GFP while samples with *E. coli*-GFP crystallize at -28°C. The melting point of both of the emulsions was around 0°C. The difference in crystallization temperature is mainly attributed to the loss in emulsion stability for emulsions without *E. coli*-GFP whereby the presence of free water due to phase separation increases the crystallization temperature of the samples. In addition, the similar melting point of the emulsions with that of bulk solutions also indicates the loss in emulsion stability due to an increase in the percentage of free water during the thawing process (Chen and He, 2003; Clausse *et al.*, 2005). It has been reported previously that the W/O emulsions solidify at a lower temperature than that of bulk water as it overcomes the free energy barrier due to homogeneous nucleation (Vanapalli, Palanuwech and Coupland, 2002). Water droplet in emulsions solidifies at a lower temperature than the temperature required to solidify bulk water (-20 °C) and are much lower than the equilibrium melting point of water of 0 °C (Lin *et al.*, 2007).

For double $W_1/O/W_2$ emulsions, a small difference in crystallization temperature was observed between samples with or without *E. coli*-GFP as samples containing *E. coli*-GFP crystallise at -21°C while samples without *E. coli*-GFP crystallizes at -23°C. Only one peak was observed which gives the crystallization peak of the W2 phase as opposed to 2 peaks reported by Kovács *et al.* (2005). The absence of the second peak indicates the loss of the inner W1 phase due to emulsion breakdown (Kovács *et al.*, 2005; Schuch, Köhler and Schuchmann,

2013). However, this may not be the case in this study as the inner W_1 droplet were intact during the freezing process as observed in Figure 5.3 f and the loss of inner W_1 phase occurred during the thawing/melting process which explains the presence of only one peak for the melting curve with a melting temperature of approximately 0°C for all samples. Schuch, Köhler and Schuchmann (2013) also described that it is possible to distinguish between the inner W_1 phase and the outer W_2 phase from the cooling curves due to the presence of two peaks that resulted from the difference in crystallization temperature but it is impossible to distinguish between these two phases from the melting curves of the $W_1/O/W_2$. Another possible explanation for the presence of only one cooling curve is due to the highly monodispersed distribution of the droplet that was prepared by using the microfluidic method with single and large size of the W_1 inner core and a thin oil layer separating the W_1 phase from the W_2 phase. A combination of these factors may have caused the outer W_2 phase and the inner W_1 phase to crystallize simultaneously within the same temperature range. Schuch, Köhler and Schuchmann (2013) previously reported that the crystallization of emulsion droplet may depend on the size of the droplet. However, further studies are still required in order to understand the effect of droplet size distribution on the crystallization temperature of the multiple emulsion.

5.3.4 Bacterial viability during storage

The effect of different storage temperatures and encapsulation in emulsion droplet on the viability of *E. coli*-GFP were determined by measuring the reduction in Log CFU/mL of the bacterial cells after the thawing process with respect to initial cell count (Figure 5.7). The samples were prepared with cells concentration of approximately 10^8 CFU/mL.

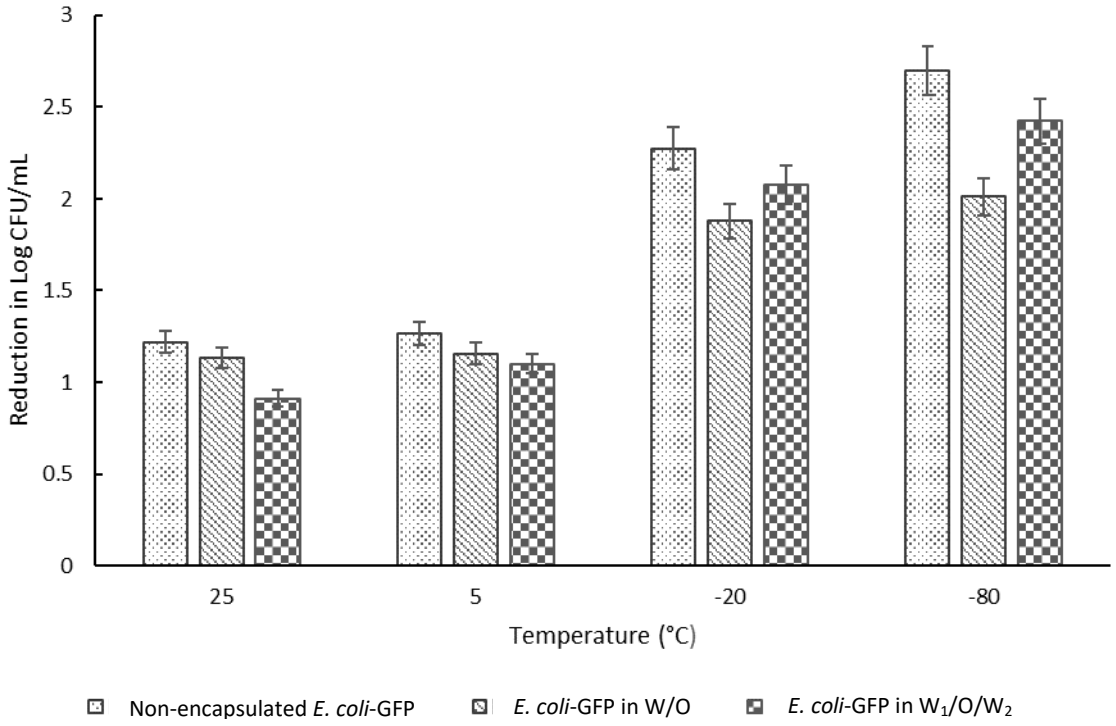

Figure 5.7 Reduction in Log CFU/mL of free *E. coli*-GFP in sterilised DIW and encapsulated in W/O or $W_1/O/W_2$ emulsion droplet. Bars represent mean SEM taken from 3 independent experiments with 3 replicates per experiment (N=3).

From the results obtained, a large reduction in *E. coli*-GFP cell count was observed with samples kept at -20℃ and -80℃ as compared to samples kept in 25°C and 5°C whereby comparing between non-encapsulated samples, 1.2 log CFU/mL and 1.3 log CFU/mL reduction in viable cell count was observed for samples kept in 25°C and 5°C respectively while 2.3 log CFU/mL and 2.7 log CFU/mL of reduction was observed for samples kept in -20°C and -80°C respectively. *E. coli*-GFP encapsulated in W/O droplet shows a smaller percentage of bacterial reduction as compared to samples encapsulated in $W_1/O/W_2$ droplet and control samples of free *E. coli*-GFP cells in sterilised DIW.

It has been reported previously that freeze-thawing may cause detrimental effects on bacterial cells that lead to a reduction in bacterial viability (Souzu, 1980, 1989; Souzu, Sato and Kojima, 1989; Strocchi *et al.*, 2006). Cell damage during the freeze-thaw process occurred due to various physico-chemical reactions (Simonin *et al.*, 2015; Wang *et al.*, 2019). Some of the factors responsible for cell damage during storage at low temperatures are the nature of the cells (O'Brien *et al.*, 2016; Wang *et al.*, 2019), whereby different bacterial species exhibit different resistance to cell damage depending on cell conformation. Furthermore, the use of cryoprotectant with various formulations (Wang *et al.*, 2019) and the freeze-thawing conditions (Fonseca, Béal and Corrieu, 2002; Powell-Palm *et al.*, 2018) of the samples may also affect the degree of cell damage during storage.

The effect of water crystallization is one of the most common factors responsible for cell damage (Souzu, 1980; Mazur, 2017; Powell-Palm *et al.*, 2018). The detrimental effect of water-crystallization on bacterial viability depended on the freezing rate whereby the decrease in bacterial viability is minimized at a low-freezing rate as compared to high-freezing rate. This is due to the cryoconcentration effect as the crystallization of the external medium resulted in cell dehydration thus preventing the lethal intracellular crystallization. The crystallization of the extracellular medium forces the cells to be concentrated in the unfrozen region of the

medium whereby a continuous decrease in temperature caused the region to be increasingly concentrated. This leads to cell dehydration as the cells were exposed to a highly concentrated solution during the freezing process. Meanwhile, the rapid freezing of bacterial suspension resulted in extensive supercooling that crystallizes intracellular water as it is not able to flow out of the cells fast enough causing extensive cell damage (Simonin *et al.*, 2015). These indicate that the degree of cell damage during the freezing process depended on the availability of intra- and extracellular water. Referring to the DSC thermograms (Figure 5.6), the broader crystallization temperature of the aqueous phase of the emulsion as compared to the bulk bacterial solution (Figure 5.5) indicates that the encapsulation of bacteria in emulsion droplet promotes slow freezing of the samples and thus minimizes cell damage during the freezing process. Encapsulation in W/O emulsion droplet shows a smaller reduction in cell count as compared to samples encapsulated in $W_1/O/W_2$ emulsion droplet and free cells in DIW due to the thick oil layer and the low water ratio that minimizes cells damage due to water crystallization.

The effect of encapsulation in improving bacterial viability during the freeze-thaw process has also been reported previously (Goderska and Czarnecki, 2008; Priya, Vijayalakshmi and Raichur, 2011; Dianawati, Mishra and Shah, 2013). The microencapsulation of *Lactobacillus acidophilus* in the self-assembled polyelectrolyte layers of chitosan and carboxymethyl cellulose has been reported to protect bacteria not only from the adverse effect of simulated GI tract but also during the freeze and freeze-drying processes (Priya, Vijayalakshmi and Raichur, 2011). Furthermore, the microencapsulation of *Bifidobacterium longum* in milk proteins and sugar alcohols aids in improving the protection effect of cryoprotectants such as glycerol resulting in better bacterial viability and function after the freeze and freeze-drying processes (Dianawati, Mishra and Shah, 2013). Moreover, the freezing of emulsion based products such as milk has also been reported to cause small

changes in the viability of bacteria indicating the ability of the emulsion structure in protecting bacteria against extensive cell damage. A study done by Sánchez *et al.* (2003) shows that the freezing of goat milk at -20°C or even after extended storage at -80°C does not significantly affect the viability of *E. coli* as opposed to cow milk due to differences in milk composition. A similar result was also reported by Nurliyani, Suranindyah and Pretiwi (2015) whereby the frozen storage of Ettawah Crossed bred goats milk samples for 60 days does not cause changes in the total bacteria while changes in emulsion stability were observed after 30 days of storage. Therefore, the encapsulation of bacteria in emulsion droplet especially W/O may help in improving bacterial viability during the freezing process due to the protective effect of the emulsion structure as it reduces available water ratio and prevents the lethal crystallization effect of the water phase.

5.3.5 The release of bacteria from double emulsions

As discussed in section 5.3.1 and 5.3.2, the storage of emulsions in freezing temperatures caused extensive droplet destabilization and complete release of the W_1 phase into the W_2 phase. The instability of double emulsions during cold temperature storage may be beneficial for the controlled release of bacteria for various applications. In order to study the effect of temperature on the release of bacteria, samples of $W_1/O/W_2$ with *E. coli*-GFP in the W_1 inner phase were prepared and kept at 25°C, 5°C, -20°C and -80°C. A bacterial cell count of the outer W_2 phase was done immediately after sample preparation and after the thawing process in order to determine the log CFU/mL of bacteria that were released into the W_2 phase from the overall viable cell in a sample as described in Table 5.2.

Table 5.2 The effect of storage temperature on the release of bacteria from $W_1/O/W_2$ droplet. Samples were prepared with 99.9% encapsulation efficiency and the release of bacteria into the W_2 phase was determined after 24 hours of storage. Data represent mean ± standard deviation taken from 3 independent experiments (N=3).

Temperature (°C)	Overall viability (log CFU/mL)	Released (log CFU/mL)
25	6.42 ± 0.03	2.75 ± 0.02
5	6.18± 0.01	2.77 ± 0.01
-20	5.19± 0.02	5.10 ± 0.01
-80	4.93± 0.03	4.90 ± 0.01

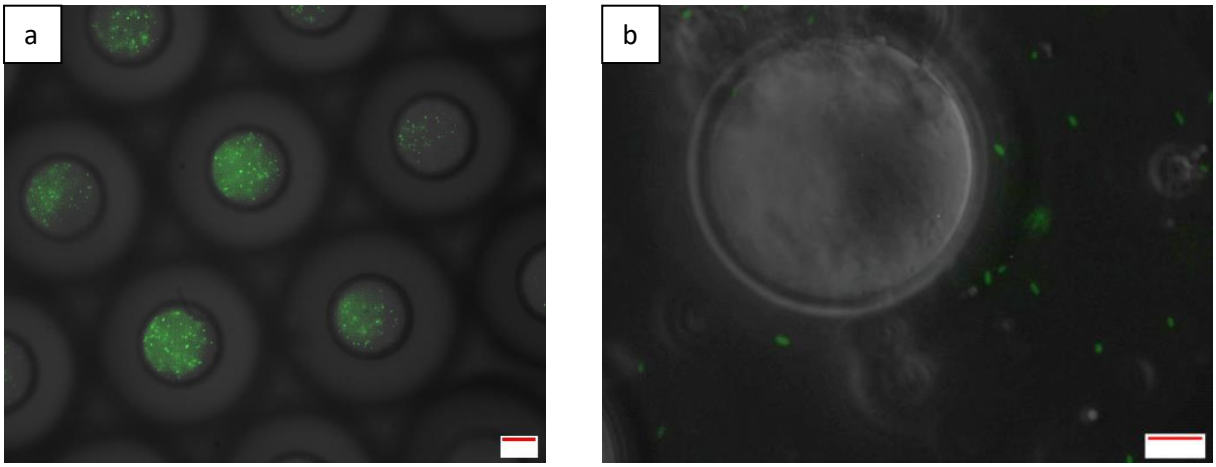

Figure 5.8 Photomicrographs of double emulsion droplet before (a) and after (b) storage at -80°C for 24 hours. The bacteria were seen encapsulated in the W_1 phase of the $W_1/O/W_2$ droplet prior to storage at -80°C and were released into the W_2 phase after being thawed at 25°C. Scale bar represents 20 µm.

As discussed previously in section 4.3.2, high encapsulation efficiency was achieved by using microfluidic for bacteria encapsulation in $W_1/O/W_2$ indicating successful encapsulation of bacteria. The increase in cell count of the W_2 phase, therefore, resulted from the release of bacteria from the W_1 phase due to emulsion destabilization process during storage as presented in Table 5.2. From the results obtained, it is determined that the percentage of bacteria released into the W_2 phase increased with a decrease in storage temperature. Complete bacterial release into the W_2 phase was observed for samples kept in freezing temperatures of -20°C and -80°C with 5.10 log CFU/mL of viable bacteria were observed in the W_2 phase from the overall viable cell of 5.19 log CFU/mL (for samples kept at -20°C) and 4.90 log CFU/mL of viable bacteria were observed in the W_2 phase from the overall viable cell of 4.93 log CFU/mL (for samples kept at -80°C). Only 2.75 log CFU/mL of cells were released into the W_2 phase from the overall viable cell of 6.42 log CFU/mL for samples kept in 25°C and 2.77 log CFU/mL of cells were released from the overall viable cells of 6.18 log CFU/mL at 5°C. The release of bacteria for samples kept in 25°C and 5°C was mainly attributed to the rupture of the thin film that separates the W_1 phase from the W_2 phase, induced by the change in the osmotic balance of the droplet due to the production of bacterial by-products during the storage period. On the other hand, the complete destabilization of the $W_1/O/W_2$ emulsion droplet that was kept in frozen temperature is due to the freeze-thawing process that leads to phase separation forming bulk oil phase and external coalescence of the W_1 and W_2 phase as reported previously in section 5.3.1 and 5.3.2. The thawing process of the samples kept at freezing temperatures leads to the melting of the oil phase first followed by the aqueous phase. During this process, the liquid oil flows out of the emulsion structure through the cracks and gaps created while the aqueous phase melts and therefore caused the immediate destabilization of the emulsion structure as the big oil droplet coalesce leading to bulk oil separation while the still-frozen W_1 oil phase coalesces with the W_2 phase as it melts (Figure 5.3 e-h). These

processes resulted in the complete release of the encapsulated bacteria as the emulsion destabilizes into a layer of the bulk oil phase, O/W emulsion and the aqueous phase containing the released bacteria.

As the inner W_1 phase remains intact during the freezing process (Figure 5.3 f), the frozen $W_1/O/W_2$ may serve as an alternative for bacterial microencapsulation whereby the controlled release of the encapsulated bacteria at the desired time can be achieved by simply thawing the frozen emulsion samples causing immediate and complete release of the bacteria into the W_2 phase. Emulsion destabilization induced by the freeze-thawing process has been used extensively in various applications such as in emulsion liquid membrane (ELM) processing (Hirai, Hodono and Komasawa, 2000; Hirai *et al.*, 2002) and waste emulsion treatment such as in oil sludge demulsification (He and Chen, 2002; Chen and He, 2003). Moreover, a study by Rojas and Papadopoulos (2007) also revealed the potential application of $W_1/O/W_2$ emulsion droplet for the controlled release of encapsulated materials that is triggered by the thawing of the oil phase. Similar to the results obtained in this study, the internal coalescence of the inner W_1 phase and the external coalescence of the outer W_2 phase were not observed during the freezing stage but occurred extensively during the thawing of the oil phase which leads to complete release of the encapsulated material. These results are followed by a study on its potential application for the controlled release of protein from the bulk emulsion systems (Rojas *et al.*, 2008). As expected, similar results were also obtained in bulk emulsion systems whereby the stability of the droplet was maintained during the freezing process while the thawing of the oil phase leads to an instant release of the encapsulated protein.

The results obtained in the present study shows the potential use of double emulsions for the controlled release of bacteria triggered by the freeze-thaw process. However, further studies are still required in order to gain a better understanding of the process especially in improving the viability of bacteria during storage.

5.4 Conclusion

This chapter revealed the feasibility of using emulsion droplet for bacterial encapsulation and storage not only in ambient but also in cold temperatures. The information gained from this chapter provides a better understanding of the stability of emulsions with the presence of bacteria in cold temperatures and showed the benefits of encapsulation in maintaining the viability of the bacteria by providing protection against the lethal effect of the freezing process. These characteristics are beneficial for the production of emulsions containing bacteria for laboratory-based and industrial applications. In addition, it also displayed the potential use of the freeze-thaw technique for the controlled release of not only bacteria but also applicable to other applications that used temperature-sensitive compounds such as in drug delivery.

Nevertheless, further studies are still required in order to compare the freeze-thaw mechanism of highly monodispersed $W_1/O/W_2$ droplet containing single W_1 inner phase with a droplet containing multiple W_1 inner phases as it may exhibit different mechanism as observed in the absence of a second peak in the cooling curves of the double emulsion droplet. In addition, further studies are also required in order to investigate the process behind the ability of bacterial cells in maintaining droplet stability during cold temperature storage and also to improve bacterial stability during the freezing process especially for samples encapsulated in double $W_1/O/W_2$ droplet.

Chapter 6

Conclusions and future works

The experiments conducted in this study have been focusing on the effects of bacterial encapsulation in single and double emulsion droplet on droplet stability together with the effect of encapsulation on bacterial growth and viability during storage in ambient and cold temperature. The use of microfluidics for emulsion droplet generation and for the encapsulation of bacteria in emulsion droplet has been proved beneficial for the production of a highly monodispersed droplet with high bacterial encapsulation efficiency. In addition, the interesting application of the double emulsion droplet in the controlled release of bacteria was also investigated in this study. The research begins by investigating the effects of bacterial encapsulation on the stability of single W/O emulsions and the effects of encapsulation on bacterial growth and viability during storage (chapter three), followed by the study of bacterial encapsulation in double emulsions $W_1/O/W_2$ droplet that further explores the effects of encapsulation on bacterial viability along with a study on the effects of osmotic balance alterations on droplet stability and release of bacteria (chapter four). In addition, a study on the effects of cold temperature storage on the stability of both single and double emulsion droplet was also conducted in order to further explore the application of bacterial encapsulation in emulsion droplet for industrial and lab-based applications (chapter five). A summary of the key findings obtained from each chapter presented in this thesis is listed and explained in the following paragraphs.

The application of droplet microfluidics for single W/O and double $W_1/O/W_2$ emulsions ensures the production of a highly monodispersed droplet with high bacterial encapsulation efficiency. The usage of a flow-focusing device with single junction (for producing W/O droplet) and double junction (for the production of $W_1/O/W_2$) allows for the generation of the monodispersed droplet in a highly controlled manner. Various droplet sizes and formats can be produced by tuning the flow or pressure rate of the phases. In addition, high encapsulation efficiency of 99.9% was also achieved when using microfluidics for the encapsulation of bacteria in $W_1/O/W_2$.

The presence of bacteria improves the stability of W/O droplet during storage as compared to control samples of emulsions droplet without bacteria. This is mainly attributed to the ability of bacteria to act as particles in stabilizing the W/O droplet due to their attachment on the interfacial layer that helps in reducing interfacial tension. The stabilization effects were apparent with the presence of dead cells whereby the inability of bacteria to survive in W/O droplet during storage resulted in the presence of dead cells with high affinity towards the interface (due to hydrophobic nature). In addition, encapsulation also promotes the formation of bacterial clustering due to stress that may also contribute to the stability of W/O droplet. *E. coli*-GFP shows a better stabilization effect during the storage period as compared to *L. paracasei* due to difference in lipid content between the strains. From the results obtained, it can be concluded that the effects of bacteria on droplet stability depend on several factors such as the type of bacteria, bacterial viability and bacterial concentration whereby these factors play a major role in ensuring the effectiveness of bacteria as particles in promoting droplet stability. Further studies are still required in order to fully understand the mechanism behind the attachment of bacteria onto the emulsion droplet and droplet stabilization effects of the bacterial cells.

The encapsulation of bacteria in $W_1/O/W_2$ droplet improves bacterial viability as compared to encapsulation in single W/O droplet. The presence of an outer W_2 phase allows for the addition of nutrients to support bacterial growth in the inner W_1 phase by nutrient replenishment. This allows for the continuous supply of nutrients throughout the storage period. The presence of an oil layer that separates the inner W_1 phase from the outer W_2 phase not only acts as a buffer that protects bacteria against harsh environmental conditions but also as a semi-permeable membrane which allows for the transport of nutrients from the outer W_2 phase into the inner W_1 phase. The addition of LB broth in the outer W_2 phase helps in improving bacterial viability and metabolic activity thus making it suitable for long term storage or study of bacteria. However, the effectiveness of the $W_1/O/W_2$ droplet to support bacterial growth is highly depended on the stability of the droplet during storage. Therefore, future studies are still required to improve the stability of the thermodynamically unstable $W_1/O/W_2$ emulsions.

The controlled release of bacteria from $W_1/O/W_2$ droplet can be achieved by osmotic balance alterations of the inner W_1 phase and outer W_2 phase. The application of droplet microfluidics in this study allows for a detailed study on droplet destabilization that leads to the release of bacteria due to the production of a highly monodispersed droplet with a single core. Droplet destabilization mechanisms that aid in bacterial release was proposed in this study that begins with droplet breakup/split as the difference in density between oil and the aqueous phase caused the oil droplet to escape from the $W_1/O/W_2$ droplet leaving the inner W_1 phase that is retained in the W_2 phase by a very thin and complex film of oil and surfactants. This process does not cause the release of bacteria into the W_2 phase as the bacteria were still encapsulated in these "secondary double emulsions". The controlled release of bacteria is, therefore, depending on the stability of the thin film whereby changes in osmotic balance leads to the release of bacteria into the W_2 phase as the droplet destabilizes and ruptures. The

controlled release of bacteria depended on several factors such as the NaCl concentration balance between the inner and outer aqueous phase as well as the Tween 80 surfactant concentration. The present study provides valuable information on the application of $W_1/O/W_2$ droplet for the controlled release of materials that will be beneficial for its industrial applications. However, further studies are still required to understand the nature and composition of the thin film that surrounds the droplet after the splitting process and the mechanism behind the droplet breakup/split in order to control this process. In addition, it is also worth to investigate the effect of other factors that may induce the release of bacteria from $W_1/O/W_2$ droplet such as a change in temperature or pH on the droplet breakup/split in order to further improve and widen the applications of $W_1/O/W_2$ droplet in the encapsulation of bacteria.

The storage of emulsions in freezing temperatures caused extensive droplet destabilization compared to samples stored in an ambient temperature of 25°C and refrigeration temperature of 5°C for both single W/O and double $W_1/O/W_2$ emulsion droplet. The W/O and $W_1/O/W_2$ droplet exhibited a different destabilization mechanism due to the difference in the continuous phase. The destabilization of W/O emulsion is due to the partial coalescence process whereby gradual freezing of the water droplet caused the formation of protruding ice crystals that puncture the still-liquid neighbouring droplet and linked the droplet together. This resulted in droplet flocculation followed by complete coalescence upon thawing that leads to the presence of free bulk water. No significant difference in droplet stability was observed for samples stored in 25°C ($P = 0.24$) or 5°C ($P = 0.07$) and presence of bacteria in the droplet improved droplet stability as it prevents extensive coalescence during thawing. For double $W_1/O/W_2$ droplet, droplet destabilization occurred due to external coalescence of the W_1 phase and W_2 phase as the structure of the droplet collapsed upon thawing. The double emulsion structure remains stable during the freezing process with intact

W_1 phase. This reveals the potential use of the freeze-thawing technique for controlled release of bacteria. Nevertheless, further studies are required in order to confirm the stabilization effect of bacterial cells on emulsions droplet during cold temperature storage and also to understand the mechanism behind droplet stabilization in the presence of bacteria.

Bacterial viability during cold temperature storage was improved with encapsulation in W/O droplet as compared to free cells and encapsulation in $W_1/O/W_2$. This is mainly due to the presence of a high oil to water ratio in W/O emulsions that prevents the detrimental effect of water crystallization that leads to cell damage. A study on the release of bacteria from the double $W_1/O/W_2$ droplet reveals the potential use of double $W_1/O/W_2$ droplet for the controlled release of bacteria whereby complete bacterial release was achieved upon thawing of samples stored in freezing temperatures. This shows the potential use of emulsions for bacterial encapsulation in cold temperatures and the use of double $W_1/O/W_2$ droplet for the controlled release of not only bacteria but also applicable for other applications that used temperature-sensitive compounds such as in drug delivery. Further studies are still required in order to improve the viability of bacteria encapsulated in double $W_1/O/W_2$ droplet during freezing temperature storage. An example of future work that can be conducted, is the development of suitable cryoprotectant formulation that not only improves bacterial viability but also its functions after storage in freezing temperature

References

Aguilera, J. M. and Lillford, P. J. (2007) *Food Materials Science: Principles and Practice*. New York: Springer (Food Engineering Series).

Altman, D. G. and Bland, J. M. (2005) 'Standard deviations and standard error', *BMJ*, 331 (7521), pp. 903.

Amalvy, J. I. *et al.* (2003) 'Use of sterically-stabilised polystyrene latex particles as a pH-responsive particulate emulsifier to prepare surfactant-free oil-in-water emulsions', *Chemical Communications*, 15, p. 1826.

Anal, A. K., Singh H. (2007). 'Recent advances in microencapsulation of probiotics for industrial applications and targeted delivery', *Trends in Food Science and Technology,* 18, pp. 240-251

Annan, N. T. *et al*. (2008) 'Encapsulation in alginate coated gelatin microspheres improves survival of probiotic *Bifidobacterium adolescentis* 15703T during exposure to simulated gastro-intestinal conditions', *Food Research International*, 41, pp. 184–193.

Aronson, M. P. *et al.* (1994) 'Origins of freeze-thaw instability in concentrated water-in-oil emulsions', *Colloids and Surfaces A: Physicochemical and Engineering Aspects*, 85(2–3), pp. 199–210.

Aronson, M. P. and Petko, M. F. (1993) 'Highly Concentrated Water-in-Oil Emulsions: Influence of Electrolyte on Their Properties and Stability', *Journal of Colloid and Interface Science*, Academic Press, 159(1), pp. 134–149.

Barlow, J. *et al.* (2017) 'High throughput microencapsulation of *Bacillus subtilis* in semi-permeable biodegradable polymersomes for selenium remediation', *Applied Microbiology and Biotechnology*, 101(1), pp. 455–464.

Bauer, W. A. C. *et al.* (2010) 'Hydrophilic PDMS microchannels for the high-throughput formation of oil-in-water microdroplet and water-in-oil-in-water double emulsions', *Lab on a Chip*, 10(14), pp. 1814–1819.

Berk, Z. (2013) 'Chapter 7 - Mixing', in Berk, Z. (ed.) *Food Process Engineering and Technology*. second edn. San Diego: Academic Press (Food Science and Technology), pp. 193–216.

Bernath, K. *et al.* (2004) 'In vitro compartmentalization by double emulsions: Sorting and gene enrichment by fluorescence-activated cell sorting', *Analytical Biochemistry*, 325(1), pp. 151–157.

Binks, B. P. *et al.* (1998) *Modern Aspects of Emulsion Science*. Royal Society of Chemistry

Binks, B. P., Philip, J., and Rodrignes, J. A. (2005) 'Inversion of silica-stabilized emulsions induced by particle concentration', *Langmuir*, 21, pp.3296−3302.

Binks, B. P. and Horozov, T. S. (2006) *Colloidal Particles at Liquid Interface*, Cambridge University Press: Cambridge.

Boedicker, J. Q., Vincent, M. E. and Ismagilov, R. F. (2009) 'Microfluidic confinement of single cells of bacteria in small volumes initiates high-density behaviour of quorum sensing and growth and reveals its variability', *Angewandte Chemie - International Edition*, 48(32), pp. 5908–5911.

Boekel, M. A. J. S. and Walstra, P. (1981) 'Stability of oil-in-water emulsions with crystals in the disperse phase', *Colloids and Surfaces*, 3(2), pp. 109–118.

Boitard, L. *et al.* (2012) 'Monitoring single-cell bioenergetics via the coarsening of emulsion droplet', *Proceedings of the National Academy of Sciences of the United States of America*, 109(19), pp. 7181–7186.

Boode, K., Walstra, P. and de Groot-Mostert, A. E. A. (1993) 'Partial coalescence in oil-in-water emulsions 2. Influence of the properties of the fat', *Colloids and Surfaces A: Physicochemical and Engineering Aspects*, 81(C), pp. 139–151.

Bozoğlu, T. F., Özilgen, M. and Bakir, U. (1987) 'Survival kinetics of lactic acid starter cultures during and after freeze-drying', *Enzyme and Microbial Technology*, 9(9), pp. 531–537.

Brizuela, M. A., Serrano, P. and Ferez, Y. (2001) 'Studies on probiotics properties of two lactobacillus strains', *Brazilian Archives of Biology and Technology*, 44(1), pp. 95–99.

Burgess, D. J. and Yoon, J. K. (1995) 'Influence of Interfacial Properties of Lipophilic Surfactants on Water-in-Oil Emulsion Stability', *Colloids and Surfaces B: Biointerfaces*, 4(5), pp. 297–308.

Casadevall i Solvas, X. and deMello, A. J. (2011) 'Droplet microfluidics: recent developments and future applications.', *Chemical communications (Cambridge, England)*, 47(7), pp. 1936–42.

Chan, H. F. *et al.* (2013) 'Rapid formation of multicellular spheroids in double-emulsion droplet with controllable microenvironment', *Sci. Rep.*, 3, p. 3462.

Chan, H. F. *et al.* (2017) 'High-throughput screening of microchip-synthesized genes in programmable double-emulsion droplet', *Nanoscale*. The Royal Society of Chemistry, 9(10), pp. 3485–3495.

Chang, C. B. *et al.* (2015) 'Monodisperse Emulsion Drop Microenvironments for Bacterial Biofilm Growth', *Small*, 11(32), pp. 3954–3961.

Chappat, M. (1994) 'Some applications of emulsions', *Colloids and Surfaces A: Physicochemical and Engineering Aspects*, 91(C), pp. 57–77.

Chavarri, M., Maranon, I. and Carmen, M. (2012) 'Encapsulation Technology to Protect Probiotic Bacteria', in Rigobelo, E.C. (ed.) *Probiotics*. IntechOpen, pp. 502-529.

Chen, G. and He, G. (2003) 'Separation of water and oil from water-in-oil emulsion by freeze/thaw method', *Separation and Purification Technology*, 31(1), pp. 83–89.

Chen, H. *et al.* (2015) 'Response Surface Optimization of Lyoprotectant for *Lactobacillus bulgaricus* during Vacuum Freeze-Drying', *Preparative Biochemistry and Biotechnology*, 45(5), pp. 463–475.

Chen, Y. Y. and Wang, H. Y. (2016) 'Fabrication and characterization of polyelectrolyte microcarriers for microorganism cultivation through a microfluidic droplet system', *Biomicrofluidics*, 10(1). pp. 0140126

Choi, S. W., Zhang, Y. and Xia, Y. (2010) 'A temperature-sensitive drug release system based on phase-change materials', *Angewandte Chemie - International Edition*, 49(43), pp. 7904–7908.

Christopher, G. F. and Anna, S. L. (2007) 'Microfluidic methods for generating continuous droplet streams', *Journal of Physics D: Applied Physics*, 40(19), pp. R319-R336.

Chung, H. J., Bang, W. and Drake, M. A. (2006) 'Stress response of *Escherichia coli'*, *Comprehensive Reviews in Food Science and Food Safety*, pp. 52–64.

Clausse, D. *et al.* (2005) 'Morphology characterization of emulsions by differential scanning calorimetry', *Advances in Colloid and Interface Science*, 117(1–3), pp. 59–74.

Colard, C. A. L., Teixeira, R. F. A. and Bon, S. A. F. (2010) 'Unraveling mechanistic events in solids-stabilized emulsion polymerization by monitoring the concentration of nanoparticles in the water phase', *Langmuir*, 26, pp. 7915−7921.

Coupland, J. N. and McClements, D. J. (1996) 'Lipid oxidation in food emulsions', *Trends in Food Science and Technology*, 7(3), pp. 83–91.

Cramp, G. L. *et al.* (2004) 'On the stability of oil-in-water emulsions to freezing', *Food Hydrocolloids*, 18(6), pp. 899–905.

Damin, M. R. *et al.* (2008) 'Effect of cold storage on culture viability and some rheological properties of fermented milk prepared with yoghurt and probiotic bacteria', *Journal of Texture Studies*, 39(1), pp. 40–55.

Damodaran, S. (2005) 'Protein Stabilization of Emulsions and Foams', *Journal of Food Science*, 70(3), pp. R54–R66.

Degner, B. M. *et al.* (2013) 'Influence of freezing rate variation on the microstructure and physicochemical properties of food emulsions', *Journal of Food Engineering*. Elsevier Ltd, 119(2), pp. 244–253.

Degner, B. M. *et al.* (2014) 'Factors influencing the freeze-thaw stability of emulsion-based foods', *Comprehensive Reviews in Food Science and Food Safety*, 13(2), pp. 98–113.

Destribats, M. *et al*. (2014) 'Emulsions stabilised by whey protein microgel particles: towards food-grade Pickering emulsions', *Soft Matter*, 10(10), pp.6941–6954.

Devanthi, P. V. P. *et al.* (2018) 'Segregation of *Tetragenococcus halophilus* and *Zygosaccharomyces rouxii* using W1/O/W2 double emulsion for use in mixed culture fermentation', *Food Research International*. Elsevier, 105(September 2017), pp. 333–343.

Devanthi, P. V. P. *et al.* (2018) 'Water-in-oil-in-water double emulsion for the delivery of starter cultures in reduced-salt moromi fermentation of soy sauce', *Food Chemistry*. Elsevier, 257(March), pp. 243–251.

Dianawati, D., Mishra, V. and Shah, N. P. (2013) 'Survival of *Bifidobacterium longum* 1941 microencapsulated with proteins and sugars after freezing and freeze-drying', *Food Research International*. Elsevier Ltd, 51(2), pp. 503-509.

Dickinson, E. (2010) 'Food Emulsions and Foams: Stabilization by Particles', *Curr. Opin. Colloid Interface Sci*., 15, pp.40−49.

Dluska, E. *et al.* (2017) 'Drug-Core Double Emulsions for Co-release of Active Ingredients', *International Journal of Chemical Engineering and Applications*, 7(6), pp. 428–432.

Dorobantu, L. S. *et al.* (2004) 'Stabilization of oil-water emulsions by hydrophobic bacteria', *Applied and Environmental Microbiology*, 70(10), pp. 6333–6336.

El Kadri, H. *et al.* (2015) 'Understanding and controlling the release mechanism of *Escherichia coli* in double $W_1/O/W_2$ emulsion globules in the presence of NaCl in the W_2 phase', *RSC Adv.*, 5(127), pp. 105098–105110.

El Kadri, H. *et al.* (2016) 'Modulating the release of *Escherichia coli* in double $W_1/O/W_2$ emulsion globules under hypo-osmotic pressure', *RSC Advances*, 6(96), pp. 93694–93706.

El Kadri, H. *et al.* (2018) 'Utilisation of water-in-oil-water ($W_1/O/W_2$) double emulsion in a set-type yoghurt model for the delivery of probiotic *Lactobacillus paracasei*', *Food Research International*, 107(February), pp. 325–336.

Elveflow (2019) *Digital microfluidics: microfluidic droplet and emulsion science*. Available at https://www.elveflow.com/microfluidic-tutorials/microfluidic-reviews-and-tutorials/digital-microfluidics-microfluidic-droplet-emulsion-science/ (Accessed: 2 September 2019)

Erickson, M. C. and Hung, Y. C. (1997) *Quality in Frozen Food*. United States: Springer.

Fadnavis, N. W. *et al.* (1990) 'Peptide synthesis mediated by immobilized and viable baker's yeast in reverse micelles: synthesis of leucine enkephalin analogues', *J. Chem. Soc. Chem. Commun.* The Royal Society of Chemistry, (21), pp. 1548–1550.

Fair, R. B. (2007) 'Digital microfluidics: Is a true lab-on-a-chip possible?', *Microfluidics and Nanofluidics*, 3(3), pp. 245-281.

Farias, T. G. S. de *et al.* (2019) 'Viabilities of *Lactobacillus rhamnosus* ASCC 290 and *Lactobacillus casei* ATCC 334 (in free form or encapsulated with calcium alginate-chitosan) in yellow mombin ice cream', *Lwt*. Elsevier, 100(October 2018), pp. 391–396.

Ficheux, M.-F. *et al.* (2002) 'Some Stability Criteria for Double Emulsions', *Langmuir*, 14(10), pp. 2702–2706.

Firoozmand, H. and Rousseau, D. (2016) 'Microbial cells as colloidal particles : Pickering oil-in-water emulsions stabilized by bacteria and yeast', *FRIN*. Elsevier B.V., 81, pp. 66–73.

Fonseca, F., Béal, C. and Corrieu, G. (2000) 'Method of quantifying the loss of acidification activity of lactic acid starters during freezing and frozen storage', *Journal of Dairy Research*, 67(1), pp. 83–90.

Fonseca, F., Béal, C. and Corrieu, G. (2002) 'Operating conditions that affect the resistance of lactic acid bacteria to freezing and frozen storage', *Cryobiology*, 43(3), pp. 189–198.

Gao, W., Smith, D. W. and Li, Y. (2007) 'Effects of Freezing on the Survival of *Escherichia coli* and Bacillus and Response to UV and Chlorine After Freezing', *Water Environment Research*, 79(5), pp. 507–513.

Gaonkar, A. G. (1994) 'Stable multiple emulsions comprising interfacial gelatinous layer, flavour-encapsulating multiple emulsions and low/no-fat food products comprising the same', *United States Patent*, (19).

Garti, N. and Bisperink, C. (1998) 'Double emulsions : progress and applications', *Current Opinion in Colloid and Interface Science*. Current Chemistry Ltd, 3(6), pp. 657–667.

Georgala, D. I. and Hurst, A. (1963) 'The survival of food poisoning bacteria in frozen foods', *Journal Applied Bacteriology,* 26, pp. 346-358.

Ghosh, S. and Coupland, J. N. (2008) 'Factors affecting the freeze-thaw stability of emulsions', *Food Hydrocolloids*, 22(1), pp. 105–111.

Ghosh, S. and Rousseau, D. (2009) 'Freeze-thaw stability of water-in-oil emulsions', *Journal of Colloid and Interface Science*. Elsevier Inc., 339(1), pp. 91–102.

Giroux, H. J. *et al.* (2019) 'Effect of oil phase properties on peptide release from water-in-oil-in-water emulsions in gastrointestinal conditions', *Lwt*. Elsevier, 109(April), pp. 429–435.

Goderska, K. and Czarnecki, Z. (2008) 'Influence of microencapsulation and spray drying on the viability of Lactobacillus and Bifidobacterium strains', *Polish Journal of Microbiology*, 57(2), pp. 135–140.

González-Ochoa, H., Ibarra-Bracamontes, L. and Arauz-Lara, J. L. (2003) 'Two-stage coalescence in double emulsions', *Langmuir*, 19(19), pp. 7837–7840. doi: 10.1021/la0349323.

Gravesen, P., Branebjerg, J. and Jensen, O. S. (1993) 'Microfluidics-a review', *Journal of Micromechanics and Microengineering*. IOP Publishing, 3(4), pp. 168–182.

Grumezescu, A. M. (2019) *Biomedical Applications of Nanoparticles*. Elsevier Science.

Harada, T. and Yokomizo, K. (2000) 'Demulsification of oil-in-water emulsion under freezing conditions: Effect of crystal structure modifier', *Journal of the American Oil Chemists' Society*, 77(8), pp. 859–864.

He, G. and Chen, G. (2002) 'Lubricating oil sludge and its demulsification', *Drying Technology*, 20(4–5), pp. 1009–1018.

Hirai, T. *et al.* (2002) 'Biomimetic Synthesis of Calcium Carbonate Particles in a Pseudovesicular Double Emulsion', *Langmuir*, 13(25), pp. 6650–6653.

Hirai, T., Hodono, M. and Komasawa, I. (2000) 'Preparation of spherical calcium phosphate fine particles using an emulsion liquid membrane system', *Langmuir*, 16(3), pp. 955–960.

Hong, Y. and Brown, D. G. (2009) 'Variation in bacterial ATP level and proton motive force due to adhesion to a solid surface', *Applied and Environmental Microbiology*, 75(8), pp. 2346–2353.

Hou, L. *et al.* (2017) 'Osmolarity-controlled swelling behaviours of dual-cored double-emulsion drops', *Microfluidics and Nanofluidics*. Springer Berlin Heidelberg, 21(4), pp. 1–8.

Hughes, E. *et al.* (2013) 'Microfluidic preparation and self-diffusion PFG-NMR analysis of monodisperse water-in-oil-in-water double emulsions', *Journal of Colloid and Interface Science*. Elsevier Inc., 389(1), pp. 147–156.

Hunter, R. J. and White, L. R. (1987) *Foundations of colloid science*. Clarendon Press (Oxford science publications).

Hussein, H. *et al*. (2019) 'Determination of cell viability using acridine orange/propidium iodide dual-spectrometry assay', *Cogent Food and Agriculture,* 5(1), pp. 1-9.

Idalia, V.-M. N. and Bernardo, F. (2017) '*Escherichia coli* as a Model Organism and Its Application in Biotechnology'*, Escherichia coli - Recent Advances on Physiology, Pathogenesis and Biotechnological Applications*. IntechOpen.

Ishibashi, C., Hondoh, H. and Ueno, S. (2016) 'Influence of morphology and polymorphic transformation of fat crystals on the freeze-thaw stability of mayonnaise-type oil-in-water emulsions', *Food Research International*. Elsevier Ltd, 89, pp. 604–613.

Jaimes-Lizcano, Y. A., Lawson, L. B. and Papadopoulos, K. D. (2011) 'Oil-Frozen W1/O/W2 Double Emulsions for Dermal Biomacromolecular Delivery Containing Ethanol as Chemical Penetration Enhancer', *Journal of Pharmaceutical Sciences*, 100(4), pp. 1398–1406.

Jankowski, T. *et al*. (1997) 'Encapsulation of lactic acid bacteria with alginate/starch capsules', *Biotechnology Techniques*, 11, pp. 31–34.

Jiao, J., Rhodes, D. G. and Burgess, D. J. (2002) 'Multiple emulsion stability: Pressure balance and interfacial film strength', *Journal of Colloid and Interface Science*, 250(2), pp. 444–450.

Kalashnikova, I. *et al* (2011) 'New Pickering Emulsions Stabilized by Bacterial Cellulose Nanocrystals', *Langmuir*, 27, pp. 7471−7479.

Kanouni, M., Rosano, H. . and Naouli, N. (2002) 'Preparation of a stable double emulsion ($W_1/O/W_2$): role of the interfacial films on the stability of the system', *Advances in Colloid and Interface Science*, 99(3), pp. 229–254.

Kawakatsu, T. *et al.* (2000) 'Effect of microchannel structure on droplet size during crossflow microchannel emulsification', *Journal of Surfactants and Detergents*, 3(3), pp. 295–302.

Kawakatsu, T., Kikuchi, Y. and Nakajima, M. (1997) 'Regular-sized cell creation in microchannel emulsification by visual microprocessing method', *JAOCS, Journal of the American Oil Chemists' Society*, 74(3), pp. 317–321.

Kebary, K. M. K. *et al* (1998) 'Improving viability of bifidobacterium and their effect on frozen ice milk', *Egyptian Journal of Dairy Science*. 26, pp. 319–337.

Khalil, A. H., and Mansour, E. H. (1998) 'Alginate encapsulated bifidobacteria survival in mayonnaise', *Journal of Food Science*. 63, pp. 702–705.

Kim, J. et al. (2010) 'Graphene Oxide Sheets at Interfaces', *J. Am. Chem. Soc*., 132, pp.8180−8186.

Kim, P. et al. (2008) 'Soft lithography for microfluidics: a Review', *Biochip Journal*, 2(1), pp. 1-11.

Klojdová, I., Štětina, J. and Horáčková, Š. (2019) 'W/O/W Multiple Emulsions as the Functional Component of Dairy Products', *Chemical Engineering and Technology*, 42(4), pp. 715–727.

Koop, T. (2004) 'Homogeneous ice nucleation in water and aqueous solutions', *Zeitschrift fur Physikalische Chemie*, 218 (11), pp. 1231-1258.

Kovács, A. *et al.* (2005) 'Structural analysis of W/O/W multiple emulsions by means of DSC', *Journal of Thermal Analysis and Calorimetry*, 82(2), pp. 491–497.

Krebs, T., Schroen, C. P. G. H. and Boom, R. M. (2012) 'A microfluidic study of oil-water separation kinetics', *WIT Transactions on Engineering Sciences*, 74, pp. 427–438.

Lalou, S., El Kadri, H. and Gkatzionis, K. (2017) 'Incorporation of water-in-oil-in-water (W1/O/W2) double emulsion in a set-type yoghurt model', *Food Research International*, 100(August), pp. 122–131.

Larsen, N. *et al.* (2018) 'The effect of pectins on survival of probiotic *Lactobacillus spp* . in gastrointestinal juices is related to their structure and physical properties', *Food Microbiology*. Elsevier Ltd, 74, pp. 11–20.

Leal-Calderon, F., Bibette, J. and Schmitt, V. (2007) 'Stability of Concentrated Emulsions', in *Emulsion Science: Basic Principles*. New York, NY: Springer New York, pp. 143–172.

Lebeer, S. *et al.* (2007) 'Impact of Environmental and Genetic Factors on Biofilm Formation by the Probiotic Strain *Lactobacillus rhamnosus* GG', *Applied and Environmental Microbiology*, 73(21), pp. 6768–6775.

Lee, K. Y. and Heo, T. R. (2000) 'Survival of *Bifidobacterium longum* immobilized in calcium alginate beads in simulated gastric juices and bile salt solution', *Applied and Environmental Microbiology*, 66, pp. 869–873.

Lehtinen, J., Nuutila, J. and Lilius, E. (2004) 'Green fluorescent protein-propidium iodide (GFP-PI) based assay for cytometric measurement of bacterial viability', *Cytometry part A-Journal of Quantitative Cell Science*, 60A(2), pp. 165-172.

Li, J., Mcclements, D. J. and Mclandsborough, L. A. (2001) 'Interaction between Emulsion Droplet and *Escherichia coli* Cells', *Journal of Food Science*, 66(4), pp. 570–657.

Lin, C. *et al.* (2007) 'Freeze/thaw induced demulsification of water-in-oil emulsions with loosely packed droplet', *Separation and Purification Technology*, 56(2), pp. 175–183.

Lin, C. *et al.* (2008) 'Effect of oil phase transition on freeze/thaw-induced demulsification of water-in-oil emulsions', *Langmuir*,24(10), pp.5291-5298.

Link, D. R. *et al.* (2006) 'Electric control of droplet in microfluidic devices', *Angewandte Chemie - International Edition*, 45(16), pp. 2556–2560.

List, G. R. (2016) ' Oilseed composition and modification for health and nutrition', in Sanders, T. (ed) *Functional Dietary Lipids: Food Formulation, Consumer Issues and Innovation for Health.* Woodhead Publishing Series in Food Science, Technology and Nutrition. Elsevier Science, pp. 23-46.

Liu, F., and Tang, C. -H. (2013) 'Soy protein nanoparticle aggregates as Pickering stabilizers for oil-in-water emulsions', *Journal of Agricultural and Food Chemistry*, 61(37), pp. 8888–8898.

Loizou, K., Wong, V.-L. and Hewakandamby, B. (2018) 'Examining the Effect of Flow Rate Ratio on Droplet Generation and Regime Transition in a Microfluidic T-Junction at Constant Capillary Numbers', *Inventions*, 3(3), p. 54.

Lowry, P. D. and Gill, C. O. (1985) 'Microbiology of frozen meat and meat products', in Robinson, R. K. (ed) *Microbiology of Frozen Foods.* London: Elsevier Applied Science, pp. 109-168.

Lu, H. *et al*. (2017) 'High throughput single cell counting in droplet-based microfluidics', *Scientific reports*, 7(1366), pp. 1-9.

Lyngberg, O. K. *et al.* (1999) 'A patch coating method for preparing biocatalytic films of *Escherichia coli'*, *Biotechnology and Bioengineering*, 62(1), pp. 44–55.

Maan, A. A., Schroën, K. and Boom, R. (2013) 'Monodispersed water-in-oil emulsions prepared with semi-metal microfluidic EDGE systems', *Microfluidics and Nanofluidics*, 14(1–2), pp. 187–196.

Magdassi, S. and Garti, N. (1987) 'Formation of water/oil/water multiple emulsions with solid oil phase', *Journal of Colloid And Interface Science*, 120(2), pp. 537–539.

Malvern instruments Ltd. (2013) ' Zetasizer nano accessories guide', *Manual 0487*, 11, pp. 1-25.

Mao, L. and Miao, S. (2015) 'Structuring Food Emulsions to Improve Nutrient Delivery During Digestion', *Food Engineering Reviews*. United States: Springer, 7(4), pp. 439–451.

Marcoux, P. *et al.* (2011) 'Micro-confinement of bacteria into w/o emulsion droplet for rapid detection and enumeration', *Colloids and Surfaces A: Physicochemical and Engineering Aspects*. Elsevier, 377, pp. 54–62.

Marefati, A. *et al.* (2013) 'Freezing and freeze-drying of Pickering emulsions stabilized by starch granules', *Colloids and Surfaces A: Physicochemical and Engineering Aspects*. Elsevier B.V., 436, pp. 512–520.

Mariani, L. *et al.* (2006) 'The use of a test battery in marine ecotoxicology: The acute toxicity of sodium dodecyl sulfate', *Environmental Toxicology*, 21(4), pp. 373–379.

Mazur, P. (2017) 'Freezing of living cells: mechanisms and implications', *American Journal of Physiology-Cell Physiology*, 247(3), pp. C125–C142.

McClements, D. J. (1998) *Food Emulsions: Principles, Practice, and Techniques*. Taylor and Francis (Contemporary Food Science).

McClements, D. J. (2004) *Food Emulsions: Principles, Practices, and Techniques.* Second edn. CRC Press (Contemporary Food Science).

McClements, D. J. (2009) *Modern Biopolymer Science*. First edn. Elsevier Inc.

Mesquita, A. R. C. *et al.* (2017) 'Activity of metabolites produced by new strains of Lactobacillus in modified de Man, Rogosa and Sharpe (MRS) medium against multidrug-resistant bacteria', *African Journal of Microbiology Research*, 11(8), pp. 345–355.

Mezzenga, R., Folmer, B. M. and Hughes, E. (2004) 'Design of double emulsions by osmotic pressure tailoring', *Langmuir*, 20(9), pp. 3574–3582.

Miles, B. Y. A. A. and Misra, S. S. (1931) 'The estimation of the bactericidal power of the blood', *Department of Pathology*, British Postgraduate Medical School, pp. 732–749.

Miyazawa, K. and Yajima, I. (2000) 'Preparation of a new soft capsule for cosmetics', *Journal of cosmetic*, 252, pp. 239–252.

Morales Chabrand, R. *et al.* (2008) 'Destabilization of the Emulsion Formed during Aqueous Extraction of Soybean Oil', *Journal of the American Oil Chemists' Society*, 85(4), pp. 383–390.

Muijlwijk, K., Berton-Carabin, C. and Schroën, K. (2016) 'Cross-flow microfluidic emulsification from a food perspective', *Trends in Food Science and Technology*, 49, pp. 51–63.

Muschiolik, G. and Dickinson, E. (2017) 'Double Emulsions Relevant to Food Systems: Preparation, Stability, and Applications', *Comprehensive Reviews in Food Science and Food Safety*,16, pp. 532-555

Nakae, T. (1976) 'Outer membrane of Salmonella. Isolation of protein complex that produces transmembrane channels.', *Journal of Biological Chemistry*, 251(7), pp. 2176–2178.

Neethirajan, S. *et al.* (2011) 'Microfluidics for food, agriculture and biosystems industries', *Lab on a Chip*, 11(9), pp. 1574.

Ngai, T., Behrens, S. H. and Auweter, H. (2005) 'Novel emulsions stabilized by pH and temperature-sensitive microgels.', *Chemical communications (Cambridge, England)*, (3), pp. 331–333.

Nguyen, B. T., Nicolai, T., and Benyahia, L. (2013) 'Stabilization of water-in-water emulsions by addition of protein particles', *Langmuir*, 29(34), pp.10658–10664.

Nurliyani, Suranindyah, Y. and Pretiwi, P. (2015) 'Quality and Emulsion Stability of Milk from Ettawah Crossed Bred Goat During Frozen Storage', *Procedia Food Science*. Elsevier Srl, 3, pp. 142–149.

O'Brien, K. V. *et al.* (2016) 'Short communication: The effects of frozen storage on the survival of probiotic microorganisms found in traditionally and commercially manufactured kefir', *Journal of Dairy Science*. Elsevier, 99(9), pp. 7043–7048.

Okushima, S. *et al.* (2004) 'Controlled production of monodisperse double emulsions by two-step droplet breakup in microfluidic devices', *Langmuir*, 20(23), pp. 9905–9908.

Oppermann, A. K. L. *et al.* (2015) 'Effect of gelation of inner dispersed phase on stability of (W1/O/W2) multiple emulsions', *Food Hydrocolloids*. Elsevier Ltd, 48, pp. 17–26.

Oppermann, A. K. L. *et al.* (2016) 'Descriptive sensory profiling of double emulsions with gelled and non-gelled inner water phase', *Food Research International*. Elsevier Ltd, 85, pp. 215–223.

Osborn, M. J. *et al.* (1972) 'Mechanism of assembly of the outer membrane of Salmonella typhimurium isolation and characterization of cytoplasmic and outer membrane', *Journal of Biological Chemistry*, 247(12), pp. 3962–3972.

Park, Y. *et al.* (2015) 'Monodisperse Micro-Oil Droplet Stabilized by Polymerizable Phospholipid Coatings as Potential Drug Carriers', *Langmuir*, 31(36), pp. 9762–9770.

Parker, M. L. *et al.* (1995) 'Growth of foodborne pathogenic bacteria in oil--in--water--emulsions: I Methods for investigating the form of growth of bacteria in model oil--in--water emulsions and dairy cream', *Journal of Applied Bacteriology*, 78, pp. 601–608.

Patel, A. R. *et al.* (2013) 'Fabrication and characterization of emulsions with pH-responsive switchable behaviour', *Soft Matter*, 9(29), pp. 6747–6751.

Pegg, D. E. (2007) 'Principles of cryopreservation', in Day, J. G. and Stacey, G. N. (eds) *Cryopreservation and Freeze Drying Protocols*. Methods in Molecular Biology. Vol 368. Humana Press, pp. 39-57.

Petruzzi, L. *et al*. (2017) 'Thermal treatments for fruit and vegetable juices and beverages: A literature overview', *Comprehensive Reviews in Food Science and Food Safety,* 16(4), pp. 668-691.

Phipps, L. W. and National Institute for Research in Dairying (1985) 'The high-pressure dairy homogenizer', *Technical bulletin*. National Institute for Research in Dairying.

Pimentel-Gonzalez, D. J. *et al.* (2009) 'Encapsulation of *Lactobacillus rhamnosus* in double emulsions formulated with sweet whey as emulsifier and survival in simulated gastrointestinal conditions', *Food Research International*. Elsevier Ltd, 42(2), pp. 292–297.

Powell-Palm, M. J. *et al.* (2018) '*Escherichia coli* viability in an isochoric system at subfreezing temperatures', *Cryobiology*. Elsevier, 85(August), pp. 17–24.

Priya, A. J., Vijayalakshmi, S. P. and Raichur, A. M. (2011) 'Enhanced survival of probiotic *Lactobacillus acidophilus* by encapsulation with nanostructured polyelectrolyte layers through layer-by-layer approach', *Journal of Agricultural and Food Chemistry*, 59(21), pp. 11838–11845.

Rayner, M. et al. (2012) 'Quinoa starch granules: A candidate for stabilising food-grade Pickering emulsions', *Journal of the Science of Food and Agriculture*, 92(9), 1841–1847.

Reger, D. L., Goode, S. R. and Ball, D. W. (2009) *Chemistry: Principles and Practice*. Cengage Learning.

Rezvani, F., Ardestani, F. and Najafpour, G. (2017) 'Growth kinetic models of five species of Lactobacilli and lactose consumption in batch submerged culture', *Brazilian Journal of Microbiology*. Sociedade Brasileira de Microbiologia, 48(2), pp. 251–258.

Rodríguez-Huezo, M. E. *et al.* (2007) 'Pre-selection of protective colloids for enhanced viability of *Bifidobacterium bifidum* following spray-drying and storage, and evaluation of aguamiel as thermoprotective probiotic', *Food Research International*. 40, pp. 1299–1306.

Rodríguez-Huezo, M. E. *et al.* (2014) 'Viability of *Lactobacillus plantarum* entrapped in double emulsion during Oaxaca cheese manufacture, melting and simulated intestinal conditions', *LWT - Food Science and Technology*, 59(2P1), pp. 768–773.

Roeßler, M., Sewald, X. and Müller, V. (2003) 'Chloride dependence of growth in bacteria', *FEMS Microbiology Letters*, 225, pp. 161-165.

Rojas, E. C. *et al.* (2008) 'Temperature-induced protein release from water-in-oil-in-water double emulsions', *Langmuir*, 24(14), pp. 7154–7160.

Rojas, E. C. and Papadopoulos, K. D. (2007) 'Induction of instability in water-in-oil-in-water double emulsions by freeze-thaw cycling', *Langmuir*, 23(13), pp. 6911–6917.

Rokka, S. and Rantamäki, P. (2010) 'Protecting probiotic bacteria by microencapsulation: Challenges for industrial applications', *European Food Research and Technology*, pp. 1–12.

Romoscanu, A. I. *et al.* (2010) 'Structure, diffusion, and permeability of protein-stabilized monodispersed oil in water emulsions and their gels: A self-diffusion NMR study', *Langmuir*, 26(9), pp. 6184–6192.

Rosenberg, M., Gutnick, D. and Rosenberg, E. (1980) 'Adherence of bacteria to hydrocarbons: A simple method for measuring cell-surface hydrophobicity', *FEMS Microbiology Letters*, 9, pp.29–33.

Rowlett, V. W. *et al.* (2017) 'Impact of Membrane Phospholipid Alterations in *Escherichia* on Cellular Function and Bacterial Stress Adaptation', *Journal of Bacteriology*. Edited by V. J. DiRita, 199(13), pp. e00849-16.

Russel, W. B. (1981) 'Brownian Motion of Small Particles Suspended in Liquids', *Annual Review of Fluid Mechanics*, 13(1), pp. 425–455.

Sánchez, A. *et al.* (2003) 'Effect of freezing goat milk samples on recovery of intramammary bacterial pathogens', *Veterinary Microbiology*, 94(1), pp. 71–77.

Schaerli, Y. *et al.* (2009) 'Continuous-Flow Polymerase Chain Reaction of Single-Copy DNA in Microfluidic Microdroplet', *Analytical Chemistry*, 81(1), pp. 302–306.

Schuch, A., Köhler, K. and Schuchmann, H. P. (2013) 'Differential scanning calorimetry (DSC) in multiple W/O/W emulsions: A method to characterize the stability of inner droplet', *Journal of Thermal Analysis and Calorimetry*, 111(3), pp. 1881–1890.

Schuster, D. (1996) *Encyclopedia of Emulsion Technology*. New York: Taylor and Francis.

Seltmann, G. and Holst, O. (2013) *The Bacterial Cell Wall*. Berlin, Heidelberg: Springer.

Sezonov, G., Joseleau-Petit, D. and D'Ari, R. (2007) '*Escherichia coli* physiology in Luria-Bertani broth', *Journal of Bacteriology*, 189(23), pp. 8746–8749.

Shang, L., Cheng, Y. and Zhao, Y. (2017) 'Emerging Droplet Microfluidics', *Chemical Reviews*, 117(12), pp. 7964–8040.

Sherman, P. and Parkinson, C. (1978) 'Mechanism of temperature-induced phase inversion in O/W emulsions stabilised by O/W and W/O emulsifier blends', in *Emulsions*. Heidelberg: Steinkopff, pp. 10–14.

Shima, M. *et al.* (2006) 'Protection of *Lactobacillus acidophilus* from the low pH of a model gastric juice by incorporation in a W/O/W emulsion', *Food Hydrocolloids*, 20(8), pp. 1164–1169.

Simonin, H. *et al.* (2015) 'Cryopreservation of *Escherichia coli* K12TG1: Protection from the damaging effects of supercooling by freezing', *Cryobiology*. Elsevier Inc., 70(2), pp. 115–121.

Soni, K. A. *et al.* (2008) 'Zeta potential of selected bacteria in drinking water when dead, starved, or exposed to minimal and rich culture media', *Current Microbiology*, 56(1), pp. 93–97.

Souzu, H. (1980) 'Studies on the damage to *Escherichia coli* cell membrane caused by different rates of freeze-thawing', *BBA - Biomembranes*, 603(1), pp. 13–26.

Souzu, H. (1989) 'Changes in chemical structure and function in *Escherichia coli* cell membranes caused by freeze-thawing. I. Change of lipid state in bilayer vesicles and in the original membrane fragments depending on rate of freezing', *BBA - Biomembranes*, 978(1), pp. 105–111.

Souzu, H., Sato, M. and Kojima, T. (1989) 'Changes in chemical structure and function in *Escherichia coli* cell membranes caused by freeze-thawing. II. Membrane lipid state and response of cells to dehydration', *BBA - Biomembranes*, 978(1), pp. 112–118. d

Srisa-art, M. *et al.* (2009) 'Analysis of Protein-Protein Interactions by Using Droplet-Based Microfluidics', *ChemBioChem*, 10, pp. 1605–1611.

Stoodley, P. *et al.* (2001) 'Growth and Detachment of Cell Clusters from Mature Mixed-Species Biofilms', *Applied and Environmental Microbiology*, 67(12), pp. 5608–5613.

Strocchi, M. *et al.* (2006) 'Low temperature-induced systems failure in *Escherichia coli*: Insights from rescue by cold-adapted chaperones', *Proteomics*, 6(1), pp. 193–206.

Sun, D. W. (2005) *Handbook of Frozen Food Processing and Packaging*. CRC Press (Contemporary Food Engineering).

Suzuki, K., Shuto, I. and Hagura, Y. (1996) 'Characteristics of the Membrane Emulsification Method Combined with Preliminary Emulsification for Preparing Corn Oil-in-Water Emulsions', *Food Science and Technology International, Tokyo*, 2(1), pp. 43–47.

Tadros, T. F. (2013) 'Emulsion Formation, Stability, and Rheology', in Tadros, T.F. (ed) *Emulsion Formation and Stability*, Weinheim. Germany: Wiley-VCH Verlag GmbH and Co. KgaA, pp. 1-72.

Tan, J. *et al.* (2008) 'Drop dispenser in a cross-junction microfluidic device: Scaling and mechanism of break-up', *Chemical Engineering Journal*, 136(2–3), pp. 306–311.

Teh, S.-Y. *et al.* (2008) 'Droplet microfluidics.', *Lab on a chip*, 8(2), pp. 198–220.

Tieko Nassu, R. and Gonçalves, L. A. G. (1999) 'Determination of melting point of vegetable oils and fats by differential scanning calorimetry (DSC) technique', *Grasas y Aceites*, 50, pp. 16–21.

Tippetts, M. and Martini, S. (2009) 'Effect of cooling rate on lipid crystallization in oil-in-water emulsions', *Food Research International*. Elsevier Ltd, 42(7), pp. 847–855.

Tsvetkov, T. and Shishkova, I. (1982) 'Studies on the effects of low temperatures on lactic acid bacteria', *Cryobiology*, 19(2), pp. 211–214.

Tzoumaki, V. M. *et al*. (2011) 'Oil-in-Water Emulsions Stabilized by Chitin Nanocrystal Particles', *Food Hydrocolloid,* 25, pp.1521−1529

Vanapalli, S. A., Palanuwech, J. and Coupland, J. N. (2002) 'Stability of emulsions to dispersed phase crystallization: Effect of oil type, dispersed phase volume fraction, and cooling rate', *Colloids and Surfaces A: Physicochemical and Engineering Aspects*, 204(1–3), pp. 227–237.

Villa, C. H. *et al.* (2003) 'Internal coalescence as a mechanism of instability in water-in-oil-in-water double-emulsion globules', *Langmuir*, 19(2), pp. 244–249.

Vladisavljevic, G. T. (2015) *Encyclopedia of Membranes*, *Encyclopedia of Membranes*. Berlin Heidelberg: Springer.

Vladisavljević, G. T., Al Nuumani, R. and Nabavi, S. A. (2017) 'Microfluidic production of multiple emulsions', *Micromachines*, 8(3). pp.75.

Walstra, P. (1993) 'Principles of emulsion formation', *Chemical Engineering Science*, 48(2), pp. 333–349.

Walstra, P. (2002) *Physical Chemistry of Foods*. New York: Marcel Dekker Inc.

Walstra, P. and Smulders, P. E. A. (1998) 'Chapter 2: Emulsion Formation', in Binks, B.P. (ed) *Modern Aspects of Emulsion Science*. The Royal Society of Chemistry, pp. 56–99.

Wang, G. *et al.* (2019) 'Optimal combination of multiple cryoprotectants and freezing-thawing conditions for high lactobacilli survival rate during freezing and frozen storage', *Lwt*, 99, pp. 217–223.

Wangqi Hou and Papadopoulos, K. D. (1996) 'Stability of water-in-oil-in-water type globules', *Chemical Engineering Science*, 51(22), pp. 5043–5051.

Ward, T. *et al.* (2005) 'Microfluidic flow focusing: drop size and scaling in pressure versus flow-rate-driven pumping', *Electrophoresis*, 26(19), pp. 3716–3724.

Wege, H. A. *et al.* (2008) 'Long-term stabilization of foams and emulsions with in-situ formed microparticles from hydrophobic cellulose', *Langmuir*, 24(17), 9245–9253.

Wei, Z. *et al.* (2012) 'Chitosan nanoparticles as particular emulsifier for preparation of novel pH-responsive Pickering emulsions and PLGA microcapsules', *Polymer*. Elsevier Ltd, 53(6), pp. 1229–1235.

Wen, L. and Papadopoulos, K. D. (2000) 'Visualization of water transport in emulsions', *Colloids and Surfaces A: Physicochemical and Engineering Aspects*, 174(1–2), pp. 159–167.

Wongkongkatep, P. *et al.* (2012) 'Bacteria interface Pickering emulsions stabilized by self-assembled bacteria-chitosan network', *Langmuir*.28, pp. 5729-5736.

Wright, C. T. and Klaenhammer, T. R. (1981) 'Calcium-induced alterations of cellular morphology affecting the resistance of *Lactobacillus acidophilus* to freezing', *Applied and Environmental Microbiology*, 41(3), pp. 807–815.

Wright, C.T and Klaenhammer, T. R. (1983) 'Survival of *Lactobacillus bulgaricus* During Freezing and Freeze-Drying After Growth in the Presence of Calcium', *Journal of Food Science*, 48(3), pp. 773–777.

Wu, N. *et al.* (2009) 'A PMMA microfluidic droplet platform for in vitro protein expression using crude *E. coli* S30 extract', *Lab Chip*, 9(23), pp. 3391–3398.

Wu, N. *et al.* (2011) 'A double-emulsion microfluidic platform for in vitro green fluorescent protein expression', *Journal of Micromechanics and Microengineering*, 21(5), p. 054032.

Yan, J. *et al.* (2013) 'Monodisperse water-in-oil-in-water (W/O/W) Double emulsion droplet as uniform compartments for high-throughput analysis via flow cytometry', *Micromachines*, 4(4), pp. 402–413.

Zeng, G. *et al.* (2007) 'Co-degradation with glucose of four surfactants, CTAB, Triton X-100, SDS and Rhamnolipid, in liquid culture media and compost matrix', *Biodegradation*, 18(3), pp. 303–310.

Zhang, W. *et al.* (2017) 'Osmotic Pressure Triggered Rapid Release of Encapsulated Enzymes with Enhanced Activity', *Advanced Functional Materials*, 27(29), pp. 1–7.

Zhang, Y. *et al.* (2013) 'A programmable microenvironment for cellular studies via microfluidics-generated double emulsions', *Biomaterials*. Elsevier Ltd, 34(19), pp. 4564–4572.

Zhu, X. F. *et al.* (2017) 'Freeze-thaw stability of Pickering emulsions stabilized by soy and whey protein particles', *Food Hydrocolloids*. Elsevier Ltd, 69, pp. 173–184.

Zur, J., Wojcieszyńska, D. and Guzik, U. (2016) 'Metabolic responses of bacterial cells to immobilization', *Molecules*, 21(7). pp. 958.

Appendix 1. Microfludic experiment setup

a

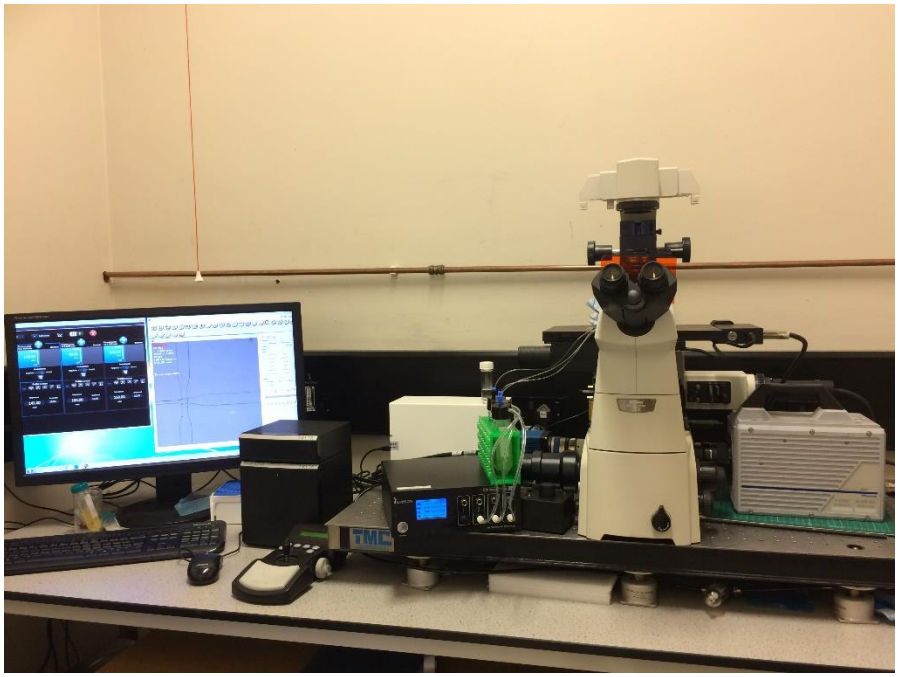

b

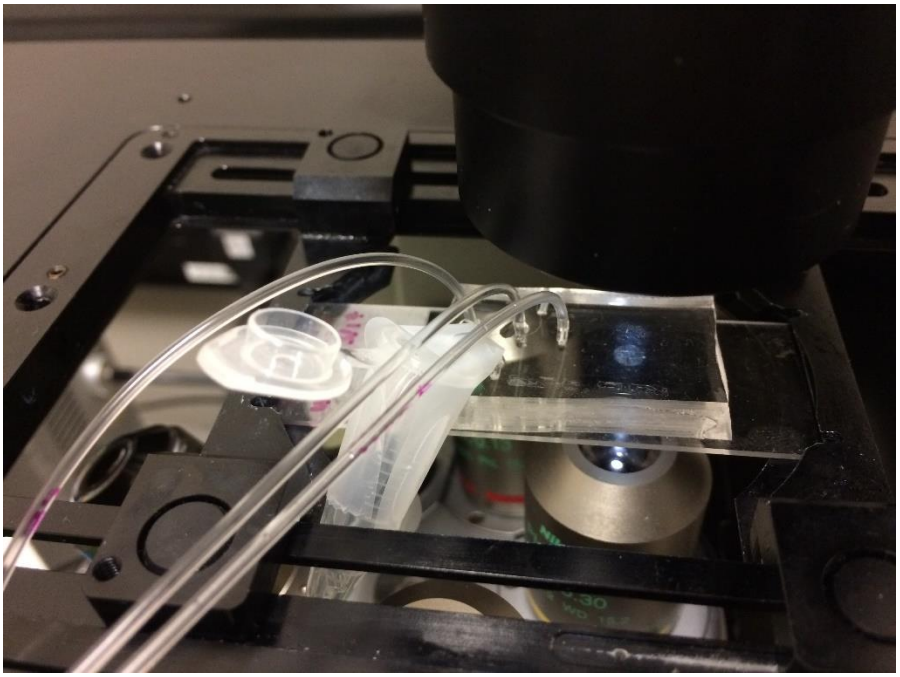

Figure A 1 Microfluidic experiment setup (a) Microfluidic droplet generation and bacterial encapsulation setup with pressure controller (b) A microfluidic device used for droplet generation

Appendix 2. Encapsulation efficiency for *E. coli*-GFP encapsulated in $W_1/O/W_2$

Table A 1 The encapsulation efficiency of *E. coli* -GFP in $W_1/O/W_2$ emulsions. Data represent mean ± standard deviation taken from 3 independent experiments.

Samples	**Encapsulation efficiency (%)**
E. coli/DI water in W1 (1% Tween 80)	99.99 ± 0.01
E. coli/DI water in W1 (5% Tween 80)	100 ± 0.05
E. coli/ LB broth in W1 (1% Tween 80)	99.98 ± 0.02
E. coli/LB broth in W1 (5% Tween 80)	99.99 ± 0.03
E. coli/ 0.5% NaCl in W1 (1% Tween 80)	99.95 ± 0.02
E. coli/ 0.5% NaCl in W1 (5% Tween 80)	99.99 ± 0.03

Appendix 3. The effect of sodium chloride, tryptone and yeast extract on the viability of *E. coli*-GFP

Table A 2 The effect of different LB broth ingredients on the viability of *E. coli*-GFP. Data represent mean standard deviation from 3 independent experiments.

Incubation time (Hour)	Sodium Chloride	Tryptone	Yeast Extract
0	6.27 ± 0.05	6.40 ± 0.04	7.03 ± 0.09
24	6.18 ± 0.03	7.98 ± 0.03	8.26 ± 0.03
Change in Log CFU/mL	-1.48	24.72	17.48

Appendix 4. Density measurements for the aqueous and oil phase of $W_1/O/W_2$ emulsions

Table A 3 Average density measurements for the aqueous and oil phase of $W_1/O/W_2$ emulsions. Data represent mean ± standard deviation taken from 3 independent experiments.

Solutions	Average density (g/ml)
DIW	0.997 ± 0.001
DIW with *E. coli*-GFP	0.973 ± 0.001
DIW with 1% w/v Tween 80	0.986 ± 0.002
DIW with 5% w/v Tween 80	0.994 ± 0.001
Mineral Oil	0.863 ± 0.001
Mineral Oil with 1.5% w/v PGPR	0.849 ± 0.003
0.5% w/v NaCl	1.004 ± 0.002
1.5% w/v NaCl	1.012 ± 0.003
2.0% w/v NaCl	1.011 ± 0.002
0.5% w/v NaCl with *E. coli*-GFP	1.004 ± 0.002
0.5% w/v NaCl w 1% w/v Tween 80	1.011 ± 0.003
0.5% w/v NaCl with 5% w/v Tween 80	1.023 ± 0.004

Appendix 5. Bacterial Adherence to Hydrocarbons (BATH) assay for soybean oil

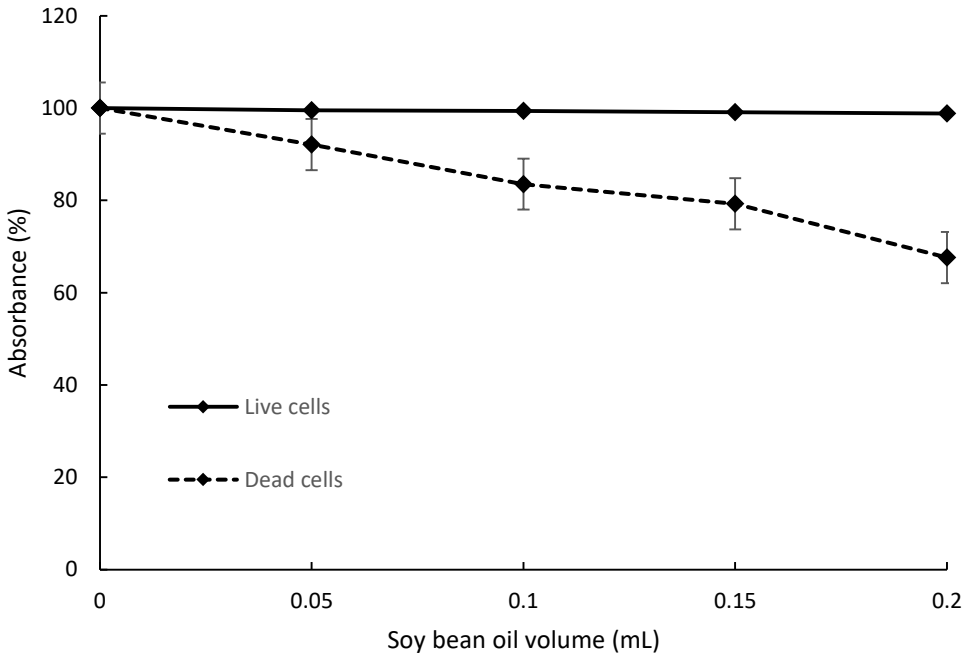

Figure A 2 The bacterial adherence to soybean oil assay for live and dead *E. coli*-GFP. Bars represent mean ± SEM taken from 3 independent experiments (N=3).